Investigation of the impact of ageing on the haematopoietic stress response

By

Charlotte Hellmich, BSc, MBChB

A thesis submitted for the degree:

Doctor of Philosophy

Norwich Medical School
Department of Molecular Haematology
The University of East Anglia, Norwich, UK

Date of submission: 1st October 2022

Declaration

I declare that the contents of this thesis entitled “Investigation of the impact of ageing on the haematopoietic stress response” was undertaken and completed by myself, unless otherwise acknowledged and has not been submitted in an application for another degree or qualification in this or any other university or institution.

This thesis is approximately 40,000 words in length

Parts of this research have been published prior to submission and are referenced in the List of Publications.

Charlotte Hellmich

Acknowledgements

The last three years have been quite an eventful journey with plenty of unexpected challenges. I have learned so many things and truly enjoyed the experience. I couldn't have reached the end of this journey without the help and support of all my amazing colleagues and friends. First, I would like to thank my fantastic supervisors Kris and Stuart, you have been the best mentors anyone could ask for and I have learned so much from you both. Thank you for your guidance, encouragement and patience with me starting as a clinician new to the world of science. You have created a unique lab in Norwich with the best support imaginable, I can't think of a better place to work!

I would like to thank all my fellow lab members, Jayna, Jamie, Aisha, Rebecca, Kat, and Edyta, for making sure there is never a boring moment in the Rushworth lab. We have had so many laughs and I'm sure there are more to come. I will always be grateful for your help and friendship. A particular big thank you goes to Jayna for everything you taught me, for your help and advice and for being an amazing friend. From the time I was your 'lab tech' for 4 months to all those random chats outside in the freezing cold, the PhD wouldn't have been the same without you.

Thank you also to the clinical team at the NNUH for supporting me coming out of clinical training and completing this PhD. A special thank you to all my registrar colleagues, for being wonderful friends and of course for helping me collect the many research samples for the lab. I especially want to thank Andra, Meha and Leo for their friendship and guidance and for helping me to find the right balance between clinical work, research and everything else.

Finally, I want to thank Pete for his patience, for always listening to me when I was stressed and for the cakes. You really are the best! I also want to thank my family, in particular my brother Moritz for proofreading this thesis for me. A big thank you goes to all the older people who have inspired me over the years, my grandparents, my aunt Louise Hennig and of course all of my patients. Vielen Dank an euch alle!

Abstract

The ageing population is gradually growing and with it the incidence of age-related diseases, including malignancies and infections. Understanding how physiological processes change during ageing is key to determining how they contribute to the development of pathologies. The regulation of the maintenance and differentiation of haematopoietic stem cells (HSCs) in the bone marrow (BM) is essential for normal blood homeostasis, as well as the haematopoietic response to stress. In order to support an increased demand for blood cell production, HSCs quickly upregulate their energy production by shifting from glycolysis to oxidative phosphorylation. During infections, this allows the rapid production and mobilisation of mature immune cells which can help to clear and overcome the infection. However, in the ageing population, symptomatic infections occur more frequently and are often associated with increased morbidity and mortality. This suggests that the immune response is diminished and, in this thesis, I examine the metabolic changes within the haematopoietic cell populations that contribute to this age-related change.

This study demonstrates that HSCs and haematopoietic progenitor cells (HPCs) acquire metabolic changes with age. These are analysed by measuring mitochondrial membrane potential, mitochondrial content and mitochondrial reactive oxygen species (ROS). Furthermore, this research shows that these age-related metabolic changes impact on the HSC and HPC stress response. The results described here show that this metabolic change is driven by senescent changes in the BM microenvironment, in particular the BM stromal cells (BMSCs). Removing HSCs from the aged BM using transplant models or targeting the BMSCs with senolytic agents can reverse some of the metabolic changes observed in aged HSCs and improve the haematopoietic stress response (1). Together, these findings demonstrate that ageing in the BM microenvironment drives intrinsic metabolic changes in the haematopoietic cell populations and this impairs their ability to effectively respond to stress.

Table of Contents

List of publications and conference papers

Hellmich, C., Wojtowicz, E., Moore, J., Mistry, J., Jibril, A., Johnson, B., Smith, J., Beraza, N., Bowles, K., Rushworth, S., **(2022)** p16INK4A dependent senescence in the bone marrow niche drives age-related metabolic changes of hematopoietic progenitors. *Blood Advances*.

Hellmich, C. and Wojtowicz, E., **(2022)** You are what you eat: how to best fuel your immune system. *Frontiers in Immunology*

Maynard, R., **Hellmich, C.,** Bowles K., Rushworth, S., **(2022)** Acute myeloid leukaemia drives metabolic changes in the bone marrow niche. Mini Review. *Frontiers of Oncology.*

Moore, J., Mistry, J., **Hellmich, C.,** Horton, R., Wojtowicz, E., Jibril, A., Jefferson, M., Wileman, T., Beraza, N., Bowles, K., Rushworth, S., **(2022)** LC3-associated phagocytosis in bone marrow macrophages suppresses acute myeloid leukemia progression through STING activation. *The journal of Clinical Investigation*

Mistry, J*., **Hellmich, C*.,** Moore, J., Jibril, A., Macauley, I., Moreno-Gonzalez, M., Di Palma, F., Beraza, N., Bowles, K. and Rushworth, S., **(2021).** Free fatty acid transport via CD36 drives β-oxidation mediated hematopoietic stem cell response to infection. *Nature Communications.* *Joint first authors

p16INK4A dependent senescence in the bone marrow niche drives age-related metabolic changes of hematopoietic progenitors. **Poster presentation. American Society of Haematology Annual Meeting 2021.**

The haematopoietic stem cell response to stress becomes impaired in ageing as a result of mitochondrial changes in the aged stromal cells. **Poster Presentation. International Society for Experimental Hematology 2021.**

Mistry, J., **Hellmich, C.,** Lambert, A., Moore, J., Jibril, A., Collins, A., Bowles, K. and Rushworth, S. **(2021).** Venetoclax and Daratumumab combination treatment demonstrates pre-clinical efficacy in mouse models of Acute Myeloid Leukemia. *Biomarker Research*

Targeting BCL-2 and CD38 in models of acute myeloid leukemia reduces tumour burden. **Poster Presentation. American Association of Cancer Research Annual Meeting 2021.**

Mitochondrial function is impaired in a subset of aged haematopoietic stem cells in response to infection. **Poster presentation with poster walk. American Society of Haematology Annual Meeting 2020. ASH abstract achievement award.**

Hellmich, C., Bowles, K. and Rushworth, S., **(2020).** ARQ531: the therapy that targets multiple pathways in acute myeloid leukemia. *Haematologica.*

Hellmich, C., Moore, J., Bowles, K. and Rushworth, S., **(2020).** Bone Marrow Senescence and The Microenvironment of Hematological Malignancies. *Frontiers in Oncology.*

Mistry, J., Moore, J., Kumar, P., Marlein, C., **Hellmich, C.,** Pillinger, G., Jibril, A., Di Palma, F., Collins, A., Bowles, K. and Rushworth, S. **(2020).** Daratumumab inhibits acute myeloid leukaemia metabolic capacity by blocking mitochondrial transfer from mesenchymal stromal cells. *Haematologica*

Mistry, J., Marlein, C., Moore, J., **Hellmich, C**., Wojtowicz, E., Smith, J., Macaulay, I., Sun, Y., Morfakis, A., Patterson, A., Horton, R., Divekar, D., Morris, C., Haestier, A., Di Palma, F., Beraza, N., Bowles, K. and Rushworth, S. **(2019).** ROS-mediated PI3K activation drives mitochondrial transfer from stromal cells to hematopoietic stem cells in response to infection. *Proceedings of the National Academy of Sciences*

List of Figures

List of Tables

List of abbreviations

3MR	Three modality Reporter
ALL	Acute lymphoblastic leukaemia
AML	Acute myeloid leukaemia
APML	acute pro-myelocytic leukaemia
ATP	Adenosine triphosphate
BH	BCL-2 homology
BM	Bone marrow
BMSC	Bone marrow stromal cells
BSA	Bovine serum albumin
CAR	Chimeric antigen receptor
CDK	Cyclin-dependent kinase
CHIP	Clonal haematopoiesis of intermediate potential
CLL	Chronic lymphocytic leukaemia
CLP	Common lymphoid progenitor
CML	Chronic Myeloid Leukaemia
CMP	Common myeloid progenitor
CoA	Coenzyme A
Con	Control
DAMPs	Danger-associated molecular patterns
DDR	DNA damage response
DMEM	Dulbecco's Modified Eagle's Medium
ECAR	Extracellular acidification rate
EPO	Erythropoietin
FABP	fatty-acid-binding proteins
FACS	Fluorescent activated cell sorting
FATP	fatty-acid-transporter proteins
FBS	Foetal calf serum
FFA	Free fatty acids
FLT-3	Flt-3 ligand
FMO	Fluorescent minus one
FSC	Forward Scatter

G-CSF	Granulocyte colony stimulating factor
GAPDH	Glyceraldehyde 3-phosphate dehydrogenase
GCV	Ganciclovir
GM-CSF	Granulocyte-macrophage colony stimulating factor
GMP	Granulocyte macrophage progenitors
HIF	Hypoxia-inducible factor
HPC	Haematopoietic progenitor cell
HSC	Haematopoietic stem cell
HSV	Herpes simplex virus
IGF	Insulin-like growth factor
IL	Interleukin
INF	Interferon
IP	Intraperitoneal
IT-HSC	Intermediate HSC
LBP	LPS binding protein
Lin	Lineage
Lin-	Lineage negative
LK	Lineage negative, C117 positive
LPS	Lipopolysaccharide
LS-K	Lineage negative, CD117 positive, Sca1 negative
LSK	Lineage negative, CD117 positive, Sca1 positive
LT-HSC	Long term HSC
MEM	Minimum Essential Medium
MEP	Megakaryocyte erythroid progenitors
MFI	Mean fluorescent index
MGUS	Monoclonal gammopathy of undetermined significance
MIP	Macrophage inflammatory proteins
$MitoSox^{hi}$	MitoSox high
$MitoSox^{lo}$	MitoSox low
MOMP	Mitochondrial outer membrane permeability
MPP	Multipotent progenitor cells
MTG	MitoTracker Green
NK	Natural killer

OCR	Oxygen Consumption rate
OXPHOS	Oxidative phosphorylation
PAMPs	Pathogen-associated molecular patterns
PB	Peripheral blood
PBS	1X phosphate buffer solution
PML-RARA	Promyelocytic leukaemia/retinoic acid receptor alpha
pRB	Retinoblastoma protein
qPCR	Real time quantitative polymerase chain reaction
renLuc	Renilla luciferase
RFP	Red fluorescent protein
ROS	Reactive Oxygen Species
SASP	Senescence associated secretory phenotype
SA-β-gal	Senescence associated beta galactosidase
SCC	Side scatter
SCF	Stem cell factor
SCT	Stem cell transplant
SNP	Single-nucleotide polymorphism
ST-HSC	Short term HSC
STING	stimulator of IFN genes
TCA	Tricarboxylic acid
tdTom	Tandem dimer Tomato
TGF-ß	transforming growth factor beta
TK	Tyrosine kinase
TLR	Toll-like receptor
TMRM	Tetramethylrhodamine, Methyl Ester
$TMRM^{hi}$	TMRM high
$TMRM^{lo}$	TMRM low
TPO	Thrombopoietin

1. Introduction

1.1. Ageing

The last 100 years have seen a dramatic change in health care, disease burdens and, as a result, life expectancy (2). Many diseases have become more treatable or curable and modern medicine has contributed to an increase in lifespan. However, this has not been associated with an equal increase in healthspan, the average length of healthy life (3). As our population continues to age, we increasingly recognise the burden of age-related diseases on individuals, the health care system and society as a whole. Ageing research aims not necessarily to change the total lifespan, but rather to improve the healthspan of our population and thereby reduce this burden (Figure 1.1.).

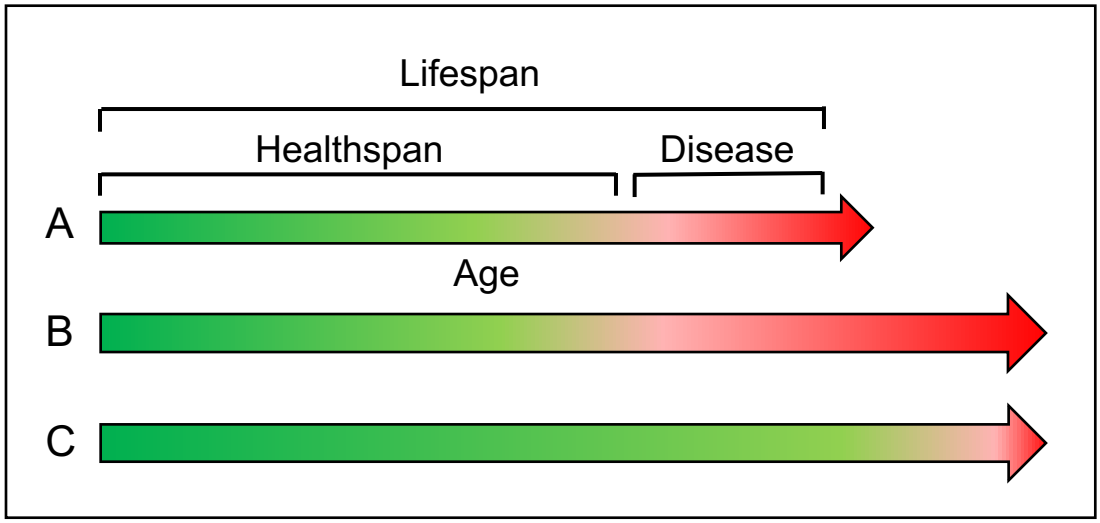

Figure 1.1. Life span and Healthspan
Lifespan is the average length of life whilst healthspan describes the disease-free lifespan. Medical interventions and treatments as well as some lifestyle changes have resulted in an increased lifespan from (A) to (B). However, this is often not accompanied by an increase in healthspan, which would be the ideal goal of improved health in ageing with an increased disease free healthspan and an increase overall lifespan (C).

Evolutionary theory of ageing stipulates that mortality rises as reproductive fitness declines but that this can be delayed if there a particular need for transfer of resources and care, as is the case in humans (4, 5). However, this

can only support the increase in life expectancy to some extent and does not explain the dramatic and rapid increase observed in the human population in the last 100-200 years. In many countries the life expectancy is now over 80 years, compared to a best life expectancy of 45 in 1840 (6) and this is predicted to continue to increase (7, 8). The decline in human mortality has been so rapid that it has only affected four of the approximately 8000 human generations and cannot be explained by the acquisition of mutations or genetic changes (9). Instead, it is thought that this change has been almost entirely driven by environmental factors, including improved hygiene, nutrition, healthcare and technological advances (2, 9, 10). Fundamental physiological and molecular processes cannot, however, change and adapt at the same speed, creating an imbalance between physiological function and longevity, which has a detrimental effect on health and drives the rise in age-related diseases. This is reflected in the gradual global transition from communicable, maternal, neonatal and nutritional diseases as the leading causes of death to an increase in the contribution of non-communicable diseases, predicted to account for more than 80% of global deaths by 2040 (7). It should be noted that significant disparity remains between countries, with communicable, maternal, neonatal and nutritional diseases continuing to be a leading cause of death in low-income countries. Nevertheless, this global rise in non-communicable diseases, many of which are associated with ageing, presents an ongoing challenge to prevent, treat and, if possible, cure these diseases in order to improve quality of life and reduce social and financial burdens. Whilst socioeconomic and lifestyle factors such as diet and smoking do contribute to disease development, it is becoming increasingly clear that the process of ageing itself can drive pathological changes and should be considered the main risk factor for diseases such as cancer, cardiovascular disease and neurodegeneration (11).

Physiological ageing, which does not necessarily correlate with chronological age (12), is likely driven by a number of processes and nine hallmarks of ageing have previously been proposed. These are genomic instability, telomere attrition, epigenetic alterations, loss of proteostasis, deregulated nutrient sensing, altered intercellular communication, stem cell exhaustion,

mitochondrial dysfunction, and cellular senescence (13). Each of these changes can directly impair tissue function and at the same time drive the acquisition of further hallmarks of ageing. Thus mitochondrial dysfunction, for example, drives development of age-related diseases such as type 2 diabetes (14, 15) and has also been shown to directly promote a senescent phenotype in fibroblasts, skin and adipose tissue (16-18). Ageing is, therefore, characterised by the failure of protective mechanisms, which would usually prevent these changes, and a gradual accumulation of each of these hallmarks. The result is reduced physiological function and development of age-related diseases.

1.1.1. Cellular Senescence

Cellular senescence, the irreversible arrest of cell proliferation was first described over 60 years ago by Leonard Hayflick (19, 20). Since then, we have gained an increasing understanding of the role of senescent cells both in health and disease. It is a process that evolved as a protective mechanism to prevent proliferation of cells following DNA damage that has an important role in tissue repair and wound healing. However, it has now become clear that this process can become detrimental if mechanisms to eliminate senescent cells are disrupted and senescent cells are allowed to accumulate (21, 22). Senescent cells have been shown to accumulate in various tissues with increasing age and have been associated with a of number of age related diseases including neurodegenerative diseases such as Alzheimer disease (23) and Parkinson's disease (24), malignancies including acute myeloid leukaemia (AML) (25) as well as osteoarthritis (26, 27) and atherosclerosis (28).

A number of pathways have been identified to drive the senescent phenotype. These can be triggered by DNA damage, telomere shortening, oncogenic activation and mitochondrial dysfunction and these can, in turn, result from direct cellular damage or external factors including oxidative stress, radiotherapy or cytotoxic chemotherapy (18, 29-31). The immediate response to any DNA damage is a rapid increase in the expression of the tumour

suppressor gene p53 and its downstream mediator p21, a cyclin-dependent kinase (CDK) inhibitor (32, 33). Normally this response is transient and reversible, however if the damage encountered becomes irreparable, persistent low levels of p53 and p21 expression are maintained and the senescent phenotype emerges (22). The irreversible nature of the senescent phenotype is primarily driven by the significant upregulation of the CDK inhibitor $p16^{INK4A}$, which occurs more slowly and is driven by external stressors as well as the effects of the persistent DNA damage response (DDR) (22). The downstream pathway of $p16^{INK4A}$ is through retinoblastoma protein (pRB) and both pRB and p53 are important transcriptional regulators, which together mediate the irreversible growth arrest of senescent cells (Figure 1.2.).

Another key characteristic of cellular senescence is the secretion of the senescent associated secretory phenotype (SASP). This has been shown to occur independently of both p53 and $p16^{INK4A}$ expression but is directly driven by the persistent DDR (34, 35). In fact, p53 has been shown to restrain the SASP (36) and the induction of senescence by p16 or p21 expression, in the absence of persistent DDR, is not associated with a SASP (35). The SASP consists of a vast number of pro-inflammatory cytokines, chemokines, growth factors and proteases; these include interleukin-1 (IL-1), IL-6, IL-7, IL-8, macrophage inflammatory proteins (MIP3α and MIP1α), Insulin-like growth factor (IGF) and matrix metalloproteinases (37). These are essential to stimulate tissue repair and wound healing in response to injury through activation of the immune system, which also contributes to the clearance of senescent cells (30). As clearance of senescent cells becomes ineffective with age, however, senescent cells accumulate and this is accompanied by persistent localised secretion of the SASP. This results in long-term changes within the tissue microenvironment, disruption of cellular and tissue functions and creates a pro-tumoural chemotherapy resistant environment (38). (Figure 1.2.)

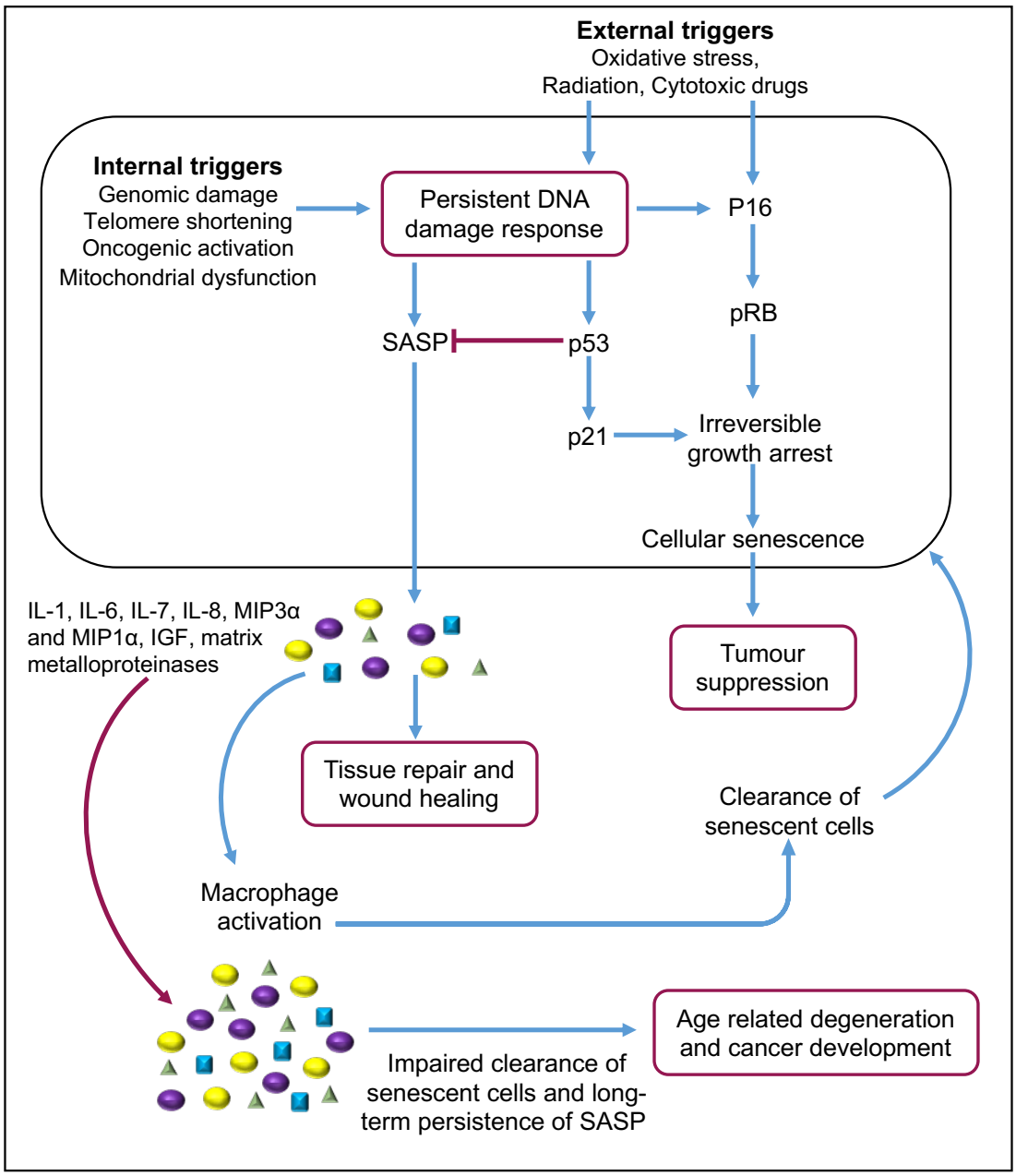

Figure 1.2. Triggers and consequences of cellular senescence
A number of internal and external triggers can lead to persistent DNA damage response (DDR), which promotes expression p21, through p53, and p16. In addition, p16 can be activated directly by some triggers in the absence of persistent DDR. p21 and p16 (through retinoblastoma protein pRB) arrest cell cycle progression and induce cellular senescence. The SASP is produced in response to persistent DDR. In the short-term favourable consequences of senescence, including tumour suppression and tissue repair, are seen and the SASP results in macrophage activation to promote the clearance of senescent cells. If this clearance is impaired, senescent cells accumulate, the SASP persist and detrimental consequences are seen in age related disease and tumour development.

It is clear that the senescent phenotype evolved as a protective mechanism. The same tumour suppressor pathways that drive it are also the initiating components that ultimately lead to apoptosis of a cell and it is not fully understood exactly how the cell's fate is determined. A number of factors have been implicated and there appears to be a fine balance that can shift the cell's fate from apoptosis to senescence. These include the cell type and the tissue microenvironment, as well as the degree of stress, such as the dose of a cytotoxic drug or the balance of pro-apoptotic and anti-apoptotic signals (39-41). Importantly once a cell commits to the senescent phenotype it becomes protected from pro-apoptotic stimuli through over-expression of the anti-apoptotic proteins such as BCL-XL and BCL-W (42). As a result, it becomes more difficult to eliminate these cells.

1.1.2. The BCL-2 family of proteins

The BCL-2 family of proteins are major regulators of apoptosis and are grouped into pro-apoptotic and anti-apoptotic proteins. These are structurally similar globular proteins, composed of α-helices and 1-4 conserved BCL-2 homology (BH) domains. In addition, many of them also contain a hydrophobic transmembrane anchoring domain which allows them to localise to intracellular membranes (43). Pro-apoptotic proteins include BAD, BID, BIK, BIM, HRK, NOXA, BAX, BAK and BOK. Of these, BAX, BAK and BOK are multidomain, pore-forming proteins containing BH 1-4, whilst the remaining only contain the BH3 domain. The anti-apoptotic proteins, including BCL-2, BCL-XL, BCL-W and MCL-1, contain all 4 BH domains (44). When all 4 domains are present this creates a highly conserved tertiary structure with a hydrophobic BH3 binding groove that allows the binding of other BCL-2 family members. Thus, these proteins interact to regulate the mitochondrial outer membrane permeability (MOMP) and the balance of expression of the different protein groups determines the cell fate (44). There are a number of theories of exactly how these proteins interact and this is likely influenced by the concentration of each protein group present as well as their relative binding affinities (45). The BH3 only pro-apoptotic proteins sense cellular stress and not only activate the pore-forming pro-apoptotic proteins but can also bind the

anti-apoptotic proteins to inhibit their function. Once activated BAX, BAK and BOK form pores in the mitochondrial outer membrane causing the release of pro-apoptotic factors such as cytochrome c and, eventually, cell death (46). The anti-apoptotic proteins, on the other hand, inhibit both the BH3 only proteins, as well as pore formation and MOMP (Figure 1.3.A). As there is bi-directional communication and competitive binding between these two groups of proteins, a fine balance is created, which is regulated by numerous signalling pathways which respond to external and internal changes and stress signals.

If this balance is disrupted, cell death may be prevented even in the presence of cellular stress or DNA damage, as is seen in senescent cells as well as in malignancies where the anti-apoptotic proteins are often over-expressed (Figure 1.3.B) (42). Whilst this evolved as a protective mechanism in senescent cells, in malignancies it gives tumour cells a survival advantage and can promote chemotherapy resistance. The over-expression of anti-apoptotic proteins, particularly BCL-2 was first described in follicular lymphoma (47) but is also seen in chronic lymphocytic leukaemia (CLL), acute lymphoblastic leukaemia (ALL), acute myeloid leukaemia (AML) as well as many other malignancies (47-50). In addition, many malignant cells carry mutations of pro-apoptotic proteins impairing their function (51). In order to directly counteract these pro-tumoural changes, drugs have been developed to target and inhibit the anti-apoptotic proteins. An example currently used in clinical practice is the BCL-2 inhibitor venetoclax, which is currently licenced for the treatment of CLL and AML (52, 53).

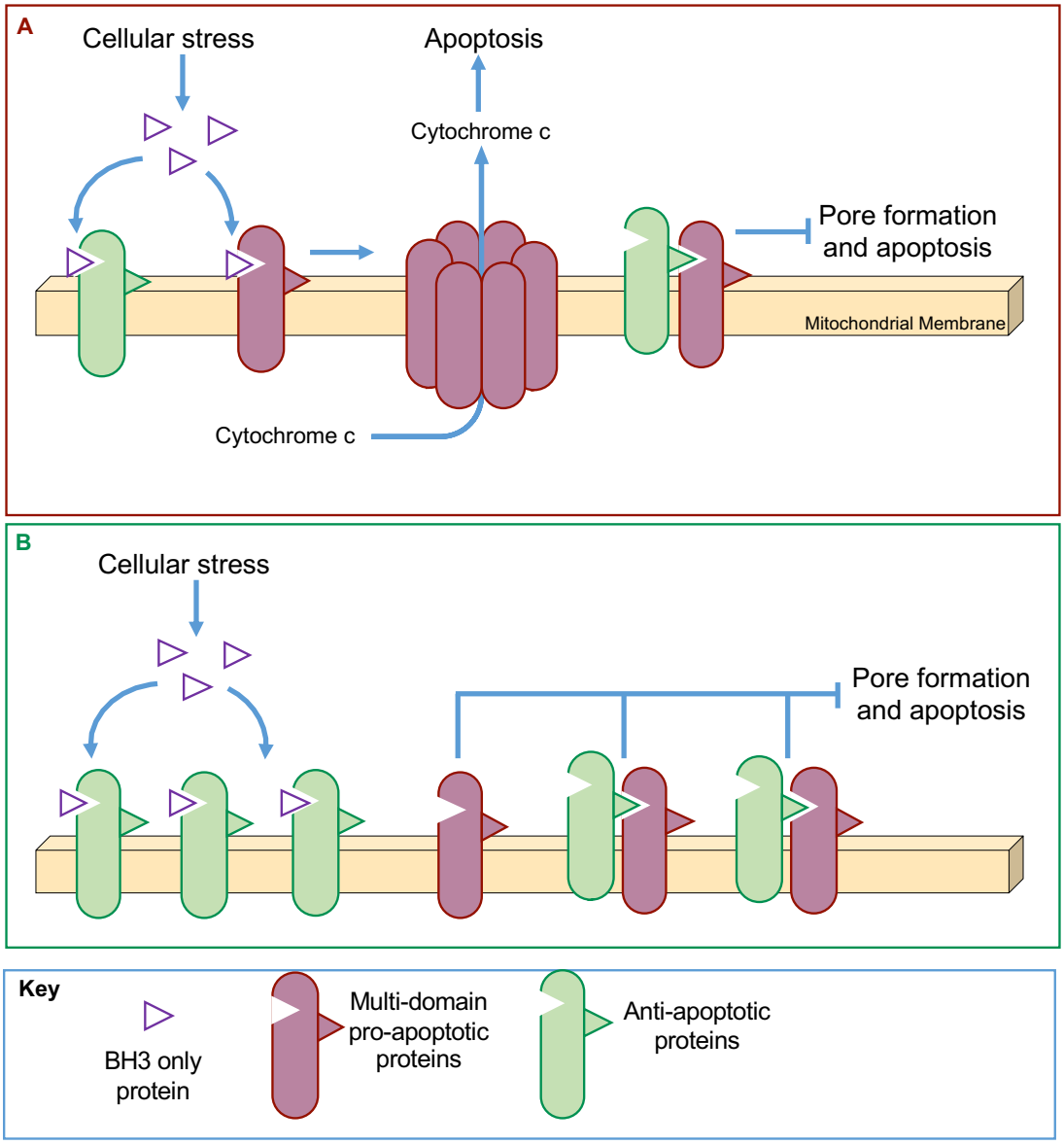

Figure 1.3.The BCL-2 family proteins

(A) Shows the potential interactions between the 3 groups of proteins. BH3 only proteins (triangles) are activated by cellular stress and competitively bind the multi-domain pro-apoptotic (red) and anti-apoptotic proteins (green) to activate or inhibit them respectively. Any BH3 only proteins bound to anti-apoptotic proteins are sequestered and can therefore no longer activate the pro-apoptotic proteins. In addition, anti-apoptotic proteins can bind the multi-domain pro-apoptotic proteins directly and inhibit pore formation and therefore apoptosis. (B) When the anti-apoptotic proteins are over-expressed, more BH3 only proteins are sequestered and cannot activate the pro-apoptotic proteins to drive pore formation. There is also increased direct inhibition of the multi-domain pro-apoptotic proteins.

1.1.3. Senolytics

As the evidence for the adverse impact of the accumulation senescent cells in ageing increases, attention has turned to the possibility of targeting senescent cells in tissues in order to reduce or reverse their effect on tissue function. Whilst various animal models have been developed to study the selective depletion of senescent cells (54, 55), the search for an agent that is selective for senescent cells and safe for use in humans has proven far more difficult (56). Initially, drugs were designed to target single molecules, such as the anti-apoptotic BCL-2 proteins. ABT-263, for example is a potent inhibitor of BCL-2, BCL-XL and BCL-W. In vivo studies have demonstrated that it can selectively deplete senescent cells in mice (57) and it has been widely used to study the impact of the depletion of senescent cells on tissues and different cellular components (58-60). In the BM treatment with ABT-263 was shown to allow recovery of haematopoietic stem cells (HSCs) and the haematopoietic system (57), although it remains unclear whether this is due to a direct effect on HSCs or due to changes in the HSC niche. However, ABT-263 and other compounds targeting single molecules, for example p53, are likely to have a much broader mode of action and have been shown to affect platelets and immune cells in addition to their senolytic activity (61-63). In particular it has been shown that ABT-263 causes severe thrombocytopenia, as platelets rely on BCL-XL to function, and this has limited its clinical use (64, 65). It is becoming increasingly evident that the pathways that drive senescence, and therefore the molecules that regulate these, are not unique to senescent cells. Consequently, any drugs targeting these single molecules, including receptors or enzymes, will have off-target effects, which could be detrimental to normal tissue function and cause significant side effects.

Newer models have instead looked to target multiple anti-apoptotic pathways in the senescent cells to increase the specificity of drugs for senescent cells (62). Two drugs have been identified; dasatinib, a tyrosine kinase inhibitor already in clinical use for the treatment of chronic myeloid leukaemia (CML), which promotes apoptosis; and quercetin, a naturally occurring flavonoid, which targets multiple components of the anti-apoptotic pathways including

BCL-XL and hypoxia-inducible factor (HIF)1α (62). Data from initial phase 1 clinical trials shows that this drug combination can reduce senescent cell burden in diabetic kidney disease (66) and may improve tissue function in idiopathic pulmonary fibrosis (67). Further trials are ongoing to investigate the role of senolytics in these conditions as well age related frailty, dementia osteoarthritis and management of accelerated ageing phenotypes observed in survivors of haematopoietic stem cell transplants or childhood cancers (62). Whilst more information is required to determine the effectiveness and safety of these drugs, as well as to identify the appropriate clinical settings for their use, it is possible that they may add to treatments in the future and may contribute to reducing age-related morbidity.

Other drugs, described as senomorphics, target one or more components of the SASP and therefore aim to reduce the pro-inflammatory effect associated with the accumulation of senescent cells. Examples include rapamycin and other naturally occurring compounds which suppress the SASP and have anti-oxidant activities (68, 69), as well as a number of drugs already in clinical use for other conditions. Clinical trials are currently ongoing to determine if treatment with metformin, a drug currently used for the treatment of type 2 diabetes, can reduce the impact of ageing and senescence (70). It has been shown to target NF-κB to inhibit a number of SASP components (71) and also reduces production of reactive oxygen species (ROS) and resulting DNA damage (72) as well as directly protecting cells from the senescent state (73). Other drugs such as ruxolitinib and glucocorticoids have also been shown to reduce the SASP and its effects on tissue function. Thus, initial data suggest that it may be possible not only to target senescent cells but also the resulting SASP and its effects. However, the practical applications of these findings and the extent to which these drugs can be used to reduce the systemic effects of ageing have not yet been determined.

1.1.4. *In vivo* models of ageing

In order to fully understand the complex interaction between cells within a tissue in both health and disease *in vivo* models are needed. To study senescence, it must first be induced in the tissue of interest. This can be done by allowing physiological ageing to take place or through chemotherapy agents or irradiation (57, 74). C57Bl/6 mice, a commonly used strain for in vivo work, are considered to be mature adults around 3-6 months, middle aged from 10-14 months and old at 18-24 months, with the estimated human equivalent ages of 20-30, 38-47 and 56-69 respectively (75).

A number of mouse models have been developed to study senescence *in vivo.* These vary in complexity and use different mechanisms to visualise or eliminate senescent cells. Most of these models rely on the same principle: Senescent cells express p16 and the p16 promotor is therefore used to promote the expression of a reporter gene by transgenic or knock in approaches (76). Moreover, the use of fluorescent tags makes it possible to identify senescent cells *ex vivo* (54), whilst incorporation of luciferase allows *in vivo* imaging of senescent cells using bioluminescence (77, 78) and further models allow the selective depletion of senescent cells following administration of a drug (54, 55). One model that combines all of these attributes is the p16-3MR model, developed by the Campisi group. In this transgenic mouse model, the p16 promotor drives the expression of a 3 modality reporter gene consisting of renilla luciferase, red fluorescent protein (RFP) and the herpes simplex virus thymidine kinase (HSV-TK). Each of these components has their own function, which helps to facilitate the study of senescent cells (Figure 1.4.). Renilla luciferase allows in vivo imaging of senescent cells when activated by luciferin and RFP can be used to isolate, image and quantify of senescent cells *ex vivo*. Finally, HSV-TK allows selective depletion of senescent cells using the pro-drug ganciclovir (GCV). GCV is a nucleoside analogue and has a high affinity for HSV-TK but a low affinity for cellular TK. It therefore specifically targets cells expressing HSV-TK, where it becomes phosphorylated, is converted into a DNA chain terminator and causes cell death by apoptosis (21). However, despite the

many functions and therefore applications of this model, it does have some limitations. Both the renilla luciferase and RFP have relatively low signals. This can make it difficult to detect the RFP signal *ex vivo* and it is not possible to detect the renilla signal in deep tissues, including the bone marrow (BM), *in vivo.* The p16-tdTom model, in contrast, is a knock-in model in which the p16INK4a promotor activates the ultrabright fluorochrome tandem dimer Tomato (tdTom). As the tdTom signal is greater this model was designed to make it easier to isolate, analyse and characterise senescent cells *ex vivo* (76). However, in this model it is not possible to eliminate senescent cells in vivo and this is an important function of the p16-3MR model. By being able to selectively deplete senescent cells it is possible to directly study the impact of senescent cells on tissue function and how their elimination affects tissue health and response to diseases, including malignancies (21, 25, 26, 55). Recently a similar mouse model to the p16-3MR model was developed but instead of using the $p16^{INK41}$ promoter it uses p21 (79). This model allows monitoring, imaging sorting and elimination of senescent cells and may allow the characterisation of distinct senescent cell populations which are known to be heterogenous and express varying levels of p16 and p21.

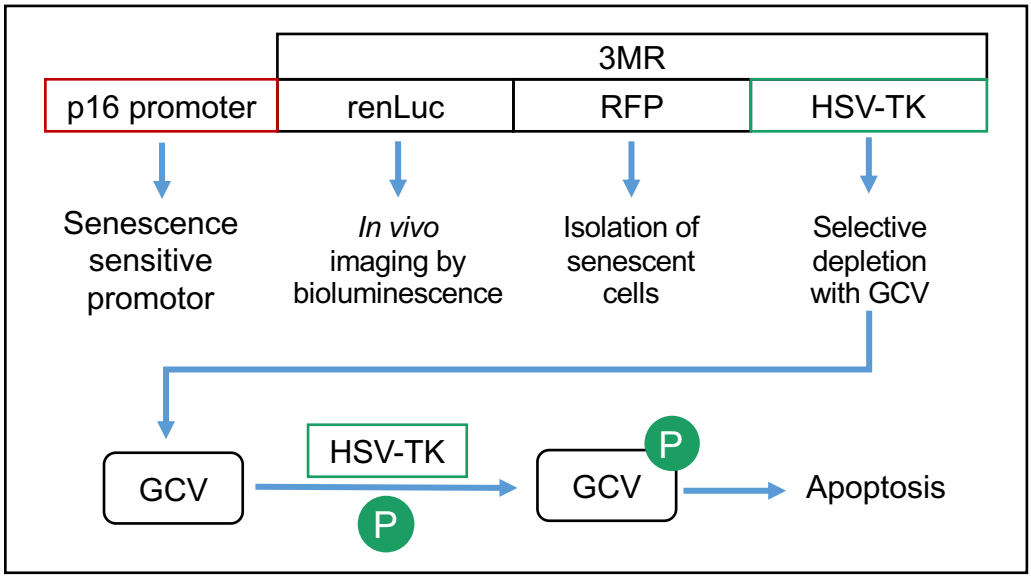

Figure 1.4. p16-3MR mouse model
The p16 promotor drives expression of the three-modality reporter (3MR) gene, including renilla luciferase (renLuc), red fluorescent protein (RFP) and herpes simplex virus thymidine kinase (HSV-TK). HSV-TK phosphorylates the pro-drug ganciclovir (GCV), which becomes a DNA chain terminator and causes apoptosis. (Adapted from Demaria et al 2014 (21))

1.2. The Bone Marrow

The bone marrow (BM) is a complex organ comprising of blood vessels, nerve tissue and a heterogenous population of cells. It can broadly be divided into red marrow, the primary site of haematopoiesis in adults, and yellow marrow, which is mostly composed of adipocytes and provides an important energy source during periods of starvation (80). Whilst in children all marrow is composed of red marrow, this is gradually replaced by yellow marrow with increasing age (81). The different cellular components of the red marrow are either directly involved in blood cell production or are part of the supportive network of cells that facilitate and regulate this (80, 82). Together these components ensure tight regulation and balanced production of mature blood cells.

1.2.1. Haematopoiesis

Haematopoiesis is the process of blood cell production and differentiation, from haematopoietic stem cells (HSCs) to haematopoietic progenitor cells (HPCs), to mature blood cells. Homeostatic mechanisms are in place to ensure a constant steady supply of mature cells to maintain stable counts of these cells in the circulating blood (83). The BM is the most regenerative tissues in the human body (84), producing, on average, 500 billion blood cells daily, including around 200 billion red blood cells, 100 billion white blood cells and 150 billion platelets (85, 86). This production can increase vastly in response to stress, such as infection, inflammation or bleeding. It is, therefore, important that the process is well regulated, can easily adapt to change and is sustainable for the entire lifespan.

The site of blood cell production changes during development. During foetal development haematopoiesis initially occurs in the yolk sac, later in the liver, spleen and placenta and from 5 months onwards also in the BM. After birth, haematopoiesis in the liver stops and the BM becomes the primary site of haematopoiesis, although the spleen and thymus maintain some haematopoietic function (87, 88). During childhood there is a progressive

replacement of BM with fat, particularly in the long bones and in adults most haematopoiesis occurs in the vertebrae, ribs, sternum, skull, sacrum, pelvis and proximal femur (81). However, it is possible for all previous sites of haematopoiesis to revert to this function, for example in BM diseases such as myelofibrosis where haematopoiesis within the BM is impaired (89).

1.2.2. Haematopoietic stem cells

HSCs are the source of all mature blood cells in the circulation, they are defined by their multipotent nature and their ability to self-renew. In mice, HSCs are defined by the expression or absence of specific cell surface markers – they are recognised to be Lineage negative (Lin-), Sca1+, cKit+, CD150+ and CD48- (Figure 1.5A) (90, 91). Traditionally HSCs were considered to be at the apex of a hierarchical model of gradual loss of self-renewal ability and differentiation. Long term (LT) HSCs, which are CD34- are unique in their self-renewal ability and full long-term reconstitution capacity (92). Short term (ST) HSCs, defined by the expression of CD34, and more recently identified intermediate (IT) HSCs on the other hand have reduced reconstitution ability but maintain their multipotent state (93, 94). There is, however, increasing evidence that HSC populations are far more heterogenous than this simple classification would suggest, and further sub-groups have been described and may also be identified in the future (95, 96). Data from single cell transcriptomics supports a more continuous model of lineage commitment and differentiation (Figure 1.5D) (92). In particular it is possible that subsets of LT-HSCs have a bias towards a particular lineage and may preferentially promote the production of specific mature blood cells (97).

1.2.3. Haematopoietic Progenitor cells

Multipotent progenitor cells (MPPs), which originate directly from the ST-HSCs, have no self-renewal capacity but remain multipotent. They differentiate further into common myeloid or common lymphoid progenitors (CMPs and CLPs). From this point the cell fate and eventual lineage of the

mature cell becomes more limited (Figure 1.5B). Common lymphoid progenitors give rise to mature lymphoid cells including B cells, T cells and natural killer (NK) cells. Common myeloid progenitors, on the other hand, differentiate further into megakaryocyte erythroid progenitors (MEPs), which produce red blood cells and megakaryocytes, and granulocyte macrophage progenitors (GMPs), which will give rise to granulocytes and monocytes (Figure 1.5C).

The process of HSC and HPC production and differentiation and the eventual cell fate is regulated by haematopoietic growth factors and cytokines, which stimulate survival and differentiation of certain cell lineages through interaction with specific receptors on the target cells. They can target cells at different stages of differentiation, for example stem cell factor (SCF) and Flt-3 ligand (FLT-3) act directly on the HSC (98, 99), interleukin (IL) 3 and granulocyte-macrophage colony stimulating factor (GM-CSF) are multipotential growth factors that act on the multipotent HPCs and support the growth of cells of different lineages (100), whilst granulocyte colony stimulating factor (G-CSF) and erythropoietin (EPO) are more specific and drive selective production of granulocytes and red cells respectively (100, 101). Thrombopoietin (TPO) is unique in its role, as it primarily regulates megakaryocyte and platelet development, but at the same time has a direct regulatory role on HSC development and maintenance (99, 102), which has been shown to express the TPO receptor Mpl (103). All these growth factors interact and work together to maintain a pool of HSCs and progenitors as well as a steady supply of mature blood cells and to drive differentiation of specific lineages in response to stress.

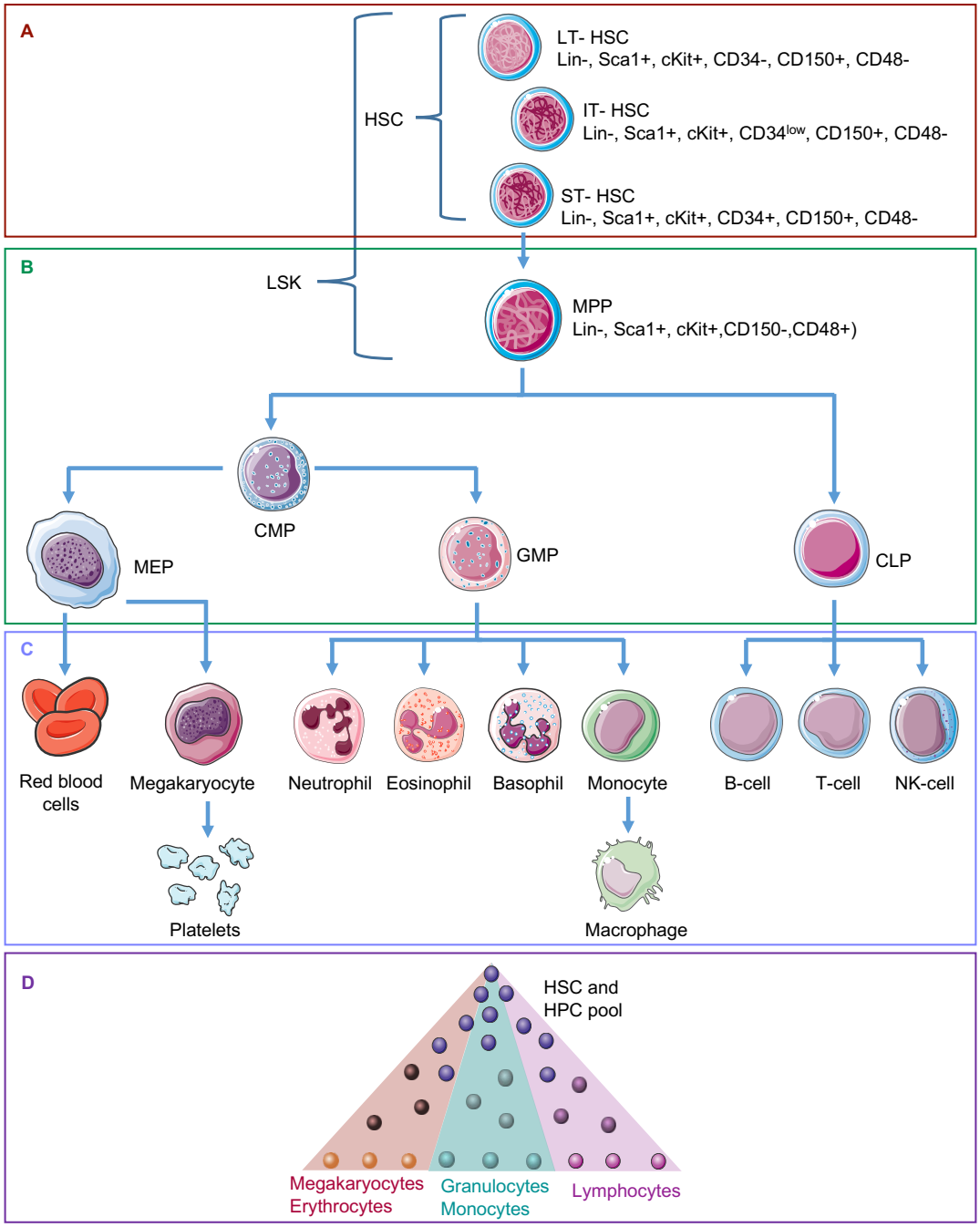

Figure 1.5. Hierarchical and continuous model of haematopoiesis
(A) Haematopoietic stem cells (HSC) are pluripotent and are classed as long-term (LT) or short term (ST) HSCs. Together with the multipotent progenitor cells (MPP) they form the LSK populations (Lin-, Sca1+, cKit+). (B) The haematopoietic progenitor cells (HPCs) are shown. MPPs differentiate into common myeloid progenitors (CMP) and common lymphoid progenitors (CLP). CMPs differentiate further into megakaryocyte erythroid progenitors (MEP) and granulocyte macrophage progenitors (GMP). (C) Mature blood cells produced include red blood cells, megakaryocytes, platelets, mature granulocytes (neutrophils, eosinophils and basophils), monocytes, macrophages B cells, T cells and NK cells. (D) The continuous model of haematopoiesis is shown, with no defined stages of differentiation and a gradual acquisition of lineage bias.

1.2.4. Mature blood cell components

Each mature blood cell has its specific role and reliable supplies are required for the healthy functioning of the human body. Red blood cells make up 84% of all cells in the human body (104), their main role is to transport oxygen and carbon dioxide between the lungs and all other tissues (105) and they are therefore vital for organs to function normally. Megakaryocytes primarily reside in the BM but can also be found in the lung and peripheral blood and are responsible for the production of platelets (106). Platelets circulate in the peripheral blood for 5-7 days and become activated following vascular insults or injury and have a key role in regulating haemostasis and thrombosis (107). However, it is becoming increasingly evident that they have a number of other functions, including as immune modulators, contributing to the innate immune response and tumour surveillance (108, 109). White blood cells are a diverse group of cells, including lymphocytes (B cells, T cells and NK cells), monocytes, which can further differentiate into macrophages, and granulocytes (neutrophils, basophils and eosinophils). Granulocytes and monocytes are key to the immediate innate immune response, they are involved in pathogen detection, driving inflammation, phagocytosis and antigen presentation (110-112). Lymphocytes on the other hand are the main effectors of the adaptive immune system, they are involved in antibody production and secretion, recognition of antigens presented to them by antigen presenting cells and are able to generate immune memory (113, 114).

1.2.5. Macrophages

Macrophages form part of the innate immune system and have an important role in tissue development, homeostasis and inflammation. They respond to a diverse range of stimuli and have many different functions including killing and controlling pathogens and promoting tissue repair and remodelling. Due to this wide range of functions the macrophage phenotype can be extremely variable and is influence by the tissue of origin of the macrophage, the local tissue microenvironment and stress signals. Importantly, it is possible for

macrophages to switch from one functional phenotype to another depending on these external factors (115).

Blood monocytes are derived from HSCs in the BM and can differentiate into BM, lymph node and splenic macrophages as well as dendritic cells. In addition, they migrate to certain tissues including the intestine, dermis and heart and differentiate to constantly replenish the tissue specific macrophage population (116-118). Other tissue specific macrophages originate from the embryonic yolk sac progenitor cells. These include microglia, which differentiate from yolk sac macrophages and lung alveolar macrophages, Langerhans cells and liver Kupffer cells which primarily arise from foetal liver monocytes (115). There is now increasing evidence that blood monocytes do not significantly contribute to the populations of these tissue specific macrophages in the steady state, but monocytes are able to migrate to these tissues and differentiate into tissue specific macrophages in response to inflammation (119).

1.2.6. The Bone Marrow Microenvironment

HSCs and HPCs reside in a highly specialised niche within the BM and their microenvironment is vital for the regulation of HSC maintenance, normal haematopoiesis and the haematopoietic response to stress. In addition to the haematopoietic cells, a number of supportive cells reside in the BM niche (Figure 1.6). These include multipotent mesenchymal stem and progenitor cells, which can differentiate into BM stromal cells (BMSCs), osteoblasts, adipocytes, endothelial cells, myocytes and chondrocytes (120-122). The mesenchymal cells have fibroblastic characteristics and have historically been difficult to distinguish from BMSCs, also sometimes called mesenchymal stromal cells (123). Similar cell surface markers have been described in the two populations, with absence of CD45, Ter119 and CD31 and expression of CD105 (121, 122, 124). However, whilst they may have some functional overlap, the mesenchymal stem cells are clearly set apart by their ability to self-renew and differentiate, and some distinguishing markers including CD140a have been identified (91, 122, 123, 125). BMSCs, on the other hand,

have immunomodulator and secretor functions and directly interact with HSCs through the secretion of chemokines and cytokines to regulate their maintenance and differentiation (125).

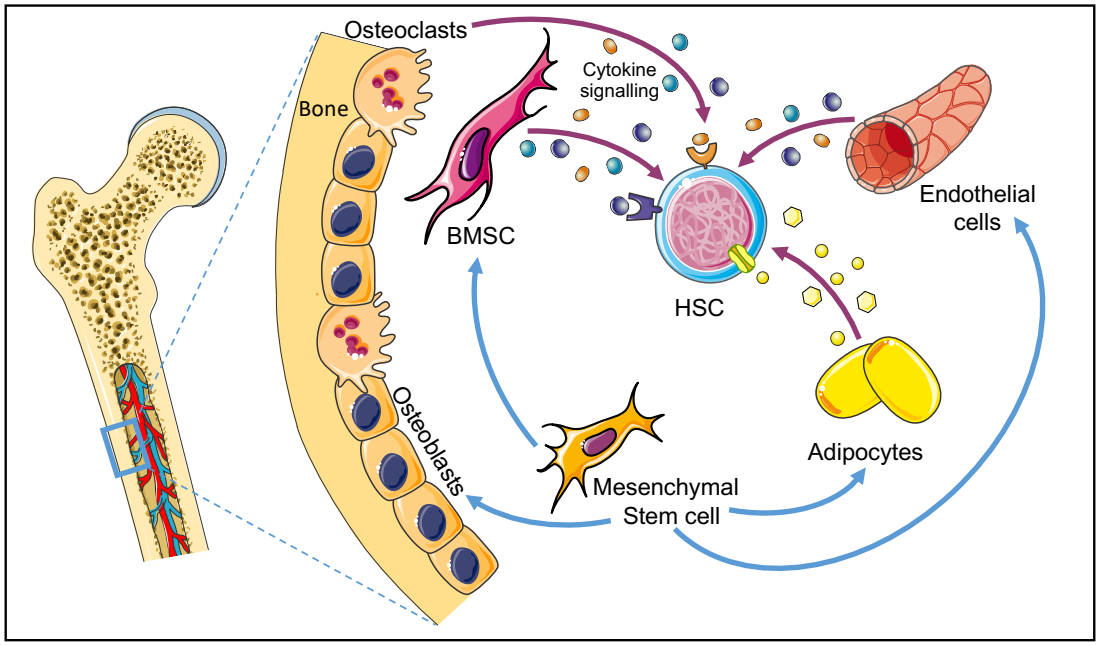

Figure 1.6. The bone marrow microenvironment
Haematopoietic stem cells (HSCs) reside in a specialised niche surrounded by supporting cells. Mesenchymal stem cells differentiate into bone marrow stromal cells (BMSCs), osteoblasts, adipocytes and endothelial cells (blue arrows). These cells, as well as osteoclasts interact with the HSCs through cytokines, chemokines, growth factors and adipokines (red arrows).

Osteoblasts and osteoclasts, which are derived from the monocyte lineage, are primarily involved in bone formation and resorption, respectively (126, 127). Although osteoblasts have no direct role in haematopoiesis, osteoclasts have been shown to be involved in HSC homing (128). Furthermore, as these osteolineage cells reside in the same microenvironment as HSC and HPCs the two processes of haematopoiesis and bone formation are undoubtedly linked and disruption or dysregulation of one can directly impact the other.

Another key component of the BM microenvironment is the adipose tissue. Adipocytes are derived from mesenchymal stromal cells and are an important source of energy as their main role is to store triglycerides, which can be

broken down into free fatty acids and glycerol during lipolysis (120). As well as maintaining and regulating the BM metabolism, adipocytes also have important endocrine functions (129). They have been shown to secrete a number of regulatory adipokines and chemokines, which contribute to the regulation of haematopoietic cell expansion and differentiation (130, 131). The proportion of adipose tissue in the BM gradually increases with age, reaching approximately 70% by the age of 70 (132). The expansion of adipose tissue either as a result of ageing, or following chemotherapy or irradiation, has been associated with impaired haematopoiesis, HSC function and an inability of the BM to recover and repopulate (133-135).

Both quiescent and cycling HSCs have been shown to preferentially reside in the perivascular and sinusoidal niche within the BM (136, 137). This places them in close proximity to endothelial cells and perivascular cells, including pericytes, and vascular smooth muscle cells, which surround the inner endothelial lining of blood vessels (138). Thus, the perivascular cells form the interface between the circulating blood and the BM and are involved in regulating HSC homing and cell trafficking to and from the BM (125, 139). Furthermore, endothelial cells have been shown to directly regulate HSC and HPC differentiation and blood cell production through the secretion of G-CSF, GM-CSF and IL-6 (139).

1.3. Ageing in the Bone Marrow

1.3.1. Haematopoiesis

The normal function of the BM depends on careful regulation and interaction of both haematopoietic cells and the supporting cells of the BM microenvironment. This becomes somewhat disrupted with age and whilst normal haematopoiesis usually continues, a number of changes have been observed in the aged BM. In aged mice, genes associated with inflammation and stress responses have been shown to be upregulated in HSCs, the self-renewal and long-term repopulation ability of HSCs is reduced and a skewing towards the myeloid lineage is observed (57, 140-142). Whether these changes occur due to intrinsic changes in the HSC, HPCs or the BM microenvironment remains to be determined. There is evidence that whilst HSCs have the self-renewal potential that gives them the status of a stem cell, this may not be unlimited and become restricted with increasing age (143). The ageing of HSCs appears to be driven by the number of divisions they have undergone and in mice changes in HSC regenerative potential and progeny production are observed after only five cell divisions (144). Overall, these changes result in impaired function of the HSC, dysregulation of normal haematopoiesis and therefore have an impact on the function of the immune system and immunosurveillance (145). This process, known as immunosenescence, has been associated with age-related conditions including infections, autoimmune disease and solid tumours (141, 146). Furthermore, the changes within in the BM niche may contribute to the development of age-related BM diseases such as leukaemia, myeloma and myelodysplastic syndrome (MDS) (147-149). Thus, the changes observed with ageing in the BM microenvironment and the HSC and HPC populations have significant health implications for our ageing population and a better understanding of these changes and of the interactions between the different components of the BM may help to improve the care of these patients.

1.3.2. Clearance of senescent cells

The impact of ageing on the BM and normal haematopoiesis in turn contributes to systemic ageing as it directly affects the function of the cells responsible for the clearance of senescent cells, the macrophages (150). The inflammation resulting from the SASP has been shown to promote macrophage migration and macrophage mediated clearance of senescent cells (151). This is essential to maintain tissue function and, in turn, helps to limit the inflammation and damage caused by the SASP (152, 153). However, macrophages themselves are not immune to the impact of ageing and the influence of the SASP. They have been shown to develop an altered phenotype and function with ageing (154) and the SASP has been shown to influence the polarisation of macrophages (30, 155, 156).

Macrophages have historically been classified into M1 and M2 macrophages (157) and whilst there is now an understanding that this binary classification may not be sufficient to incorporate all the complexities of macrophage subtypes, it remains a useful tool to understand their basic function and response to stress. M1 macrophages, also known as classically activated macrophages, are stimulated by LPS and interferon-gamma (INF-ɣ), they produce inflammatory mediators such as IL6, ROS and nitric oxide and have an anti-microbial and tumoricidal function (158). M2 macrophages or alternatively activated macrophages, on the other hand, are stimulated by IL4 and IL13 and typically secrete transforming growth factor beta (TGF-ß), IL10, arginase and metalloproteases. They have increased phagocytic activity, promote angiogenesis and tissue repair and are immunosuppressive and pro-tumoural (158).

In a senescent environment, macrophages have been shown to predominately express M2-like characteristics (155, 156, 159). This in turn affects the immunosurveillance function of macrophages, contributes to immunosenescence (160) and impairs the effective clearance of senescent cells. Thus, macrophage function diminishes with age both due to intrinsic changes and the impact of the ageing microenvironment of the BM and other

tissues (161). The interaction between senescent cells and macrophages is clearly complex and bi-directional, with each group of cells affecting the other. A better understanding of this relationship may help to identify targets to promote the clearance of senescent cells and reduce the damaging effects of the SASP on tissue function.

1.4. Age-related Bone Marrow Diseases

1.4.1. Clonal Haematopoiesis

The self-renewal capacity and the high replicative potential of HSCs, whilst needed for the function to steadily replenish circulating blood cells and respond to stress, also makes HSCs vulnerable to oncogenic changes (162). Mutations arising in HSCs or HPCs are passed down to all daughter cells and can therefore be detected in circulating mature blood cells. Clonal cell populations are present in most adults and this in itself does not directly correlate with overt pathology (163). However, if the mutation in the HSC or HPC confers a survival advantage, this can lead to an expansion of this clonal cell population and could indicate a pre-malignant state, as is the case in monoclonal gammopathy of undetermined significance (MGUS) and clonal haematopoiesis of intermediate potential (CHIP). MGUS is characterised by the clonal expansion of plasma cells and it often remains a stable asymptomatic condition that does not require treatment. However, acquisition of additional mutations will lead to progression to myeloma in 1% of patients a year, on average (164, 165).

CHIP is defined by the presence of a clone with variant frequency ≥ 2% and is present in 10% of adults over the age of 70 (166, 167). The most common somatic mutations shown to trigger CHIP occur in the DNM3TA, TET2 and ASXL1 genes and skewed X chromosome inactivation has been identified as a trigger (61, 168). Similarly to MGUS, many patients with CHIP remain asymptomatic, however there is a significant risk (0.5-1% per year) of transformation to haematological malignancies, including myeloproliferative disorders, MDS and AML (169). In addition, CHIP has been associated with other age-related pathologies, including cardiovascular disease, even in the absence of any haematological disorders (170, 171). Conversely, it has been suggested that clonal haematopoiesis may reduce the risk of Alzheimer's disease (172) and the presence of clonal haematopoiesis in the BM of stem cell donors was associated with increased rates of graft-versus host disease and reduced relapse rates (173, 174). It has therefore been hypothesised that

clonal haematopoiesis alters normal BM function and blood cell development, resulting in altered function and immunosurveillance and contributing to the systemic chronic inflammation observed with ageing (175). However, the exact mechanism of how individual mutations drive clonal haematopoiesis and, eventually, pathological changes remain unclear. This makes it difficult to risk-stratify patients and ensure appropriate monitoring to allow early diagnosis and treatment. One approach has been to determine clone size and fitness, the proliferative advantage a cell carrying the mutation in question has over other cells (176, 177). This could help predict future clonal expansion and progression to overt disease phenotypes (178) and therefore identify patients at greater risk, who require closer monitoring and follow up. Furthermore, studies using mouse models of clonal haematopoiesis, suggest that it may be possible to manipulate clone fitness and to reduce disease development whilst maintaining potential benefits associated with clonal haematopoiesis (179).

1.4.2. Haematological malignancies

Haematological malignancies are a heterogenous group of diseases that together are the fifth most common cancer group in the UK and generally increase in incidence with increasing age (180, 181). Broadly, they can be divided into malignancies derived from cells originating in the BM, including leukaemias and multiple myeloma, and those originating in the lymphoid tissue (Hodgkin and non-Hodgkin lymphomas) (182). They have been at the forefront of understanding the molecular basis of tumour development (183), as well as the implementation of targeted and immunotherapy-based treatment approaches (184). As a result, the prognosis for some haematological malignancies has significantly improved in the last 30 years, including non-Hodgkin lymphoma, especially due to the addition of rituximab to standard chemotherapy regimens (185, 186) and, perhaps most strikingly, CML since the introduction of targeted therapy with tyrosine kinase inhibitors (187-190). Notably, these are both examples where targeted treatments improved outcomes for patients irrespective of age (191, 192). In contrast other haematological malignancies, particularly AML, remain difficult to treat and the prognosis for older patients is usually significantly worse (180, 192). This

highlights the ongoing need to better understand disease development and, in particular, the interplay between ageing, disease pathogenesis and treatment tolerance and effectiveness.

1.4.3. Acute Myeloid Leukaemia

Acute myeloid leukaemia (AML) is primarily a disease of the elderly. It most commonly presents in patients over the age of 65 and has a peak incidence between the ages of 80 and 85 (193). Despite improved understanding of the disease biology, treatments have changed very little over the last 50 years and whilst some more targeted treatments have been developed, the backbone of treatment remains cytotoxic chemotherapy (194). Overall, the prognosis for patients diagnosed with AML remains poor, in part due to the fact that many of the older patients are unable to tolerate the intensive cytotoxic chemotherapy regimens recommended as first line treatments and achieving complete remission in these patients can therefore be difficult. However, even in young, fit patients who tolerate these treatments and achieve remission, treatment resistance and relapse are common and often occurs from minimal residual disease sequestered in the BM (195, 196). It appears that the BM niche adapts to hosting leukaemic cells and promotes treatment resistance and relapse (25).

1.4.3.1. Acute Myeloid Leukaemia Pathogenesis

AML is usually defined by the presence of more than 20% immature myeloid blast cells in the BM, or more than 10% blasts when certain characteristic cytogenetic or molecular abnormalities are also present (197, 198). It can be sub-classified further based on immunophenotypic markers that can help differentiate between granulocytic, monocytic, megakaryocytic and erythroid lineages or undifferentiated precursors. In contrast to solid malignancies, only a small number of mutations are required for the leukaemic transformation with an average of only 13 mutations present in AML blasts (199, 200). A two-hit model of leukaemogenesis, in which two classes of mutation collaborate to create the leukaemic blast, has been described (201). Class I mutations

include FLT-3, KIT and N-RAS gene mutations and confer a survival and proliferative advantage to the leukaemic blast. Class II mutations result in the inhibition of normal haematopoietic differentiation and apoptosis, they are often chromosomal translocations which produce fusion genes involving the Promyelocytic leukaemia/retinoic acid receptor alpha (PML-RARA), CEBPA, RUNX1, MLL or NPM1 genes but can also result from mutations within these genes (199, 202). Some of the more recently identified mutations, such as DNMT3A, TET2, IDH1 and IDH2 mutations, have not yet been classified, as the consequence of these mutations is not yet fully understood and they may not directly fit into one of these groups (202). It is likely that, as we continue to better understand the role of these different driver mutations, the classification of mutations in AML will continue to change. The reason for identifying and classifying these mutations is their significant impact on the prognosis for patients with AML. Although age and co-morbidities affect this, by far the most significant variable appear to be the genomic lesions (197). Deletion of chromosome 3q and 5q, monosomies of chromosomes 5 and 7, complex karyotypes and FLT-3 mutations have been associated with a poor prognosis. On the other hand translocation t(15;17)/PML-RARA and translocations involving core binding factor, t(8;21)/RUNX1-RUNX1T1, inversion 16 or translocations (16;16)/CBFB-MYH11 and NPM1 mutations have been associated with a more favourable prognosis (203). The genetic changes within the leukaemic blasts can therefore help to inform treatment decisions and can affect the outcome for patients. An example of a favourable mutation is the translocation between chromosome 15 and 17, t(15;17), which is seen in acute pro-myelocytic leukaemia (APML). In this subtype of AML, the single balanced translocation creates the fusion oncoprotein PML-RARA and this causes an arrest in myeloid differentiation. This can be targeted directly by all-trans retinoic acid (ATRA), which interacts with the PML-RARA fusion protein and rapidly triggers differentiation to granulocytes (204). More recently, the addition of arsenic trioxide to the treatment regimen has improved outcomes further and it is currently considered the only curative targeted cancer therapy (205, 206).

It is clear that AML is an extremely diverse disease. It is possible for multiple clonal populations of cells to develop simultaneously and AML clones have a significant ability to adapt. The evolutionary nature of the disease means that it rapidly adapts to its environment and selects clones that have not been targeted for expansion. Thus, simply targeting one mutation is often not sufficient in treating the disease and treatment resistance is common.

1.4.3.2. Acute Myeloid Leukaemia Treatment

The treatment for AML consists of induction and consolidation phases. Induction most commonly involves two cycles of DA (daunorubicin and cytarabine), although alternative regimens such as FLAG-Ida (fludarabine, high dose cytarabine, idarubicin and G-CSF) can also be used. Consolidation usually consists of further chemotherapy such as intermediate or high dose cytarabine (207, 208) and may also include an allogeneic stem cell transplant (SCT). SCTs are usually considered for patients under the age of 60 with standard or poor risk disease and reduced intensity conditioning allografts can also be considered in some older patients (197, 198). In addition, more targeted treatments have been added to treatment regimens more recently, including gemtuzumab, an anti-CD33 monoclonal antibody, and midostaurin, a FLT-3 inhibitor (194).

These treatment regimens, however, are intense and associated with high morbidity and mortality rates, especially in older, more frail, patients with co-morbidities. Intensive chemotherapy is myelosuppressive and therefore carries a high risk of treatment associated infections and complications of SCTs include infection, graft vs host disease and treatment associated toxicities, which can result in long term morbidity and increased mortality (209). As the peak incidence for AML is 80-85, these treatments are not suitable for many patients. Less intense treatments, including azacytidine or low dose cytarabine in combination with venetoclax, are available and whilst these can reduce tumour volume and improve survival, achieving remission is not possible (198). Furthermore, even these drugs are toxic and associated with morbidity and therefore, for some patients a palliative approach and best

supportive care is the most appropriate option. This highlights the need for a change in the treatment approach for AML. Increasing or changing the dose or combination of cytotoxic drugs will not alter the outcome for the majority of patients who simply cannot tolerate these treatments. Conversely, if we can identify treatment targets and suitable drugs that are tolerated by our older population then these would also benefit the young and improve outcomes for all by improving remission rates and reducing relapse. The future direction of treatments developed will likely include more mutation targeted drugs and immunotherapies including bi-specific T cell engaging antibodies, checkpoint inhibitors and chimeric antigen receptor (CAR) T cells (198). However, another aspect to consider for future treatment development is the BM microenvironment and how AML manipulates this into the pro-tumoral, leukaemia supporting environment.

1.4.3.3. The Leukaemic Microenvironment

It is becoming increasingly evident that AML and other haematological malignancies drive changes in the BM microenvironment and other BM derived cells, including macrophages, endothelial cells, adipocytes and BMSC and that this in turn promotes tumour development, survival and treatment resistance (25, 210-215). In addition, AML impairs normal haematopoietic function by blocking differentiation of normal HSCs, which leads to characteristic cytopaenias often present at diagnosis (216).

AML has been shown to modulate macrophage polarisation to a pro-tumoural M2 phenotype, thus altering their immunosurveillance and phagocytic functions (211). Targeting these changes, through direct induction of the M1 macrophage phenotype (217) or activation of LC3 associated phagocytosis via the stimulator of IFN genes (STING) pathways suppresses AML growth and increases survival in *in vivo* models of AML (218). Furthermore, the interaction between BM endothelial cells and leukemic blasts has been shown to promote AML growth and contribute to chemotherapy resistance (219). Adipose tissue provides a significant source of energy both during normal haematopoiesis and for malignant cells in the BM microenvironment. AML

blasts directly modulate adipocyte metabolism by inducing phosphorylation of lipase to activate lipolysis and facilitate the release of free fatty acids (210). As the adipose content of the BM increases with age, this may contribute to the increased incidence of AML in the older population.

Another factor that may drive AML development in ageing is the accumulation of senescent cells within the BM microenvironment. AML has been shown to induce a senescent phenotype in BMSCs and the secretion of a SASP. Superoxide derived from leukaemic blasts was shown to induce p16INK4a driven senescence in BMSCs and in vivo depletion of senescent cells slows tumour progression and prolongs animal survival (25). The temporal correlation between senescent changes in the BM microenvironment and tumour development remain to be explored further. It is possible that tumour development only occurs once age-associated senescent changes have been initiated or that the senescent changes only occur once malignant clones are present to drive them. Most likely it is combination of both, the BM microenvironment gradually accumulates senescent cells with increasing age, this creates a more favourable environment for any progenitor cells that acquire mutations and become malignant. These malignant cells in turn accelerate the ageing process within the BM microenvironment, impairing immunosurveillance and clearance of both senescent and malignant cells (Figure 1.7) (63).

It is clear that AML does not only directly alter the BM microenvironment, but also benefits from many age-related changes affecting the BM. This may in part explain the less favourable prognosis for older patients diagnosed with AML, which cannot be sufficiently explained by the differences in adverse prognostic factors (220). It also highlights the importance of improving our understanding of both leukaemia driven and age-related changes in the BM microenvironment as these will likely contribute to treatment resistance and disease relapse.

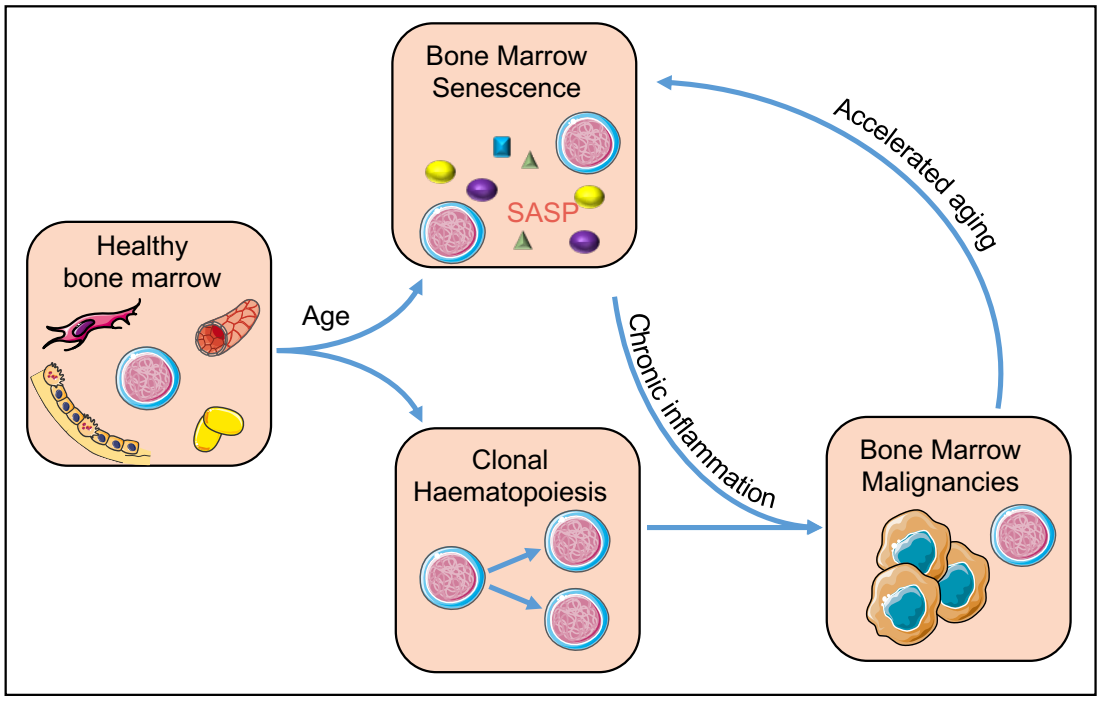

Figure 1.7. Age-related changes in the bone marrow
With increasing age senescent cells accumulate in the BM microenvironment. At the same time changes in the HSCs and HPCs drive clonal haematopoiesis. The senescent changes and secretion of the SASP cause chronic inflammation and create a pro-tumoural microenvironment, and thereby contribute to the progression of clonal haematopoiesis to haematological malignancies. These in turn further accelerate ageing of the BM microenvironment.

1.4.3.4. Chemotherapy induced senescence

When considering the role of senescence in the context of malignancy, it is important to differentiate between the tumour cells themselves and their environment. Whilst it appears that tumour cells thrive in a senescent environment, they themselves continue to actively proliferate and, although they often over-express the anti-apoptotic BCL-2 proteins that are also associated with the senescent phenotype they are not senescent. In fact, inducing senescence in tumour cells can help to impair tumour proliferation and promote immunosurveillance and subsequent clearance of malignant cells (221, 222). This is the mode of action of retinoic acid and arsenic in the treatment of APML: By activating p53 they induce a senescent phenotype in leukaemic cells (206). Several other cytotoxic chemotherapy agents including

daunorubicin have been shown to induce a senescent state. Unfortunately, these are usually non-specific and therefore induce senescence not only in tumour cells but also in non-cancerous cells (74). This, therefore, impacts on the tumour microenvironment, as well as normal tissue health and function and secretion of the SASP has been shown to create a chronic inflammatory state which may contribute to chemotherapy associated side effects (38, 223). As described above, a senescent BM microenvironment can promote tumour growth (25) and it has also been shown that, in solid tumours, depletion of senescent cells within the tumour microenvironment reduces recurrence and metastases (74). It is clear that whilst the desired effect of chemotherapy agents is to induce senescence in malignant cells, it is important to consider the impact they have on the function of normal tissue, as well their potential to actually create a pro-tumoural microenvironment that could support tumour growth, treatment resistance and relapse in the future.

1.5. Stressed Haematopoiesis

A healthy BM is not only key to normal blood cell production but also to the body's ability to respond to stressors such as infection or bleeding. In normal haematopoiesis, the production of all blood cell lineages is well balanced to produce adequate number of erythrocytes, myeloid cells, lymphocytes and platelets. However, in response to stress, this balance is disrupted and specific lineages are favoured. Thus, in response to bleeding, erythropoiesis is promoted and infections trigger expansion of myeloid progenitors. Furthermore, the numbers of mature cells produced can increase several fold in a short period of time in order to meet the increase in demand (224). This rapid expansion is regulated in a number of ways. In the case of infection, pathogen recognition has to occur first. This is mediated by Toll-like receptors (TLRs), which detect pathogen-associated molecular patterns (PAMPs) and danger-associated molecular patterns (DAMPs) and have been shown to be expressed by HSCs and HPCs (225, 226). They stimulate the release cytokines and growth factors, including IL-3, IL-6, interferons, SCF, TPO, G-CSF and GM-CSF, and promote HSC and HPC expansion and differentiation (226, 227). This drives emergency granulopoiesis and the release of increased leukocytes, in particular neutrophils, into the circulation. Emergency erythropoiesis on the other hand, is regulated by EPO, which also drives steady state red cell production, as well as SCF and glucocorticoids (228). In cases of extreme stress more immature blood cells including myelocytes and nucleated red blood cells, which are usually only present in the BM, can be release into the peripheral blood (229). Furthermore, if stress persists and high numbers of granulocytes are continuously produced in response to infection, this can occur at the expense of other lineages causing thrombocytopenia, lymphopenia and mild anaemia (224).

1.5.1. Metabolism in the Bone Marrow Niche

In order for cells to survive, proliferate and differentiate they require a constant and reliable supply of energy. Several pathways exist to allow energy production within the cells, each requires different substrates and the

efficiency and overall energy output, in the form of adenosine triphosphate (ATP), can vary significantly between pathways (Figure 1.8). Substrates include glucose, which gives rise to pyruvate during the anaerobic process of glycolysis, lactate, which is converted to pyruvate in a reversible reaction catalysed by lactate dehydrogenase (230), free fatty acids (FFAs), which produce acetyl-coenzyme A (CoA) through β-oxidation (231) and amino acids. All of these substrates can generate acetyl-CoA as the final product, to combine with oxaloacetate to form citrate in the first step of the tricarboxylic acid (TCA) cycle (232). The TCA cycle consists of a series of reactions that supply NADH and $FADH_2$ to the electron transport chain to fuel oxidative phosphorylation (OXPHOS) (232, 233). OXPHOS is the most efficient mode of energy production and produces the most ATP, however, both OXPHOS and the TCA cycle are aerobic in nature and require an abundant supply of oxygen and mitochondria. In addition, it results in the production of by-products, including ROS, which can cause DNA damage and therefore affect cell function and longevity (234).

The HSC niche is relatively hypoxic despite its perivascular location, as blood has become relatively deoxygenated by the time it reaches the BM (235-237). These hypoxic conditions promote HSC quiescence, minimise oxidative stress and are known to benefit long-term HSC health (234). As a result, in the steady state, quiescent HSCs primarily rely on anaerobic glycolysis, which only produces 2 ATP molecules, for their energy supply (235, 236). Mitochondrial mass and activity, on the other hand, is sustained at low levels and tightly regulated by a balance of biogenesis and mitophagy (235, 238). Thus, levels of OXHOS and resulting mitochondrial ROS are maintained at low levels in the HSC niche during normal homeostasis.

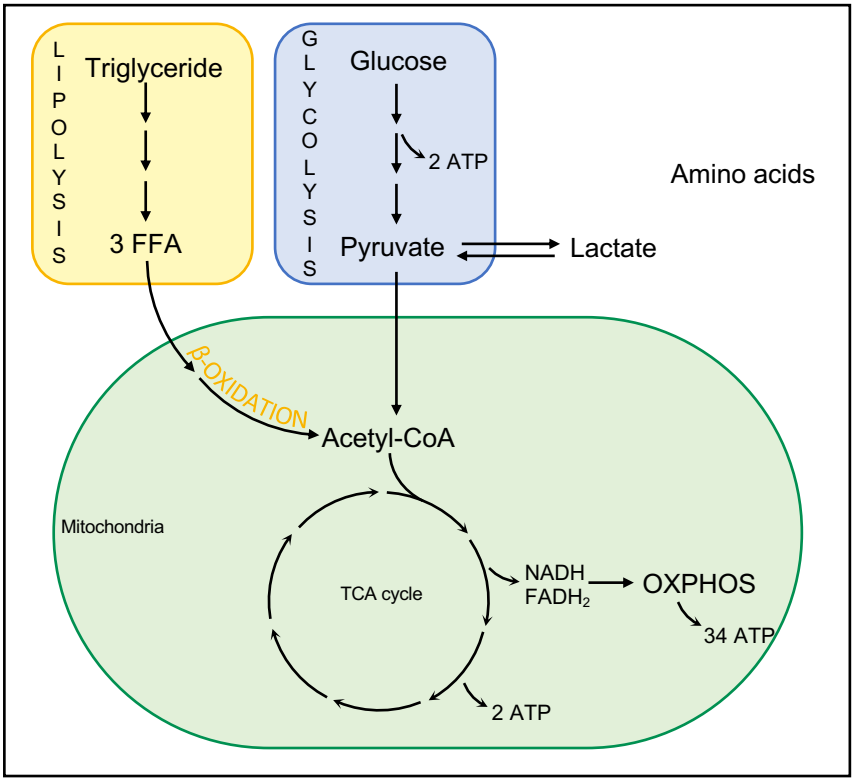

Figure 1.8. Metabolic pathways
Free fatty acids (FFA), produced during lipolysis, glucose, lactate and amino acids are used to produce acetyl-CoA. FFA are converted during β-oxidation and glucose is converted to pyruvate during glycolysis. Pyruvate in turn can be converted to acetyl-CoA or lactate in a reversible reaction. Acetyl-CoA is a substrate for the tricarboxylic acid (TCA) cycle which produces ATP as well as NADH and $FADH_2$, which enter the electron transport chain to generate a further 34 ATP molecules during oxidative phosphorylation (OXPHOS).

1.5.2. Metabolism during stressed Haematopoiesis

As the production of blood cells dramatically increases during stressed haematopoiesis, the energy requirement of HSCs and HPCs also rises. As a result, the less efficient anaerobic glycolysis is no longer sufficient to meet demands. In response to stress, HSCs are able to rapidly switch to OXPHOS for energy supply (239). This requires a rapid increase in mitochondrial mass and is facilitated by superoxide driven mitochondrial transfer from the bone marrow stromal cells (BMSC) to HSCs via connexin 43 GAP junctions (91). This allows an immediate upregulation of OXPHOS without the delay that

would result if HSCs relied solely on the upregulation of their own mitochondrial biogenesis (91).

In addition, HSCs acquire a number of metabolites from their microenvironment in order to fuel this increase in OXPHOS. Amino acids, lactate, glucose and free fatty acids can all be used to generate acetyl-CoA, which feeds directly into the TCA cycle (232). Fatty acids are in abundant supply from the BM adipose tissue and their transfer to HSCs is mediated by CD206, CD36, fatty-acid-binding proteins (FABPs) and fatty-acid-transporter proteins (FATPs) (240-242). The inducible fatty acid transporter CD36 has been shown to be upregulated in HSCs during infection to promote the uptake of free fatty acids and support the shift to OXPHOS (240). Whilst HSCs increase their energy consumption, proliferation and differentiation, a small pool of quiescent undifferentiated HSCs is always maintained to allow for the long-term replenishment of HPCs and mature blood cells.

1.5.3. The hijacking of the haematopoietic stress response

Like many physiological processes the haematopoietic stress response has been hijacked by malignant haematopoietic cells. AML cells in particular have been shown to take advantage of the diverse metabolic pathways available to them. Whilst it was traditionally thought that tumour cells rely purely on anaerobic glycolysis, which allows them to thrive in hypoxic environments (243), there is now increasing evidence that a number of cancers are able to acquire mitochondria from their tumour microenvironment. This enables them to switch to OXPHOS and thus improve their energy efficiency giving them a proliferative and survival advantage. Mitochondrial transfer has been observed in AML, where it is mediated by NOX2 derived superoxide (214). Furthermore, AML cells have been shown to utilise amino acids to fuel their increased reliance on OXPHOS and that treatment with the BCL-2 inhibitor venetoclax directly impairs the uptake of amino acids and supresses OXPHOS in ROS-low leukaemic stem cells and eventually leads to cell death (244-246). Finally, we know that AML drives the mobilisation of free fatty acids from adipocytes (210) and this is associated with an upregulation of the FABP4 and CD36

(247). Interestingly, it appears that leukaemic cells particularly rely on fatty acid metabolism in relapsed disease and therefore are able to escape targeted amino acid depletion by venetoclax (244). These examples demonstrate, not only how physiological processes can inform our understanding of mechanisms that drive tumour growth and development, but also how we can use this understanding to target these pathways and develop better ways to treat malignancies and prevent treatment resistance and relapse.

1.6. Rationale

As our population ages, the burden of age-related diseases on individuals, health care systems and society as a whole is steadily increasing. Understanding the physiological changes that occur during ageing, alter the functions of tissues and organs and contribute to disease development is thus becoming increasingly important. The BM stress response is dependent on tightly regulated interactions between HSCs and HPCs and the BM microenvironment. Any changes in the microenvironment or in the haematopoietic cell populations can disrupt these interactions and thus impair the BM response to stress. It is therefore likely that the changes observed in the ageing BM will impact on the ability of the BM to respond to stress. Increased age is associated not only with an increased incidence of infections, but also with an impaired ability to clear infections effectively and therefore an increase in infection associated morbidity and mortality (7). The rapid metabolic adaptability of HSCs and HPCs is key to their effective response to stress. This requires not only an adequate supply of metabolites but also healthy and functional mitochondria. However, mitochondrial dysfunction has been identified as one of the hallmarks of ageing (13). Whilst this may not have a significant impact of HSCs in the steady state when they primarily rely on glycolysis (14) it may contribute to the BM's ability to respond to stress, including infection. A better understanding of the interactions between HSCs and HPCs and the aged BM microenvironment will not only help to identify the how age-changes alter HSC function and the BM response to stress but in the future, it may also elucidate how these changes result in a pro-tumoural microenvironment that drives the age-associated development of haematological malignancies.

1.7. Hypothesis

I hypothesise that mitochondrial function in HSCs and HPCs diminishes with age and that this impairs their ability to respond to stress signals. I also hypothesise that depleting senescent cells in the BM microenvironment can restore HSC and HPC function and improve their response to infection. Therefore, the aim of this study is to understand age-related mitochondrial changes in the haematopoietic stem cell compartment. To address this aim I have three complementary objectives (Figure 1.9).

1.8. Objectives

1. Characterising the metabolic profile of aged HSCs.
2. Defining how age-related metabolic changes alter the haematopoietic response to stress.
3. Investigate the role of senescent cells in the haematopoietic response to stress.

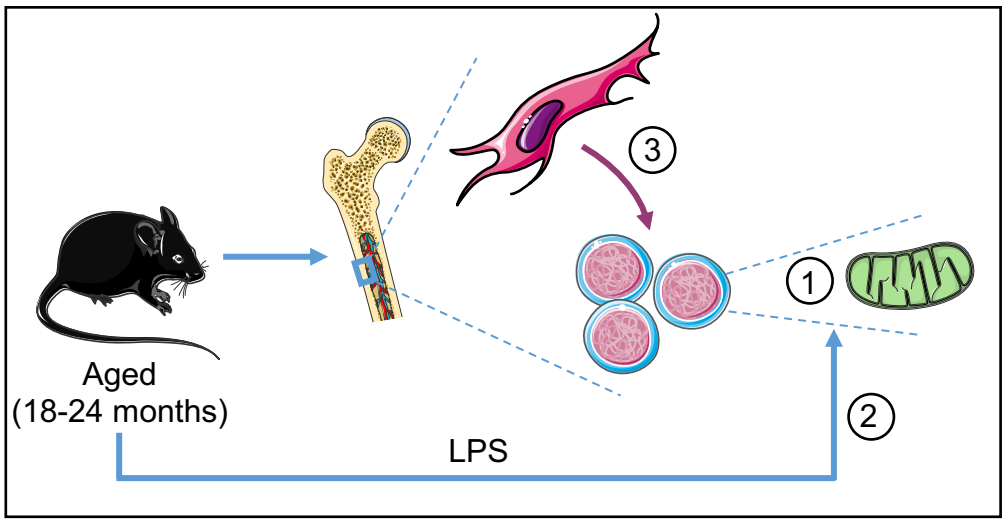

Figure 1.9. Graphical representation of the three objectives.

2. Materials and Methods

2.1. Materials

All reagents and materials used in the study are shown in Table 2.1 and described in the Methods section below. The reagents were obtained from the manufacturers as detailed below.

Table 2.1. Reagents used with Manufacturer and Catalogue Number
Agilent (Santa Clara, CA, USA), Biolog (Hayward, CA, USA), Cell Signalling (Danvers, MA, USA), Fisher Scientific (Hampton, New Hampshire, USA), GE Healthcare (Little Chalfont, UK), Medisave UK Ltd (Weymouth, UK), Miltenyi Biotec (Bergisch Gladbach, Germany), Nexcelom Bioscience (Lawrence, MA, USA), PCR Biosystems (London, UK), Peprotech (Rocky Hill, NJ, Promega (Madison, WI, USA), USA), Promega (Madison, WI, USA), Sarstedt (Nümbrecht, Germany), Selleck Chemicals LLC (Houston, TX, USA), Sigma-Aldrich (St Louis, MO, USA), Stem Cell Technologies (Cambridge, UK), Stratech (Cambridge, UK), ThermoFisher (Waltham, MA, USA), Wolf Laboratories (York, UK)

Product	Manufacturer	Catalogue number
1ml syringe	Fisher Scientific	15489199
1x MAS Buffer	Biolog	72303
26-gauge butterfly needle	Medisave UK Ltd	2674829
26-gauge needle	Fisher Scientific	12349169
27-gauge needle	Fisher Scientific	10204444
ABT-263	Selleck Chemicals LLC	S1001
Ammonium Chloride (NH_4Cl)	Stem Cell Technologies	07850
SA-β-gal	Cell Signalling	9860
Bovine Serum Albumin (BSA)	Fisher Scientific	BP1600-100
Busulfan	Sigma-Aldrich	B2635
CD117 microbeads	Miltenyi Biotec	130-091-224
Cellometer SD100 counting chamber	Nexcelom Bioscience	CHT4-SD100-002
CellTrics 40µm filter	Wolf Laboratories	04-0042-2316
DAPI	ThermoFisher	62248
DMEM Medium	ThermoFisher	10566016
EDTA	Sigma-Aldrich	E9886
EDTA tubes	Sarstedt	6.265 374
Foetal Bovine Serum (FBS)	ThermoFisher	105000056
FIX & PERM Cell Fixation & Permeabilization Kit	ThermoFisher	GAS004
Ganciclovir	Stratech	ORB322504-BOR
Human IL-6	PeproTech	200-06
Hydrogen Peroxide (H_2O_2)	Sigma-Aldrich	H1009
IsoFlo (Isofluorane)	Zoetis	In house (DMU)
Lineage cell depletion kit	Miltenyi Biotec	130-110-470
Lipopolysaccharide (LPS)	Sigma-Aldrich	L2630
LS columns	Miltenyi Biotec	130-042-401
MEM Medium	ThermoFisher	11095080
MitoPlate	Biolog	14105l

Product	Manufacturer	Catalogue number
MitoSox	ThermoFisher	M36008
MitoTracker™ Green	ThermoFisher	M46750
Mouse CD105 – PE Cy7	Biolegend	120410
Mouse CD117 – PE Cy7	Miltenyi Biotec	130-108-355
Mouse CD11b – APC	Biolegend	101212
Mouse CD150 – BV510	Biolegend	115920
Mouse CD150 – PE Cy5	Biolegend	115920
Mouse CD19 – PerCP	ThermoFisher	45-0193-82
Mouse CD31 – BV421	Biolegend	102424
Mouse CD31 – FITC	Miltenyi Biotec	130-123-675
Mouse CD31 – PerCP	Biolegend	102522
Mouse CD4 – APC Cy7	Biolegend	100414
Mouse CD45 – BV510	Miltenyi Biotec	130-119-130
Mouse CD45 – PerCP	Biolegend	103130
Mouse CD45.1 – BV605	Biolegend	110738
Mouse CD45.1 – PE	Miltenyi Biotec	130-103-009
Mouse CD45.2 – FITC	Miltenyi Biotec	130-102-312
Mouse CD48 – APC Cy7	Biolegend	103431
Mouse CD8 – APC Cy7	Biolegend	100714
Mouse IL-3	PeproTech	213-13
Mouse Ki67 – FITC	Miltenyi Biotec	130-117-691
Mouse Lineage Cocktail - Pacific blue	Biolegend	133310
Mouse Ly6G – PE Cy7	Miltenyi Biotec	130-124-208
Mouse Sca1 – APC	Miltenyi Biotec	130-102-343
Mouse SCF	PeproTech	250-03
Mouse Ter119 – APC	Miltenyi Biotec	130-102-290
OneComp eBeads™ Compensation Beads	ThermoFisher	01-1111-42
PCRBIO 1-Step Go RT-PCR Kit	PCR Biosystems	PB10.53-10
Penicillin-Streptomycin	GE-Healthcare	SV30010
Phosal 50PG	Fisher Scientific	NC0130871
Poly-D Lycine Solytion	Sigma-Aldrich	A-003-E
Polyethylene glycol 400	Sigma-Aldrich	202371
Primers for qPCR	See Table 2.3	
PureLink™ Genomic DNA Mini kit	ThermoFisher	K182002
qPCRBIO cDNA synthesis kit	PCR Biosystems	PB30.11-10
qPCRBIO SyGreen Mix	PCR Biosystems	PB20.12-51
ReliaPrep RNA Cell Miniprep System	Promega	Z6012
Saponin	Sigma-Aldrich	47036-50G-F
Seahorse XFp Base Medium	Agilent	1033335-100
Seahorse XFp Mito Stress Test Kit	Agilent	103010-100
Sodium Pyruvate	Fisher Scientific	11501871
TaqPath ProAmp MasterMix	ThermoFisher	A30865
TMRM	ThermoFisher	T668
Trypan Blue Solution	Sigma-Aldrich	T8154
Trypsin-EDTA	ThermoFisher	25200056
Verapamil	Sigma-Aldrich	V4629

2.2. Animal Models

All *in vivo* work was carried out in accordance with regulations set by the UK Home Office and the Animal Scientific Procedures Act 1986 under project licence 70/8814 (Prof. Kristian Bowles) and PP023671 (Dr Stuart Rushworth).

2.2.1. Animal maintenance

Animals were housed at the Disease Modelling Unit (DMU) at the University of East Anglia, which is a specific pathogen free, containment level 3, facility. Five different strains of mice were used for this study as described below. Breeding pairs were set up at the age of 6-8 weeks and maintained for no longer than 6 months. Offspring were weaned at the age of 3 weeks and used for experiments at the age of 8-12 weeks. Mice, including ex-breeding females, were also aged to 18-24 months. The aged colonies were closely monitored and at any sign of age-related diseases including tumour development or overgrooming the mice were sacrificed by a schedule 1 method and not used for experiments. As female mice are easier to house in the long term and their cages can continue to be merged at any age, all experiments in this study used only female mice.

2.2.1.1. Wildtype C57Bl/6 mice

C57BL/6J mice (CD45.2) were purchased from Charles River (UK). This is the most widely used inbred mouse strain and was used for the majority of the experiments described in this thesis. The C57Bl/6 mice are long lived and have good breeding records, making them optimal for routine use for in vivo work. Both young and aged C57Bl/6 mice were used to study the differences in the young and aged BM and the response to lipopolysaccharide (LPS) treatment. They were also used together with the PepCboy mice in the transplant models. BMSC and LK cells were isolated from young and aged C57Bl/6 mice to study mitochondrial transfer and senescence associated beta-galactosidase (SA-β-gal) staining respectively. Finally, aged C57Bl/6 mice were used as control

mice to compare with the p16-3MR mice, which have the same genetic background, and to study the effect of ABT-263 treatment.

2.2.1.2. Wildtype PepCboy mice

B6.SJL-Ptprca$^{Pep3b/BoyJ}$ (CD45.1) (PepCboy) were acquired from The Jackson Laboratory (Bar Harbour, ME). This is a congenic C57Bl/6 mouse strain, which differs from C57Bl/6 mice by the expression of CD45.1 rather than CD45.2. This allows identification of hematopoietic cells from one strain in the circulation or BM of the other and these two mouse strains are therefore commonly used for transplantation models. In this thesis young and aged PepCboy mice were used as donors of cells for transplantation into young C57Bl/6 mice and young PepCboy mice were also used as transplant recipients.

2.2.1.3. p16-3MR mice

p16-3MR mice were developed and provided by the Campisi Laboratory (21). This is a genetically modified mouse model developed on a C57Bl/6 genetic background. In this mouse model a 3 modality reporter gene is associated with the p16 promotor. In this study the herpes simplex virus 1 (HSV-1) thymidine kinase (HSV-TK) reporter component was used. HSV-TK phosphorylates the pro-drug ganciclovir (GCV) converting it to a DNA chain terminator and causing apoptosis of senescent cells.

2.2.1.4. p16-tdTom mice

p16-tdTom mice were purchased from The Jackson Laboratory (Bar Harbour, ME). Similarly to the p16-3MR mouse model, this model was developed on a C57Bl/6 background in order to study senescent cells. A fluorochrome tandem-dimer Tomato (tdTom) was knocked-in to the p16^{INK4A} locus. This allows the detection of tdTom fluorescence in p16 expressing senescent cells. In this study, this model was used to assess levels of p16 expression in HSCs, HPCs and BMSCs from young and aged mice.

2.2.1.5. Wildtype CBA

CBA mice were obtained from Charles River (UK). These mice differ from other mouse strains used in this study by their mitochondrial genome. Their mitochondrial DNA can be distinguished from C57B/6 mitochondrial DNA by two single nucleotide polymorphisms. LKs cells from CBA mice were therefore used to study mitochondrial transfer from young and aged BMSCs to LKs *in vitro*.

2.2.2. Transplantation models

For the transplant model C57Bl/6 and PepCboy mice were used. The recipients were first treated with busulfan 25mg/kg for 3 days. LSKs or HSCs were purified by fluorescent activated cell sorting (FACS) and the appropriate number of cells for each experiment were resuspended in 1X phosphate buffer solution (PBS) for a total volume of 200µl per recipient mouse. Engraftment was measured by the relative levels of CD45.1 or CD45.2 donor cells in the BM and peripheral blood (PB) of the recipient.

2.2.2.1. Transplantation of young and aged LSKs

Young PepCboy (CD45.1+) mice were treated with 25mg/kg busulfan for 3 days. The following day LSKs were FACS purified from young and aged C57Bl/6 (CD45.2+) mice. 100,000 LSKs were injected into the tail vein of each busulfan treated PepCboy mouse. Engraftment was assessed after 12 weeks in the PB and BM.

2.2.2.2. Transplant with TMRM staining

For this transplant model young C57Bl/6 (CD45.2+) mice were treated with 25mg/kg busulfan for 3 days. LSKs were then FACS purified from young and aged PepCboy (CD45.1+) mice based on their Tetramethylrhodamine, Methyl Ester (TMRM) levels. LSKs were also isolated from young C57Bl/6 mice. In a competitive transplant setting 150,000 $TMRM^{hi}$ or $TMRM^{lo}$ LSKs from young or aged PepCboy mice and 150,000 LSKs from C57Bl/6 mice were injected

into the tail vein of the busulfan treated C57Bl/6 mice. Engraftment was assessed in the PB at 8 and 12 weeks and in the BM at 12 weeks.

After 12 weeks a new group of young C57Bl/6 mice were treated with busulfan for 3 days. CD45.1+ HSCs were then sorted from the BM of the C57Bl/6 (CD45.2) mice engrafted with $TMRM^{lo}$ LSKs from young or aged mice. In a secondary transplant 1000 CD45.1+ HSCs were injected into busulfan young C57Bl/6 mice together with 100,000 whole BM support cells from C57Bl/6 (CD45.2) mice. Engraftment was assessed after a further 12 weeks.

2.2.2.3. Transplant with LPS treatment

Again, young C57Bl/6 (CD45.2+) mice were treated with 25mg/kg busulfan for 3 days and LSKs were then FACS purified from young and aged PepCboy (CD45.1+) mice. 100,000 LSKs from C57Bl/6 mice were injected into the tail vein of the busulfan treated C57Bl/6 mice. Engraftment was assessed in the PB at 8 and 12 weeks and the engrafted mice were treated with 0.5mg/kg LPS or vehicle control. All mice were sacrificed using two schedule 1 methods 16 hours after this treatment.

2.2.3. Animal Procedures

All procedures were carried out by myself under my personal UK Home Office license IE10ADD51, with the help from Dr Jayna Mistry (I2777C6D5) and Dr Stuart Rushworth (ICD3874DB). Training for each procedure was provided by Mr Richard Croft (IGEBEFB87) and Mrs Anja Croft (L8A2ACED).

2.2.3.1. Intraperitoneal injections

Busulfan, LPS and GCV were administered by intraperitoneal (IP) injections. For all IP injections mice were restrained using a scruff technique and a volume of 200µl was injected into the peritoneum using a sterile 26-gauge needle. Busulfan was given for 3 consecutive days prior to transplantation at a dose of 25mg/kg. LPS was administered at a dose of 0.5mg/kg for all experiments and mice were sacrificed after 16 hours, except when the overall

survival was assessed. Ganciclovir was given at a dose of 25mg/kg for 5 days followed by a seven-day rest period.

2.2.3.2. Intravenous injections

For the transplantation models, donor cells were isolated and resuspended in PBS. Busulfan pre-treated recipient mice were placed in a heat chamber and warmed to 37ºC for 10 minutes to promote vasodilation. They were then placed in a benchtop holding cone and 200µl of the cell suspension was injected into the lateral tail vein using a sterile 27-gauge needle. Pressure was applied to prevent any subsequent bleeding and the mice were monitored in a new cage for a short period before they were returned to their home cage.

2.2.3.3. Oral Gavage

ABT-263 was administered by oral gavage at a dose of 100mg/kg daily for 7 days. It was first resuspended in 10% ethanol, 30% polyethylene glycol 400 and 60% Phosal 50PG. The suspension was freshly prepared each day and, as a control, mice were administered the same combination of ethanol, polyethylene glycol 400 and Phosal 50PG but without any ABT-263. Mice were restrained using a scruff method and administered 200µl of the solution by oral gavage. Mice were monitored until fully recovered from the procedure and then returned to their home cage.

2.2.3.4. Blood sampling

Blood samples were obtained from the tail vein of mice to confirm engraftment in the transplant models. Mice were placed in a heat chamber at 37ºC for 10 minutes for vasodilation and then placed in a benchtop holding cone. Samples were taken from the lateral tail vein with a trimmed 26-gauge butterfly needled. Up to 200µl of blood was collected into an EDTA coated tube.

Terminal blood samples were obtained from mice by cardiac puncture to allow collection of larger volumes of blood. Mice were placed under deep terminal anaesthesia using isoflurane. Samples were taken from the left ventricle of the heart using a 25-gauge needle and placed directly into an EDTA coated tube.

2.2.3.5. Schedule 1

Mice were humanely sacrificed at the endpoint of each experiment or if showing any signs of being unwell, including weightloss, reduced motility, severe over-grooming, piloerection, hunched postures, signs of graft vs host disease or, in the aged colonies, spontaneous tumour development. Two schedule one methods were always used. Most commonly, gradual CO_2 asphyxiation followed by neck dislocation were used. The exception to this was when terminal blood samples were required and cardiac puncture was used followed by neck dislocation.

2.3. Isolation of primary mouse bone marrow

Mouse BM was usually isolated from the tibias and femurs of mice. The bones were dissected out and all muscle was removed. They were then cut in half and each bone was placed in a 0.5 ml Eppendorf tube with a hole at its base, which was itself placed inside a 1.5ml Eppendorf tube. These tubes were then centrifuged at maximum speed for 6 seconds and the cells from each bone were collected at the base of the 1.5ml Eppendorf tube. The BM pellets were resuspended in MACS buffer (PBS pH 7.4 containing 0.5% BSA and 1mM EDTA) and pooled for each mouse. Cells were then filtered through a 40µm filter, washed and, if needed counted before being cultured for in vitro experiments or prepared for flow cytometry or FACS.

When higher numbers of cells were required, in particular for metabolic pathway analysis, cells were isolated by bone crushing. For this the spine, sternum, hips, femurs and tibias were dissected out and carefully crushed using a pestle and mortar. Small volumes of MACS buffer were added to resuspend the BM cells throughout this process before they were filtered and washed and then processed in the same way as the centrifuged BM samples.

2.3.1. CD117 enrichment

To isolate CD117+ cells anti-CD117 magnetic microbeads were used (Miltenyi Biotec, Bergisch Gladbach, Germany). Up to 100 million BM cells were suspended in 500µl of MACS buffer and 20µl of anti-CD117 beads. They were incubated for 20 minutes at 4ºC and then spun down at 1500 rpm for 5 minutes. The supernatant was removed and the cells were resuspended in 1ml of MACS buffer. The cells were then transferred into a pre-washed LS column (Miltenyi Biotec, Bergisch Gladbach, Germany) attached to a magnet. The column was washed a further three times with 3ml of MACS buffer. At the end the CD117 positive cells were flushed from the LS column by removing it from the magnet and firmly plunging it. The CD117+ cells were then prepared for FACS purification by adding TMRM staining and the appropriate antibody panels, either in preparation for the transplantation or single cell sorting.

2.3.2. LK cells isolation

To isolated lineage negative (Lin-), CD117 positive (LK) cells, two sets of magnetic beads were used. First BM cells were lineage depleted using a direct lineage depletion kit (Miltenyi Biotec, Bergisch Gladbach, Germany). First lineage depletion beads were added to up to 100 million cells and incubated for 20 minutes at 4ºC as per the manufacturer's instructions. The same procedure was followed as for the CD117 enrichment and the flow through Lin- cells were collected at the end. These cells were subsequently spun down at 1500 rpm for 5 minutes before being resuspended in MACS buffer and CD117 magnetic beads for the CD117 enrichment as described above. The resulting LK cells were either used directly for the seahorse metabolic flux analysis, metabolic pathway analysis or beta galactosidase measurement, or cultured for later use in co-culture experiment to measure mitochondrial transfer. LK cells were cultured in Dulbecco's Modified Eagle's Medium (DMEM) containing 10% foetal calf serum (FBS) and 1% penicillin-streptomycin and supplemented with mouse stem cells factor (SCF) (100ng/ml), mouse IL-3 (10ng/ml) and human IL-6 (10ng/ml) (Peptrotech, Inc., Rocky Hill, NJ, USA)

2.3.3. Bone marrow stromal cells

BMSCs were isolated from whole BM after centrifugation as described above. BM cells were resuspended in Minimum Essential Medium (MEM) containing 20% FBS and 1% penicillin-streptomycin and then plated onto tissue culture plastic. After 96 hours any non-adherent or non-viable cells were washed of and fresh MEM was added to the adherent cells, which include BMSCs. Medium was replaced twice a week until BMSC colonies were visible and then used immediately and not passaged repeatedly to preserve the young and aged phenotype as much as possible. To remove BMSC from the flask, the serine protease trypsin-EDTA was used. Briefly, the medium was removed and the cells were washed three times with 1X PBS before the addition of 2ml of trypsin. The flask was then placed in the incubator to promote the activity of trypsin and dissociation of the adherent cells from the flask. Next, 5ml of MEM were added to the flask to inactivate the trypsin, the cells were then spun down at 1500rpm for 5 minutes and resuspended in MEM to remove any excess trypsin. BMSC markers were confirmed by flow cytometry (CD105+, CD140a+ CD31−, Ter119−, and CD45−). Finally, the cells were counted and used immediately for the mitochondrial transfer co-culture experiment or the seahorse metabolic flux analysis.

2.4. Cell culture assays

2.4.1. Cell counting with trypan blue

To determine the numbers of viable cells and ensure use of the correct cell numbers for each assay, the trypan blue exclusion assay was used. This is a widely used assay that allows easy identification of viable cells, as these have an intact cell membrane and are unable to take up trypan blue, whilst non-viable cells can take up the blue dye. To perform this assay cells to be counted where mixed with trypan blue in a 1 in 2 dilution (10µl of each) and 10µl of this mixture was then pipetted onto a haemocytometer. All viable cells were

counted in each of the four outer quadrants and the total cell count per ml of the cell suspension was calculated (Figure 2.1).

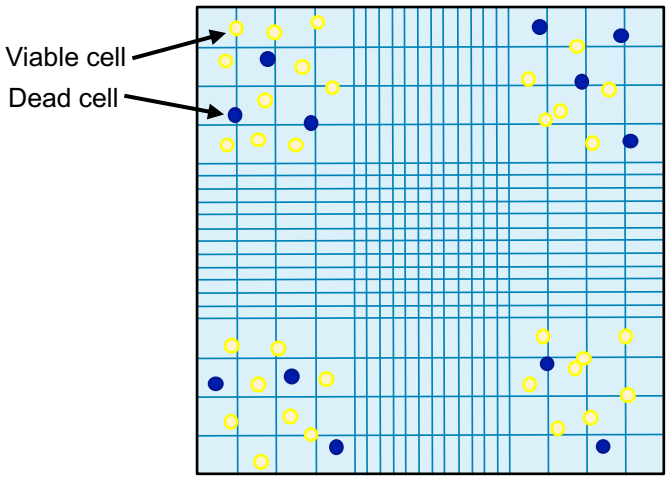

$$\text{Cell number/ml} = \left(\frac{\text{Viable cell count}}{\text{Number of quadrants counted}}\right) \times \text{Dilution factor} \times 10^4$$

Figure 2.1. Cell counting using trypan blue exclusion.
Layout of the haemocytometer layout with cells shown in the outer 4 quadrants to be counted. Dead cells are shown in blue as these take up trypan blue. Viable cells are shown in yellow. The formula to calculate total cell number per ml is shown below.

For animal experiments an automated cell counter, Cellometer T4 Bright Field Viability Cell Counter (Nexcelom Bioscience LLC Lawrence, MA, USA) was used. This uses bright field microscopy and pattern recognition software to quantify the total cell numbers, live cells and dead cells. Isolated BM cells were diluted 1 in 10 in MACS buffer and then further with trypan blue at dilution factor of 1 in 2. 20µl of this mix were then loaded onto the cell counting chamber (Nexcelom Bioscience LLC Lawrence, MA, USA) and the cell concentration was calculated accounting for the total dilution factor of 1 in 20).

2.4.2. Co-culture experiment

For the co-culture experiment BMSCs were isolated from young and aged C57Bl/6 mice and cultured as described above. Once confluent colonies of cells were visible in the flask, they were removed using trypsin-EDTA and counted using the trypan blue exclusion assay. They were then replated onto a 24 well tissue culture plate with 100,000 cells in each well. At the same time, LK cells were isolated from young CBA mice as described above and cultured. 24 hours after the stroma had been plated and fully adhered, the medium was removed and the cells were washed with PBS. Subsequently 10,000 CBA LK cells were added to the wells, leaving a few without LK cells as negative controls. The co-cultured cells were then treated with 5μMol of H_2O_2 and, again, some wells left untreated as controls. After 24 hours the LK cells were carefully removed from the wells without disturbing the adherent stroma. Their DNA was then extracted for Taqman PCR analysis.

2.4.3. Senescence associated beta-galactosidase assay

LK cells were isolated from young and aged mice as described above and immediately stained using the senescence associated beta-galactosidase (SA-β-gal) staining kit (Cell Signaling Technology, MA). Cells were placed in a 35mm wells and stained according to the manufacturer's instructions. Briefly, cells were fixed and 1ml of β-gal staining solution was added to each 35mm well. They were then incubated at 37ºC. The cells were evaluated for the blue colour change indicative of SA-β-gal positive cells. This assay was kindly performed by Dr Stuart Rushworth.

2.5. Flow cytometry and cell sorting

Flow cytometry was used extensively in the study, not only to identify cell populations and determine cell counts, but also to measure mitochondrial content, membrane potential and ROS using a number of dyes. Furthermore, flow cytometry was used to sort specific cell populations, including HSCs, LSK and BMSCs for both transplants or analysis of RNA expression levels. All of these processes rely on staining of BM cells with antibodies conjugated with a detectable fluorophore or fluorescent dyes. A number of flow cytometers were used in this study, primarily dependent on the number of lasers of each cytometer, which determines the number of fluorophores that can be detected on each sample and also the ability to sort cells. However, at times the access to some flow cytometers was limited due to Covid-19 restrictions and as a result alternatives were used.

The antibody panels used for analysis and cell sorting are shown in Table 2.2, some of these vary depending on the flow cytometer used and the colours that could be detected. All antibodies were purchased from Miltenyi Biotech (Bergisch Gladbach, Germany), BioLegend (San Diego, CA, USA) or ThermoFisher (Waltham, MA, USA). For each antibody panel a compensation was set up at the relevant flow cytometer and these were repeated at regular intervals or after any servicing of the flow cytometer. Each flow cytometer was cleaned and primed before use. OneComp eBeads^{TM} Compensation Beads (ThermoFisher, Waltham, MA, USA) were stained individually with each antibody and fluorophore emission cross-over was measured. When dyes were included in the panels, compensation was carried out using live cells instead. In addition, fluorescence minus one controls were run for each panel to allow accurate identification of positively and negatively stained cell populations.

All data was downloaded as flow cytometry standard (FCS) files and analysed using FlowJo version 10.8.1 software (FlowJo, LLC, Ashland, OR, USA).

Table 2.2. Antibody panels used for Flow Cytometry Assays

Antibody Panel		Fluorophores						
		APC	PE Cy7	PE Cy5	BV421	BV510	PE	FITC
			APC Cy7	PerCP	Pacific blue	BV605	tdTom	
TMRM	HSC	Sca1	CD117	CD48	Lin Cocktail	CD150	TMRM	
	BMSC	Ter119	CD105	CD45	TMRM	CD31		
MTG	HSC	Sca1	CD117	CD48	Lin Cocktail	CD150	MTG	
	BMSC	Ter119	CD105	CD31	CD45	TMRM	MTG	
MitoSox	HSC	Sca1	CD117	CD48	Lin Cocktail	CD150	MitoSox	
Ki67	HSC	Sca1	CD117	CD48	Lin Cocktail	CD150	Ki67	
	PB	CD11b	Ly6G	CD4/CD8	CD19	DAPI		
Transplant	HSC	Sca1	CD117	CD48	Lin Cocktail	CD150	CD45.1	CD45.2
	Mature cells	CD11b	Ly6G	CD4/CD8	CD19	CD45.1	CD45.2	
with TMRM	HSC	Sca1	CD117	CD48	CD150	Lin Cocktail	Cd45.1	TMRM
with MitoSox	HSC	Sca1	CD117	CD48	Lin Cocktail	CD150	MitoSox	CD45.2
tdTom	HSC	Sca1	CD117	Lin Cocktail	CD150	tdTom		
	BMSC	Ter119	CD105	CD31	CD45	tdTom		
Cell sorting	LSK	Sca1	CD117	Lin Cocktail				
	HSC	Sca1	CD48	CD150	CD45.1			
	BMSC	Ter119	CD105	CD45	CD31			
with TMRM	LSK	Sca1	CD117	Lin Cocktail	TMRM			
	HSC	Sca1	CD117	CD48	Lin Cocktail	CD150	TMRM	

2.5.1. BM sample preparation for flow cytometry

Once the BM was isolated, centrifuged and resuspended as described above, cells were then counted and 5 million cells were aliquoted out for each antibody panel. A master mix of the antibody panel was prepared with 1µl of each per sample. Antibodies were added to the cells suspended in 200µl of MACS buffer and incubated for at least 20 minutes at 4ºC in the dark. For sorting of $TMRM^{hi}$ and $TMRM^{lo}$ cells for both the transplant and single cell sorting, CD117 enrichment was first performed as described above and the CD117+ cells were then stained with TMRM and the appropriate antibody panels.

If dyes were used, these were applied before antibody staining. Cells were incubated with 200nMol MitoTracker Green (MTG) (ThermoFisher Waltham, MA, USA), 400nMol Tetramethylrhodamine, Methyl Ester (TMRM) (ThermoFisher Waltham, MA, USA) or 2µMol MitoSox (ThermoFisher Waltham, MA, USA) and 50µMol verapamil (Sigma-Aldrich, St Louis, MO, USA) in a total volume of 500µl for 30 minutes at room temperature. They were then washed twice with MACS buffer and centrifuged at 1500 rpm for 5 minutes before being resuspended in 200µl of MACS buffer and stained with the antibody cocktail. Frequencies of $TMRM^{hi}$ and $TMRM^{lo}$ or $MitoSox^{hi}$ and

MitoSox^{lo} cell populations were calculated as the percentage of the total number of cells of each population. For example, the TMRM^{hi} frequency of HSCs represents the percentage of HSCs with high levels of TMRM staining.

To measure Ki67 expression the aliquoted cells were first fixed and permeabilised using the FIX & PERM Cell Fixation & Permeabilization Kit (ThermoFisher, Waltham, MA, USA). The cells were first stained with the antibody cocktail and incubated for 20 minutes at 4ºC in the dark. They were then centrifuged at 1500 rpm for 5 minutes and resuspended in 100µl of MACS buffer and 100µl of Reagent A (Fixation Medium) was added. After a 15-minute incubation at room temperature the cells were washed with MACS buffer and centrifuged at 1500 rpm for 5 minutes. The supernatant was removed and the pellet was resuspended in 100 µL of Reagent B (Permeabilisation Medium) and 1 µL of the Ki-67 antibody (Miltenyi Biotec, Bergisch Gladbach, Germany). After a further 20 minutes incubation at room temperature the cells were centrifuged again at 1500 rpm for 5 minutes and re-suspended in 200µL of MACS buffer.

2.5.2. Peripheral blood sample preparation

To analyse PB cells, blood samples were collected into EDTA coated tubes. Samples were mixed carefully and 10µl of each sample were placed in 100µl Ammonium Chloride (NH_4Cl) (Stem Cell Technologies, Cambridge, UK) for red cell lysis. After 5 minutes 800µl of MACS buffer were added and the samples were vortexed. They were then spun down at 500 x g for 5 minutes supernatant was removed. The samples were resuspended in 50µl of the pre-prepared antibody master mix. To prepare the antibody mix 0.5µl of each antibody per sample were added to 50µl of MACS buffer per samples. Once the antibody was added to each sample, they were incubated at 4ºC for 15 minutes. Finally, 300µl of DAPI diluted in MACS buffer to a concentration of 80ng/ml were added to each sample.

2.5.3. Flow Cytometers

2.5.3.1. BD FACSCanto II

The FACSCanto II flow cytomter (BD, Franklin Lakes, NJ, USA) is located at the Norfolk and Norwich University Hospital in the Pathology Laboratory and is maintained by Dr Allyson Tyler. It has three lasers, 488, 633 and 405nm and can therefore detect eight fluorophores at a time - FITC, PE, PE Cy5, PE Cy7, APC, APC Cy7, BV421 and BV510. This flow cytometer has an automated carousel which facilitates the running of numerous samples. The FACSCanto II was used for most of the experiments in this study and most antibody panels were set up for the parameters that can be detected with this flow cytometer.

2.5.3.2. BD Fortessa LSR

The BD Fortessa LSR flow cytometer is located at the Quadram Institute on the Norwich Research Park. Samples were run by Dr Stuart Rushworth or Katherine Hampton. The flow cytometer has five lasers (355, 405, 488, 561 and 640nm) and can detect 18 fluorophores simultaneously. It was used for PB panel and the Ki67 HSC panel

2.5.3.3. BD FACSymphony A1

The BD FACSSymphony A1 is located at the Bob Champion Research and Education Building at the University of East Anglia and only became available towards the end of this study. This flow cytometer has four lasers (405, 488, 561 and 637nm) and can detect up to 16 colours at a time. It was used for analysis of the competitive transplant with $TMRM^{hi}$ and $TMRM^{lo}$ LSKs and the subsequent secondary transplant.

2.5.3.4. Sony SH800 Cell Sorter

The Sony Cell Sorter is located at the Quadram Institute at the Norwich Research Park. It has four lasers (405, 488, 561 and 637nm), but is limited to only detect 6 colours at a time. It can, however, detect tdTom and was therefore used to analyse the expression of p16-tdTom in LSKs and BMSCs. Furthermore, it can be used to sort cells and was used to sort LSKs and HSCs

for all transplant experiments. It was also used to sort LSKs and BMSCs directly into RNA lysis solution for RNA expression analysis. All samples were run and sorted by Dr Stuart Rushworth.

2.5.3.5. BD FACSAria Fusion

The BD FACSAria Fusion flow cytometer and cell sorter is located the Earlham Institute at the Norwich Research Park and was operated by Dr Edyta Wojtowicz. It has the same numbers of lasers and therefore fluorophore detection capability as the BD Fortessa LSR but also has the ability to sort cells. This cell sorter was used to isolate $TMRM^{hi}$ and $TMRM^{lo}$ HSCs for single cell sequencing.

2.6. Seahorse Metabolic Flux analysis

The Seahorse XFp Analyser (Agilent Technologies, Santa Clara, CA, USA) was used to measure metabolic activity of LK cells using the XFp Cell Mito Stress Kit. This was carried out with the help of Dr Jamie Moore. In preparation for the assay, XFp flux cartridges were hydrated with XF Calibrant overnight at 37°C. On the next day Seahorse XFp culture plates were coated with poly-D lysine for at least 2 hours. BM was isolated from each mouse and pooled for each treatment condition. LK cells were isolated using lineage depletion and CD117 enrichment and subsequently counted by trypan blue exclusion. They were then spun down and resuspended in Seahorse base media supplemented with pyruvate (1mM), L-Glutamine (2mM), Glucose (10mM). 150,000 cells in 180µl were plated onto each well of the Seahorse XFp culture plate and centrifuged briefly to achieve a uniform monolayer of cells. Cells were equilibrated in a humidified non-CO2 incubator until the start of the assay.

For analysis of the metabolic activity of BMSCs, cells were isolated and cultured as described above. Once confluent BMSC colonies were visible, cells were removed from the tissue culture flask using trypsin-EDTA and counted. 2000 BMSCs were plated onto each well of the Seahorse XFp culture

plate and incubated over night to allow adherence of the cells. The following day the media was removed and the cells were washed before 180µl of Seahorse base media supplemented with pyruvate (1mM), L-Glutamine (2mM), Glucose (10mM) was added to each well.

The XFp Cell Mito Stress Kit is designed to measure the oxygen consumption rate (OCR), which reflects the levels of oxidative phosphorylation and basal extracellular acidification rate (ECAR) of cells, which is a measure of glycolysis. It uses timed injections of Oligomycin (2 µM), carbonyl cyanide-4-(trifluoromethoxy) phenylhydrazone (FCCP) (1 µM), and Rotenone (0.5 µM), in accordance with the manufacturer's instructions. These agents inhibit ATP synthase to reduce OCR, increase OCR by targeting the inner mitochondrial membrane, and reduce OCR through inhibition of complex 1 and 3 in the electron transport chain, respectively (Figure 2.2). This assay therefore allows measurement of basal and maximal respiration. These were calculated by subtracting the non-mitochondrial oxygen consumption from the basal and maximal respiration readings. All results were normalised to input cell number and analysed using Microsoft Excel and GraphPad Prism software version 9.4.1 (GraphPad Software, San Diego, CA, USA).

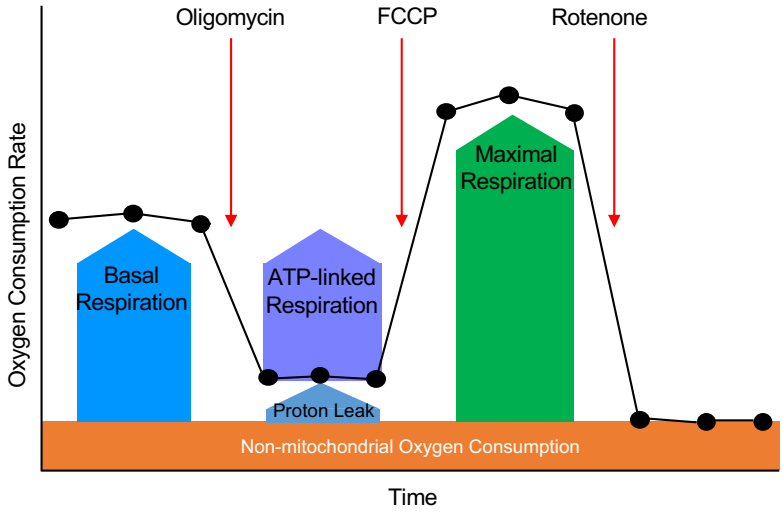

Figure 2.2. Seahorse Metabolic Flux Cell Mito Stress Kit.
Samples were injected with Oligomycin, FCCP and Rotenone at pre-determined time points. The OCR was measured at 3 time points before and after each drug was injected to allow calculations of basal and maximal respiration in each sample.

2.7. Metabolic Pathway Analysis

This assay was completed and analysed by Benjamin Johnson. This assay uses MitoPlates from Biolog (Hayward, CA, USA) to measure the utilisation of different metabolic substrates by cell populations. MitoPlates were prepared following manufacturer's instructions, 30 µL Assay mix containing 50 µg/mL Saponin (Sigma-Aldrich, St Louis, MO, USA) were pipetted into the wells and incubated at 37ºC for 1 hour. During this incubation time BM was isolated from mice and pooled for each treatment group. LK cells were harvested as described above, filtered using a 40µm nylon filter and counted. Cells were pelleted, and resuspended in 1x MAS Buffer (Biolog, Hayward, CA, USA) to give a final concentration of $2.5x10^6$ cells/ml. Next, 30µL of the cell suspension were pipetted into each well of the MitoPlate (Biolog, Hayward, CA, USA). Triplicate repeats were plated for each sample. The MitoPlate was read for 6 hours with 5-minute intervals at OD590 using the OmniLog plate reader. The initial and final OD readings were separated and organised per well. Data was restructured to fit the correct MitoPlate format, the final OD reading was subtracted from the initial OD and any negative results were set to 0 and later marked as not detected (ND). The triplicate and substrate control wells were averaged, each individual calculated OD value was subtracted from this value and averaged, creating the average aggregate minus no substrate table. The negatives were removed from this table and the data reorganised to match each substrate. Finally, all data was normalised to young control mice and heatmaps were created using 3 colour conditional formatting.

2.8. Molecular Biology

2.8.1. RNA extraction

RNA was extracted for the analysis of gene expression in FACS purified BMSCs and LSKs. The ReliaPrep RNA cell miniprep system (Promega, Southampton, UK) was used for this. Cells were directly sorted into BL+TG lysis buffer, the volume was varied depending on the numbers of cells sorted according to the manufacturer's instructions. The appropriate recommended volume of Isopropanol was next added to each sample and mixed well by vortexing. The lysates were loaded into the ReliaPrep mini-columns and centrifuged at 13,000 x g for 30 seconds. The columns were washed with 500µl of RNA wash solution and again spun at 13,000 x g for 30 seconds. Next, 30µl of DNase incubation mix (24µl yellow core buffer, 3µl Manganese Chloride and 3µl DNase I) were added to each sample and the samples were incubated for 15 minutes at room temperature. They were then washed with 200µl of Column Wash solution followed by 500µl of RNA wash solution and spun at 13,000 x g for 30 seconds each time. A final wash step with 300µl of RNA Wash Solution was performed and the samples were spun at 13,000 x g for 2 minutes. The columns were then placed into the 1.5ml elution tubes and the correct volume of nuclease free water was added (depending on the initial cell numbers used). The samples were centrifuged at 13,000 x g for 1 minute and the isolated RNA was stored at -80ºC until use.

2.8.2. DNA extraction

To analyse changes in mitochondrial DNA content in BMSC cells from young and aged mice and in LKs in the co-culture experiment, DNA was extracted using the PureLink™ Genomic DNA Mini kit (ThermoFisher, Waltham, MA, USA), which includes all the reagents used below. BMSCs were FACS purified and DNA was then immediately extracted, whilst LK cells were carefully removed from the co-culture assay and DNA was then extracted. Cells were pelleted, resuspended in 200µl PBS and 20µl of Proteinase K and 20µl of

RNase A) were added to each sample. The samples were vortexed and after a 2-minute incubation 200µl of PureLink Genomic Lysis/Binding Buffer were added and the samples were mixed again by vortexing. The samples were incubated for 10 minutes at 55ºC using a heat block to promote protein digestion and then 200µl of 96-100% ethanol were added to the lysate. The lysate was transferred into the PureLink Spin Column and centrifuged at 10,000 x g for 1 minute. Next, the spin column was washed with 500µl of Wash Buffer 1, before being centrifuged at 10,000 x g for 1 minute, and 500µl of Wash Buffer 2 followed by a 3-minuted centrifugation at 15,000 x g. Finally, the spin column was placed into a 1.5ml Eppendorf tube and 100µl of PureLink Genomic Elution buffer were added to each sample and incubated for 1 minute before being centrifuged at 15,000 x g for 1 minute. The DNA samples were stored at -20ºC until used.

2.8.3. Quantification of extracted RNA/DNA

The NanoDrop Spectrophotometer (ThermoFisher, Waltham, MA, USA) was used to quantify the DNA or RNA isolated from each sample. First, a blank sample of 1µl nuclease free water was run and then 1µl of each sample was analysed to measure the RNA or DNA concentration in ng/ml, as well as sample purity. Sample purity was measured using the absorbance threshold of nucleic acids, which is maximum at 260nm and the ratio of absorbance at this level to absorbance at 280nm is used to define the purity of DNA or RNA samples. A 260/280 ratio of 1.7 to 2.3 was considered sufficiently pure.

2.8.4. cDNA synthesis

The extracted RNA was used to synthesise cDNA through reverse transcription using the qPCRBIO cDNA synthesis kit (PCR Biosystems, London, UK). For a 10µl reaction a master mix was made up containing 2µl of 5X cDNA Synthesis Mix, 0.5µl of 20XRTase per samples. Each RNA sample was diluted to an equal concentration with nuclease free water to a total volume of 7.5µl and 2.5µl of the master mix were added. The PCR tubes were

placed into a Thermocycler (Bio-Rad, Watford, UK) and run on a pre-defined program with 30 minutes at 42ºC, 10 minutes at 85ºC, to denature the RTase, and then a return to 4ºC until the samples were removed and stored at -20ºC until used.

An alternative method used for some samples was a one-step PCR using the PCRBIO 1-Step Go RT-PCR Kit (PCR Biosystems, London, UK). This does not require the cDNA synthesis step and samples are directly prepare for qPCR with a RTase containing master mix.

2.8.5. Real time quantitative PCR

Real time quantitative PCR (qPCR) was performed on a Roche Lightcycler 480 (Roche, Basel, Switzerland) using SYBR-green technology (PCR biosystems, UK) to analyse gene expression or Taqman based analysis of mitochondrial DNA content. Primers were obtained from Qiagen (Hilden, Germany), Sigma-Aldrich (St Louis, MO, USA) or ThermoFisher (Waltham, MA, USA) and details of each primer are shown in Table 2.3. For the KiCqStart® SYBR Green primers, forward and reserve primers were first combined using 5µl of each and diluted in 90µl of nuclease free water.

Table 2.3. Primers used in qPCR analysis

QuantiTect SYBR-Green Primers (Qiagen)		
Gene	Assay name	GeneGlobe ID
GAPDH	Mm_Gapdh_3_SG QuantiTect Primer Assay	QT01658692
p16	Mm_Cdkn2a_1_SG QuantiTect Primer Assay	QT00252595
p21	Mm_Cdkn1a_va.1_SG QuantiTect Primer Assay	QT01752562
IL-6	Mm_Il6_1_SG QuantiTect Primer Assay	QT00098875
Laminin B1	Mm_Lmnb1_1_SG QuantiTect Primer Assay	QT00101346
KiCqStart® SYBR-Green Primers (Sigma-Aldrich)		
Gene	Forward primer 5'-3'	Reverse primer 5'-3'
BCL-2	ATGACTGAGTACCTGAACC	ATATAGTTCCACAAAGGCATC
BCL-XL	GCTTGGGATAATGAGACAAG	GAGAACATTCAGACCACAAG
Taqman® Primers (ThermoFisher)		
Gene	Assay name	Assay specifics
Mouse Tert	Taqman® copy number reference assay mouse	4458368
Mouse ND1	ND1 Taqman gene expression assay	4331182
COX3 9348snp	Custom Taqman® COX3 Assay	ANNKVUR
ND3_9461snp	Custom Taqman® ND3 Assay	ANPRPEN

2.8.5.1. Gene expression

To analyse gene expression in LSKs and BMSCs qPCR was performed with SYBR-Green technology (PCR Biosystems, UK), using either diluted synthesised cDNA samples or the PCRBIO 1-Step Go RT-PCR Kit (PCR Biosystems, London, UK) as described above. When cDNA was used, a master mix was made with 1µl of the primer, 4µl of SYBR-Green Mix and 1µl of nuclease free water. 6µl of this mix was of this mix was plated onto a 384-well plate before 4 µl of diluted cDNA were added. For the 1-step qPCR assay a master mix containing 0.1µl RTase Go 1-Step, 2.5µl of SYBR-Green Mix and 0.4µl of the PCR primer per sample was made and added directly to a 384-well plate. 2µl of RNA was then added to each well.

Once all sampled were plated, the plate was sealed and centrifuged at 1000 rpm for 1 minute. It was placed in a Roche Lightcycler 480 (Roche, Basel, Switzerland) for qPCR and run on a pre-programmed cycle as outlined in Table 2.4.

Table 2.4. qPCR SYBR-Green Lightcycler programming

qPCR with cDNA	Cycles	Temperature	Time
Pre-amplification	1	95ºC	2 minutes
Amplification	45	95ºC 60ºC 72ºC	15 seconds 10 seconds 10 seconds
Melt curve	1	95ºC 65ºC 97ºC	5 seconds 1 minute Continuous
Cooling	1	40ºC	30 seconds
1-step qPCR			
Reverse transcription	1	45ºC	10 minutes
Polymerase activation	1	95ºC	2 minutes
Amplification	40	95ºC 60ºC 72ºC	10 seconds 10 seconds 30 seconds
Melt curve	1	95ºC 65ºC 97ºC	5 seconds 1 minute Continuous
Cooling	1	40ºC	30 seconds

The output from the Lightcycler is the cycle threshold (Ct) value. The Ct value for each gene of interest was normalised to the housekeeping gene Glyceraldehyde 3-phosphate dehydrogenase (GPADH). GAPDH is present in every cell and its expression is not altered by other genetic changes. To determine the relative expression of each gene in young controls and aged mice first the ΔCt value for a specific gene was quantified by subtracting the Ct of the housekeeping gene from the Ct of the gene. The ΔΔCt could then be calculated by subtracting the ΔCt of the test condition (samples from aged mice) from the young control. The fold change in expression was then determined relative to control young cells by $2^{-\Delta\Delta Ct}$. Each sample was replicated at least four times.

2.8.5.2. Taqman based mitochondrial DNA analysis

For the co-culture experiment assessing mitochondrial content and to quantify mitochondrial DNA content in BMSCs, DNA was extracted as described above. qPCR using Taqman probes Tert, ND1 and ND3 and COX3 (ThermoFisher, Waltham, MA, USA) was then performed. Tert is a genomic probe whereas ND1, ND3 and COX3 are mitochdrial DNA probes. The ND3 and COX3 probes have two sequence specific fluorophores, 2′-chloro-7′phenyl-1,4-dichloro-6-carboxy-fluorescein (VIC) and 6- Carboxyfluorescein (FAM), that can be used to differentiate between single nucleotide polymorphisms (SNP) in the mitochondrial DNA of C57Bl/6 mice and CBA mice. In CBA mice ND3 is detected on FAM and on VIC, whilst COX3 is only detected on FAM. In C57Bl/6 mice on the other hand, both ND3 and COX3 only show positive fluorescence on VIC (Table 2.5). Therefore, any COX3 detected on VIC must originate from a C57Bl/6 mouse. The Taqman assays were run in simplex reactions so that both fluorescence of both VIC and FAM could be analysed.

Table 2.5. Table to show detection of COX3 and ND3 SNPs in CBA and C57Bl/6 mice on FAM and VIC fluorophores

	COX3	ND3
FAM	CBA	CBA
VIC	C57Bl/6	CBA and C57Bl/6

To analyse the mitochondrial DNA content of BMSCs, the Tert and ND1 probes were used. The COX3 and ND3 probes were used together with Tert for the mitochondrial transfer experiment. A master mix was made for each primer containing 0.25µl of primer, 2.5µl TaqPath and 1.25µl nuclease free water per sample. 4µl of master mix and 1 µl of DNA were plated onto a 384 plate. The plate was sealed and centrifuged at 1000 rpm for 1 minute. It was then run on pre-defined programme in a Roche LightCycler 480 (Roche, Basel, Switzerland) (Table 2.6). Ct values were obtained and mitochondrial DNA Ct values were normalised to genomic Ct values. The ΔΔCt method described above was used to calculate the relative mitochondrial copy numbers in each sample. For the mitochondrial transfer experiment detection of COX3 on VIC was used to quantify the relative mitochondrial content originating from C57Bl/6 mice in the LK cells from which the DNA was extracted.

Table 2.6. Taqman® assay Lightcycler programming

	Cycles	Temperature	Time
Pre-amplification	1	60ºC 95ºC	30 seconds 5 minutes
Amplification	50	95ºC 60ºC	15 seconds 1 minute
Cooling	1	40ºC	30 seconds

2.9. Quantification and Statistical Analysis

All analysis in this study was carried out using FlowJo software version 10.8.1 (FlowJo, LLC, Ashland, OR, USA), GraphPad Prism software version 9.4.1 (GraphPad Software, San Diego, CA, USA) and Microsoft Excel (Alburquerque, NM, USA). Due to variability in the data, particularly when carrying out *in vivo* work, statistical comparison was performed without an assumption of normal distribution using the Mann-Whitney test. For comparison of more than two groups the Two-way ANOVA followed by Tukey's multiple comparison test was used. Differences among groups were considered significant when the probability value, p, was less than 0.05 (*P < 0.05, **P < 0.01, ***P < 0.001, ****P<0.0001, ns = not significant). Results are represented showing each sample value and the standard deviation. Sample size (n) represents number of biological replicates. No statistical methods were used to pre-determine sample size.

3. Characterising the metabolic profile of aged HSCs

3.1. Introduction

Some age-related changes in the BM microenvironment and haematopoietic stem cell (HSC) population have been well characterised. These include overall expansion of cell populations, a shift to favour myeloid differentiation and a reduced self-renewal capacity of the HSCs (141, 148). It is becoming increasingly clear that HSC health and, consequently, also these age-related changes are strongly influenced by the BM microenvironment (135). It is therefore important to consider ageing of the HSC population in the context of the ageing BM microenvironment.

The metabolic profile of HSCs is vital, not only to maintain their state of quiescence and long-term health (234), but also to appropriately upregulate energy production in the response to stress (91). Mitochondrial health in particular is key to HSC function and has been shown to decline with age (248). Moreover, HSCs have been shown to become more heterogenous with age and it is therefore possible that different sub-populations of HSCs exist with varying functional capacities (143). Any changes in HSC metabolism and overall health will likely impact on the function and health of the downstream haematopoietic progenitor cells (HPCs). In this thesis I will study both the HSC and HPC populations, as defined in Figure 1.5, and determine how their metabolic profile changes with age and how this in turn is influenced by changes in the aged BM microenvironment.

Mitochondrial content, function and health can be measured using a number of well characterised mitochondrial dyes using flow cytometry. MitoTracker Green (MTG) is a fluorescent dye which localises to mitochondria irrespective of their mitochondrial membrane potential and can, therefore be used to measure total mitochondrial content (249). Mitochondrial membrane potential can be measure using Tetramethylrhodamine, Methyl Ester (TMRM). This is a lipophilic cationic fluorescent dye which accumulates in active mitochondria proportionately to the mitochondrial membrane potential (250). Finally,

MitoSox is a positively charged probe that accumulates in mitochondria, where it is oxidised by superoxide. The oxidised product is fluorescent and directly reflects the levels of mitochondrial superoxide production and is therefore a measure of mitochondrial reactive oxygen species (ROS) (251). Others have shown that these dyes can be exported by HSCs and HPSs through calcium channels and this can impact the staining and detection of these dyes (252). Therefore, all stains were applied together with the calcium channel blocker verapamil, which has been shown to effectively block this efflux of these mitochondrial dyes (253).

In this chapter I aim to define the age-related changes of HSCs and HPCs and, in particular, to characterise the mitochondrial changes in these cell populations. Furthermore, I will also determine how the BM microenvironment may influence these changes. Finally, I will examine whether mitochondrial function can be used to define sub-populations of HSCs with different functional profiles.

3.2. Defining age-related mitochondrial changes in HSCs and HPCs

To analyse the age-changes in HSC and HPC populations young (8-12 weeks old) and aged (18-24 months old) female C57Bl/6 mice were sacrificed. BM was extracted from the femurs and tibias by centrifugation and stained with antibodies for cells surface markers and different mitochondrial dyes in preparation flow cytometric analysis (Figure 3.1A). Figure 3.1B shows the gating strategy for the HPC populations of LS-Ks (Lin-, CD117+, Sca1-), LSKs (Lin-, CD117+, Sca1+) and MPPs (Lin-, CD117+, Sca1+, CD150-, CD48+) and the HSC population (Lin-, CD117+, Sca1+, CD150+, CD48-). All gating was determined using fluorescent minus one (FMO) controls.

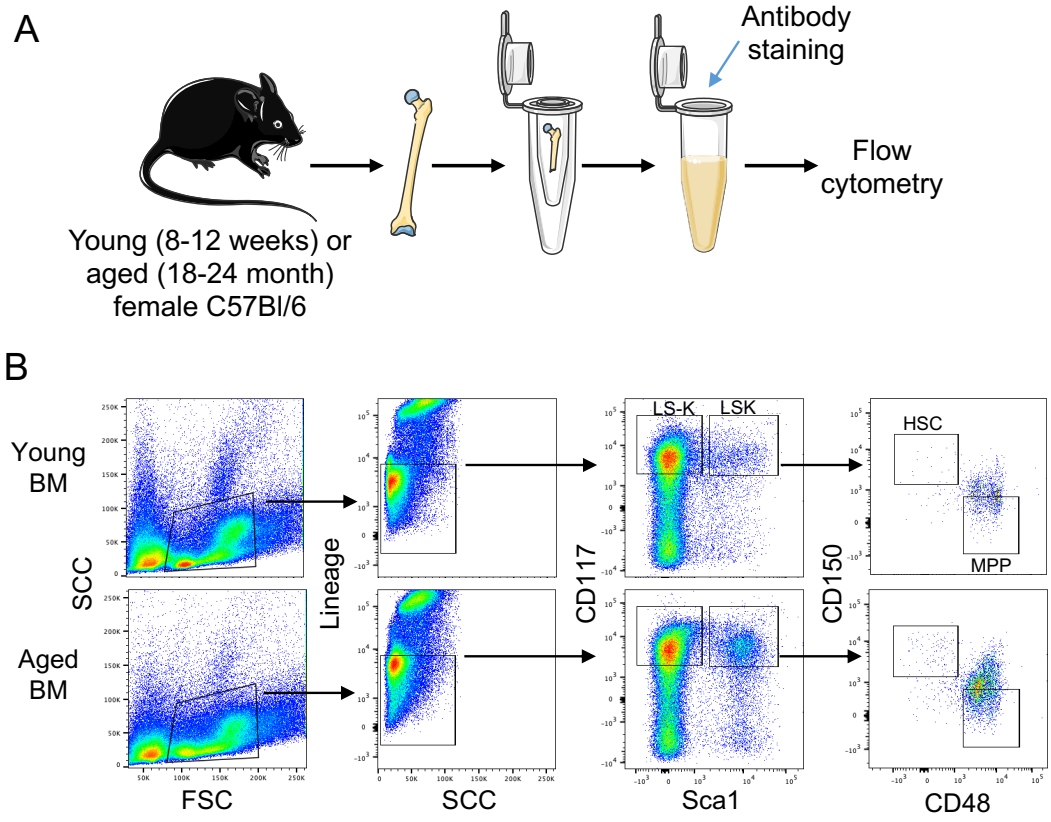

Figure 3.1. Gating strategy for HSCs and HPCs in young and aged mice. *(A) Schematic to show BM was isolated from the femurs and tibias of 8–12-week-old mice and 18-24 months old mice and subsequently stained for flow cytometry to identify different HSC and HPC populations. (B) Using one example from a young and one example of an aged mouse, the gating strategy for LS-Ks (Lin-, CD117+, Sca1-), LSKs (Lin-, CD117+, Sca1+), HSCs (Lin-, CD117+, Sca1+, CD150+, CD48-) and MPPs (Lin-, CD117+, Sca1+, CD150-, CD48+) is shown.*

First, the cell counts of each of these populations was determined and HSC, LSK and MPP counts were found to be increased in aged mice compared to young mice. Although there was no significant difference in the cell counts of LS-Ks (Figure 3.2).

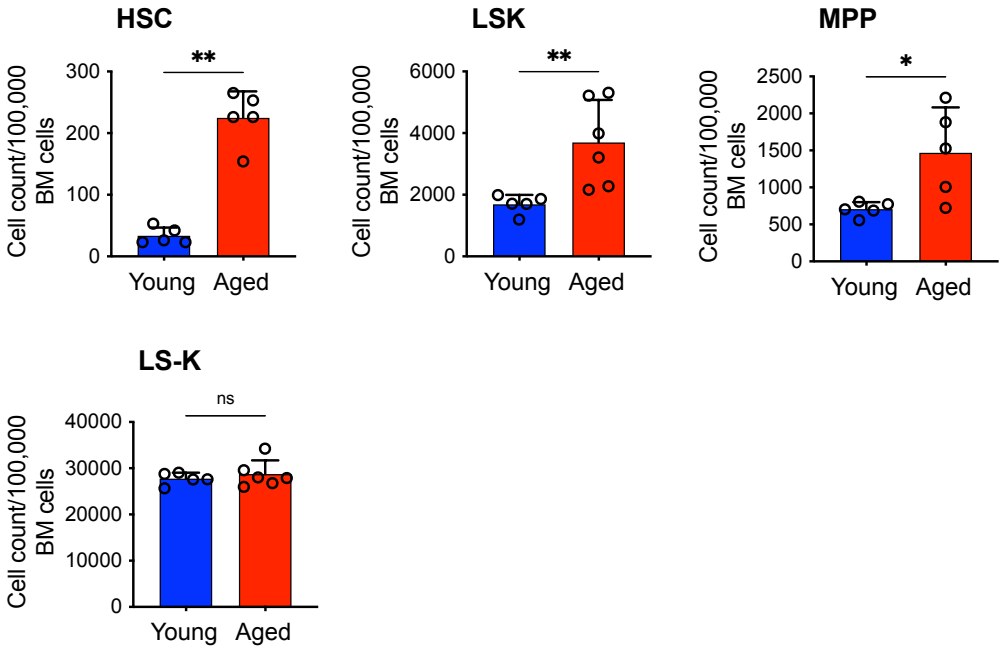

Figure 3.2. Haematopoietic cell populations expand in aged mice.
*Cells were isolated from young and aged mice and cell counts of HSCs, LSKs, MPPs and LS-Ks, per 100,000 BM cells were determined by flow cytometry. *P < 0.05, **P < 0.01, ns = not significant using Mann-Whitney U test.*

Next, peripheral blood samples were taken from both young and aged mice and, following red cell lysis, samples were stained for flow cytometry analysis of nucleated peripheral blood (PB) cell populations. Staining with DAPI was used to define the live cell populations. Frequencies of monocytes (CD11b+, Ly6G-), neutrophils, CD11b+, Ly6G+), T cells (CD4+ or CD8+) and B cells (CD19+) were measured (Figure 3.3A) and the relative myeloid to lymphoid frequency was determined. Figure 3.3B shows that, as expected, there is shift towards increased myeloid cell production in aged mice. This data is consistent with previously published data, showing increased BM cellularity and myeloid shift (141, 148).

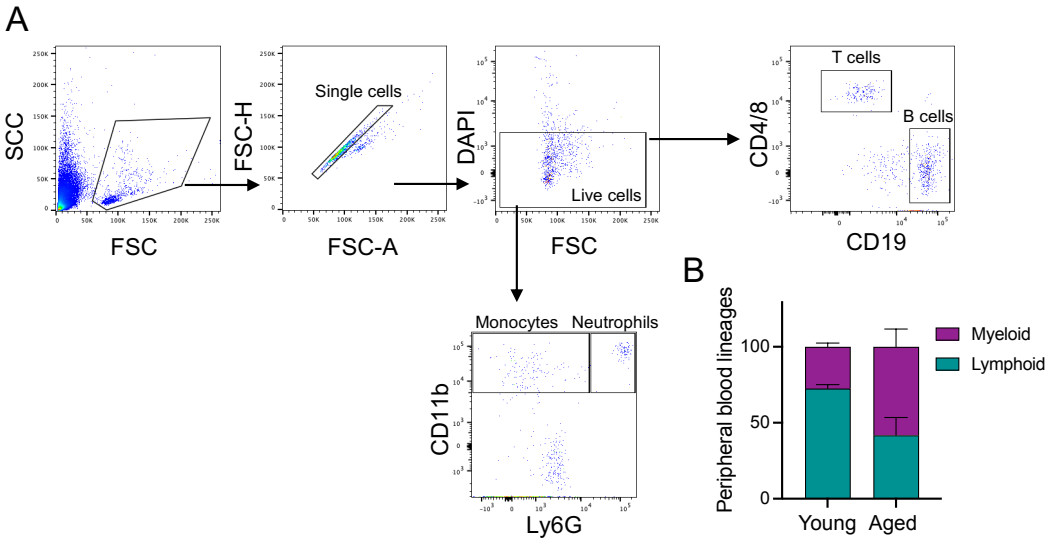

Figure 3.3. Nucleated peripheral blood cells from aged mice show myeloid bias.
(A) The gating strategy for nucleated PB cells is shows: First single mononuclear live cells were identified using FSC-Area (FSC-A) and FSC-Height (FSC-H) as well as DAPI staining. Next gating was applied to define lymphoid cells, CD19+ B cells and CD4+ or CD8+ T cells and myeloid cells, monocytes (CD11b+, Ly6G-) and neutrophils, (CD11b+, Ly6G+). (B) The relative frequency of lymphoid and myeloid cell populations in young and aged mice is shown.

Mitochondrial membrane potential, mitochondrial content and mitochondrial ROS were measured to assess how mitochondrial health changes in aged HSCs and HPCs. As previously described (248), staining with TMRM revealed two distinct cell populations, TMRM high ($TMRM^{hi}$) cells and TMRM low ($TMRM^{lo}$) cells, in both young and aged mice (Figure 3.4A). The results show that the frequency of $TMRM^{hi}$ HSCs, LSKs, MPPs and LS-Ks is significantly reduced in the BM of aged mice (Figure 3.4B). This may suggest a reduction in overall mitochondrial function or activity in the aged HSCs and HPCs.

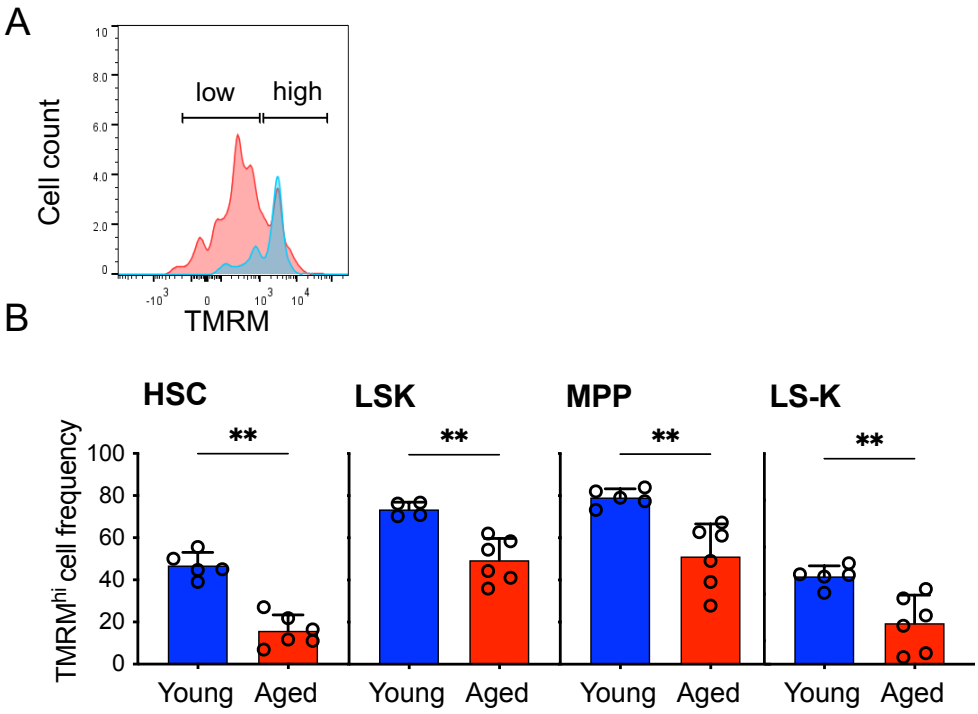

Figure 3.4. Mitochondrial membrane potential declines in haematopoietic cells of aged mice.
*(A) Representative flow cytometry plot of TMRM staining of HSCs in young (blue) and aged (red) mice with $TMRM^{hi}$ and $TMRM^{lo}$ cell populations shown. (B) $TMRM^{hi}$ cell frequencies of HSCs, LSKs, MPPs and LS-Ks is shown in BM isolated from young and aged mice. *P < 0.05, **P < 0.01, ns = not significant using Mann-Whitney U test.*

Next, mitochondrial content of the cells was measured using MitoTracker Green (MTG). Mitochondrial content was found to be increased in HSCs and LSKs from aged mice (Figure 3.5). It is possible that this is a compensatory mechanism to counteract the decline in mitochondrial function but it may also reflect in inability to effectively clear dysfunctional mitochondria. No change was observed in the MPPs or LS-Ks.

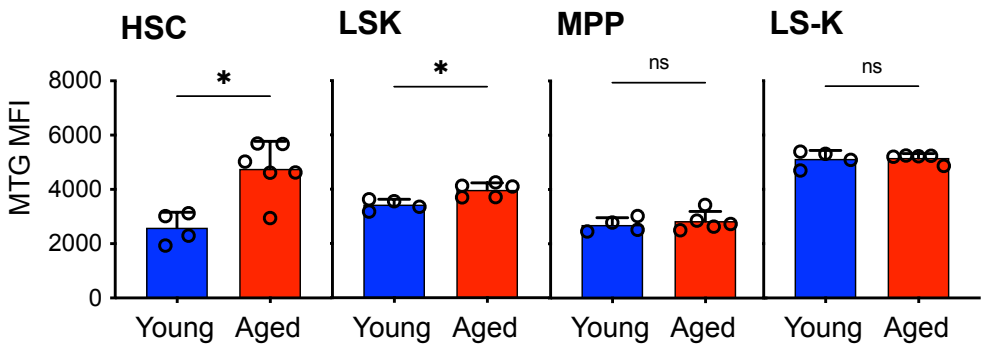

Figure 3.5. Mitochondrial content increases in HSCs and LSKs from aged mice.

*Mean fluorescent index (MFI) of MTG staining in HSCs, LSKs, MPPs and LS-Ks isolated from young and aged mice is shown. *P < 0.05, ns = not significant using Mann-Whitney U test.*

Finally, MitoSox dye was used as a measure for mitochondrial ROS. As with TMRM, two cell populations, MitoSox high (MitoSox^{hi}) and MitoSox low (MitoSox^{lo}) were identified (Figure 3.6A). The frequency of MitoSox^{hi} HSCs was, in fact, found to be reduced in aged mice (Figure 3.6B), which suggests reduced levels of mitochondrial ROS. However, this could be a result of the overall reduced mitochondrial activity and function in the HSCs. No changes were observed in the MitoSox levels of the LSKs or MPPs of aged mice and there was also a reduction in the MitoSox^{hi} cell frequency of the LS-Ks (Figure 3.6C). Together this data suggests that in HSCs and HPCs from aged mice there is an accumulation of mitochondria but this coincides with a decline in mitochondrial function.

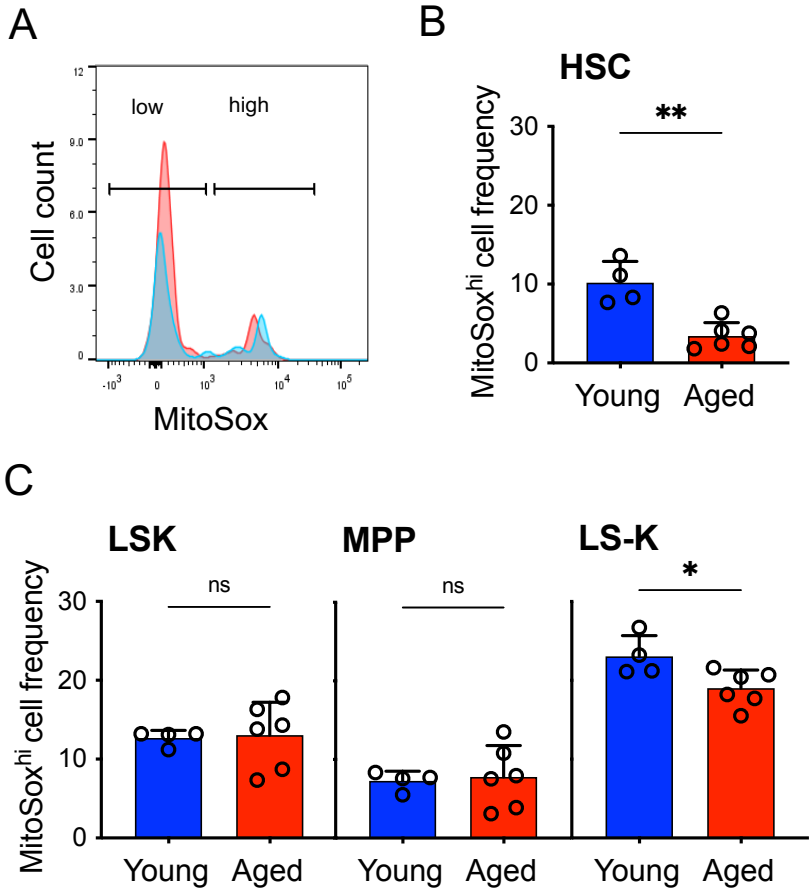

Figure 3.6. Changes in mitochondrial ROS in HSCs and HPCs of aged mice compared to young.

*(A) Example of MitoSox staining of HSCs isolated from young (blue) and aged (red) mice with MitoSox^{hi} and MitoSox^{lo} cell populations shown. (B) MitoSox^{hi} cell frequency of HSCs from young and aged mice. (C) MitoSox^{hi} cell frequencies of LSKs, MPPs and LS-Ks. *P < 0.05, **P < 0.01, ns = not significant using Mann-Whitney U test.*

To define the proliferative activity of HSCs in the steady state in the aged and young mice, BM cells were fixed and permeabilised and cell cycling was measured using Ki-67. Ki-67 is a nuclear protein expressed by proliferating cells and can therefore be used to assess the proportion of actively dividing cells amongst cell populations (254). The Ki-67 positive population was defined using FMO controls (Figure 3.7A). HSCs from aged mice showed no change in cycling activity compared to young mice (Figure 3.7B) and the same was true in LSKs, MPPs and LS-Ks. Overall, HSCs, LSKs and MPPs from both young and aged mice had low levels of cell cycling, whilst a higher percentage of LS-Ks were found to be cycling (Figure 3.7C). This suggests that the mitochondrial changes in the HSCs and HPCs of aged mice does not directly affect cell cycling in the steady state.

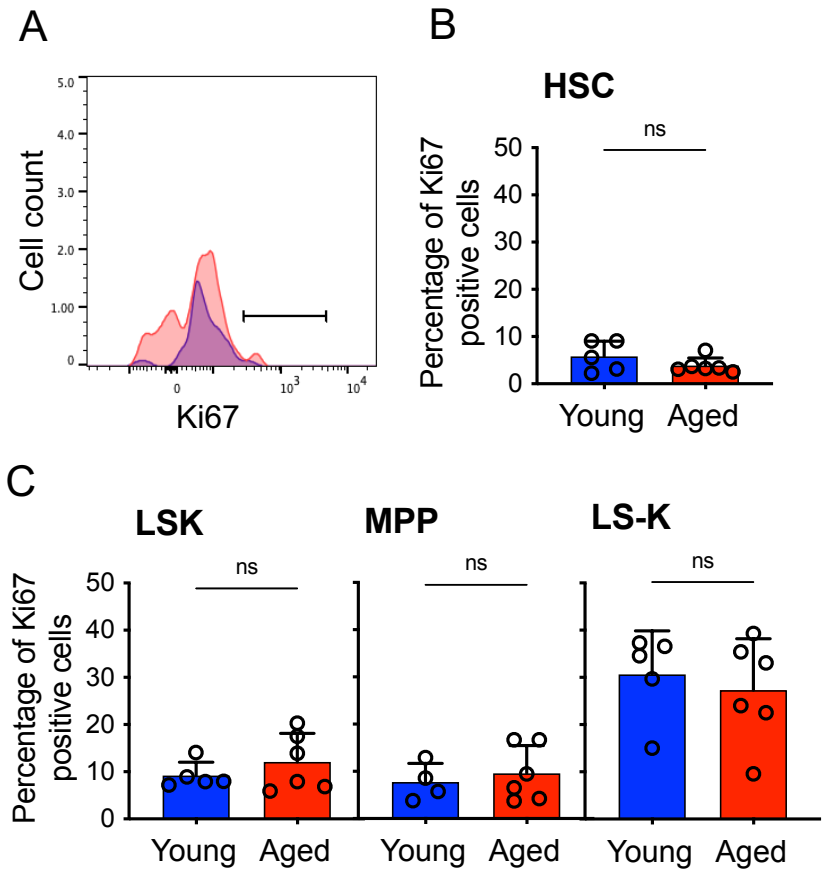

Figure 3.7. Ki67 is not changed in HSCs and HPCs from aged mice.
*(A) Flow plot example of Ki67 staining in young (blue) and aged (red) HSCs with a representative gate for the Ki67 positive cell population identified by the FMO control. (B) Percentage of Ki67 positive HSCs in young and aged mice. (C) Percentage of Ki67 positive LSKs, MPPs and LS-Ks is shown. *P < 0.05, ns = not significant using Mann-Whitney U test.*

3.3. Transplantation into a young BM microenvironment improves HSC mitochondrial health

The BM microenvironment plays a vital role in regulating and maintaining HSC and HPC function. To determine whether the BM microenvironment can influence the mitochondrial health of aged HSCs and HPCs, a previously established transplant model was adapted (240). This model uses PepCboy and C57Bl/6 mice as these two mouse strains express different alleles of the CD45 cell surface marker, PepCboy mice express CD45.1 and C57Bl/6 mice express CD45.2 (255, 256). As CD45 is commonly expressed on all haematopoietic cells, this model allows tracking of any engrafted haematopoietic cells from one mouse strain in the other (257, 258). Here, young female PepCboy (CD45.1+) mice were treated with 25mg/kg of busulfan for 3 days. One day later LSKs from young and aged female C57B/6 (CD45.2+) mice were purified by fluorescent activated cell sorting (FACS) and injected by tail vein injection into busulfan conditioned PepCboy mice (Figure 3.8). LSKs were used in this transplant model as this allows quicker isolation of more cells using FACS and therefore reduces the ex-vivo time of the cell populations to maximise their viability for transplantation. A proportion of the LSK cells isolated are the HSCs which have the ability to engraft and repopulate the host BM. After 12 weeks the mice were sacrificed, PB samples were taken and the BM was extracted and analysed by flow cytometry.

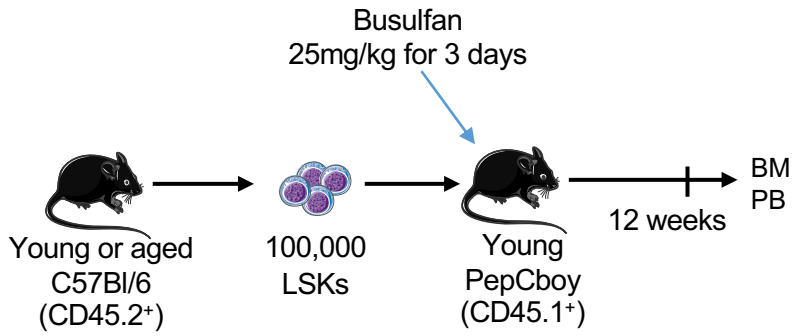

Figure 3.8. Schematic of the transplant model.
The set-up of the transplant is shown. LSKs were isolated from young and aged C57Bl/6 (CD45.2+) mice and 100,000 cells transplanted into each young PepCboy (CD45.1) mouse that was previously treated with 25mg/kg busulfan for 3 days. After 12 weeks engraftment was confirmed by analysis of PB and isolated BM.

Figure 3.9A shows an example of the gating strategy to determine engraftment of the CD45.2+ donor cells in the CD45.1+ host mice. Although LSKs from aged mice were able to re-populate the BM of young mice this was slightly reduced when compared to the engraftment of LSKs from young mice (Figure 3.9B).

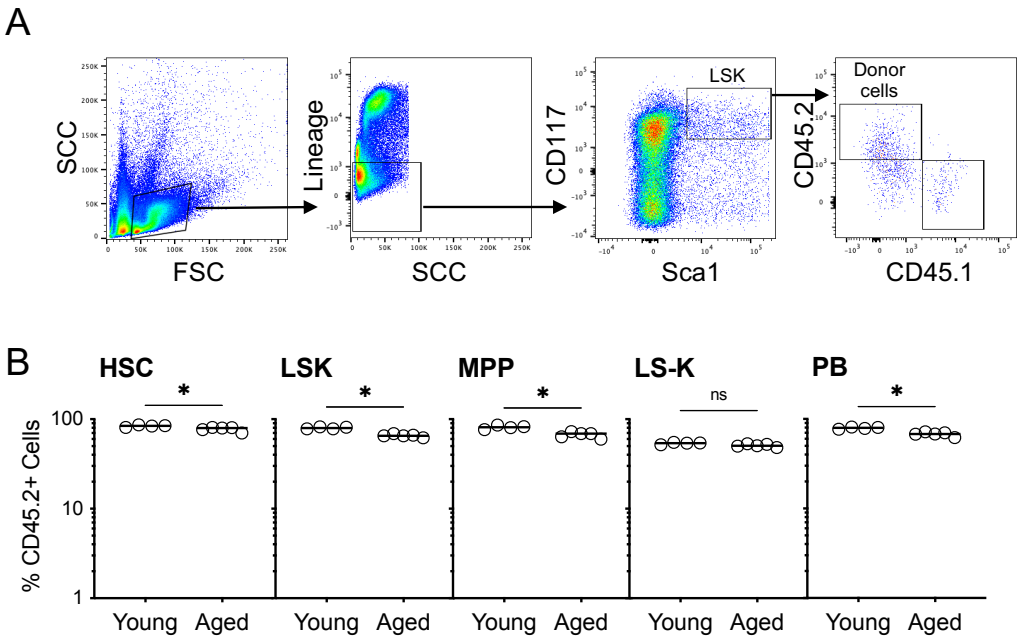

Figure 3.9. LSKs from aged mice are able to re-populate the young BM. *(A) Representative flow cytometry plot showing the gating strategy for identifying engrafted CD45.2 donor LSKs in the BM isolated from young CD45.1+ PepCboy mice 12 weeks after transplantation. (B) Percentage engraftment (CD45.2+ cells) of HSCs, LSKs, MPPs and LS-Ks as well as PB cells is shown in PepCboy mice transplanted with LSKs from either young or aged C57Bl/6 mice. *P < 0.05, ns = not significant using Mann-Whitney U test.*

Next, to determine if the young BM microenvironment can alter the HSC and HPC populations, the engrafted CD45.2 cells were analysed further by flow cytometry. Cell counts of CD45.2+ HSCs, LSKs and LS-Ks were found to be the same in mice engrafted with aged LSKs compared to those engrafted with young LSKs, although there was a small reduction in MPP counts (Figure 3.10A). Furthermore, examination of the CD45.2+ nucleated PB cells revealed that the myeloid bias observed in aged mice was corrected following the transplant into young mice (Figure 3.10B). This data suggests that transplantation of LSKs from aged mice into a young BM microenvironment reverses some of the age-related changes observed, including the increase in BM cellularity and the shift towards myeloid differentiation.

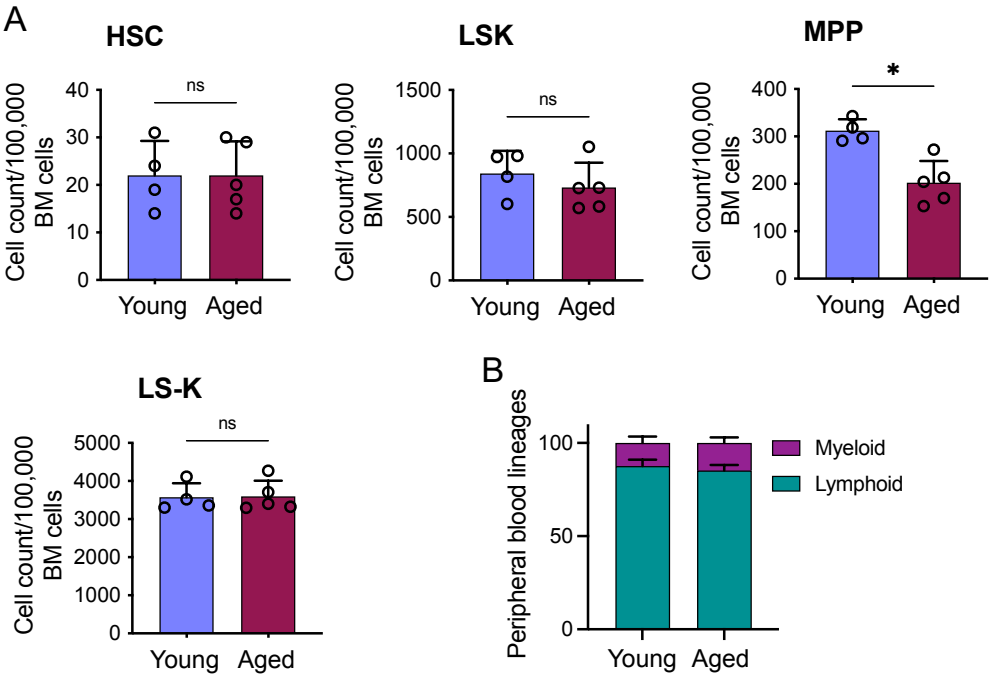

Figure 3.10. BM cell counts and PB lineage distribution following transplantation of young and aged LSKs.
(A) Cell counts per 100,000 BM cells of donor CD45.2+ HSCs, LSKs, MPPs and LS-Ks are shown in young PepCboy (CD45.1+) mice transplanted with LSKs from young or aged C57Bl/6 (CD45.2+) mice. (B) Relative distribution of donor myeloid and lymphoid lineages in the PB blood of mice engrafted with young or aged LSKs. ns = not significant using Mann-Whitney U test or Two-way Anova.

Furthermore, when the mitochondrial membrane potential of the HSCs, LSKs, MPPs and LS-Ks was measured, the frequency of $TMRM^{hi}$ cells was found to be the same in cells originating from young and aged mice (Figure 3.11). This suggests that haematopoietic cells from aged mice are able to recover some of their mitochondrial function when transplanted into young mice.

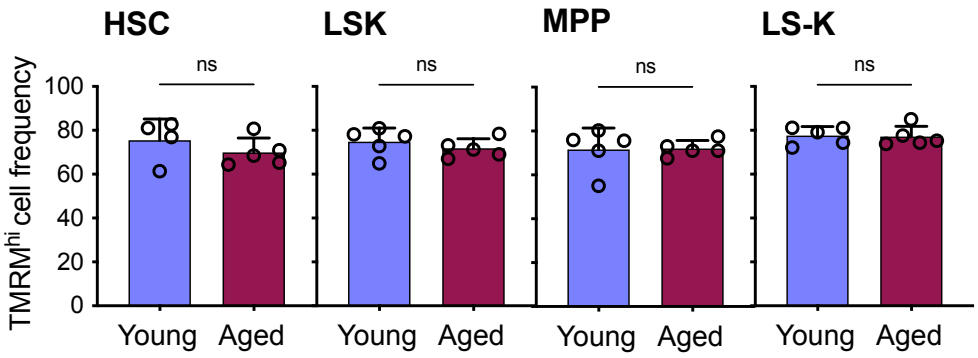

Figure 3.11. Transplantation of aged LSKs into young mice increases their mitochondrial membrane potential.
BM was isolated from mice engrafted with LSKs from young or aged mice and the frequency of $TMRM^{hi}$ donor HSCs, LSKs, MPPs and LS-Ks is shown. ns = not significant using Mann-Whitney U test.

Similarly, little change was observed in the levels of mitochondrial ROS, measured by MitoSox in the HSC and HPC populations of the engrafted CD45.2 positive cells from aged and young transplanted cells (Figure 3.12).

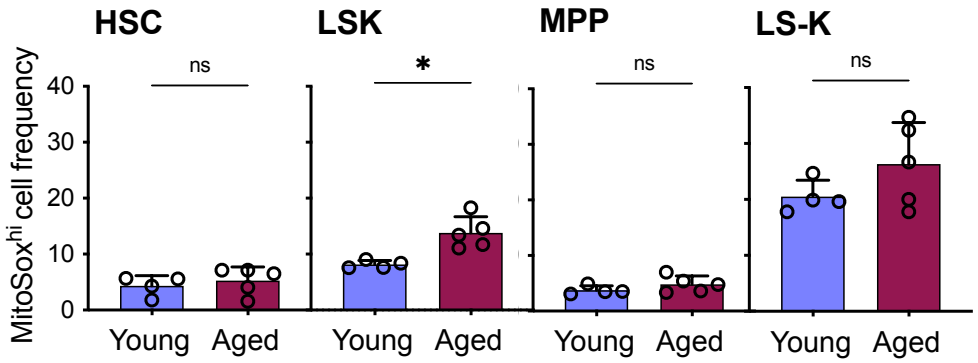

Figure 3.12. MitoSox levels in young and aged HSCs and HPCs following transplantation into young mice.
*$MitoSox^{hi}$ cell frequency in engrafted HSCs, LSKs, MPPs and LS-Ks following transplantation of LSKs from young and aged mice into young mice. *P < 0.05, ns = not significant using Mann-Whitney U test.*

3.4. Mitochondrial membrane potential defines sub-populations of young and aged HSCs

Maintenance of low mitochondrial activity in HSCs has been associated with increased long-term HSC health and improved self-renewal capacity in young mice (259). However, HSCs from aged mice have a significant increase in the frequency of $TMRM^{lo}$ HSCs. To investigate whether all of these cells maintain their function and repopulation ability, a competitive transplant model was set up. BM was isolated from young and aged PepCboy (CD45.1+) mice and first enriched for CD117+ cells using magnetically labelled anti-CD117 microbeads. They were then stained with TMRM, Lineage cocktail, CD117 and Sca1 and $TMRM^{hi}$ and $TMRM^{lo}$ LSKs were FACS purified. The CD117 enrichment prior to cell sorting reduces the time required to sort adequate numbers of $TMRM^{hi}$ and $TMRM^{lo}$ cells and therefore improves overall cell viability. As described above these sorted LSK populations contain either $TMRM^{hi}$ or $TMRM^{lo}$ HSCs (Figure 3.13A). This transplant model was used to determine how mitochondrial membrane potential affects the repopulation potential of HSCs from young and aged mice. Figure 3.13B shows again that the HSCs isolated from aged mice have a significant increase in $TMRM^{lo}$ cell frequency compared to HSCs from young mice. 150,000 $TMRM^{hi}$ or $TMRM^{lo}$ LSKs were adoptively transferred into busulfan conditioned young C57Bl/6 (CD45.2+) mice, together with an equal number of competitive young C57Bl/6 LSKs (Figure 3.13C).

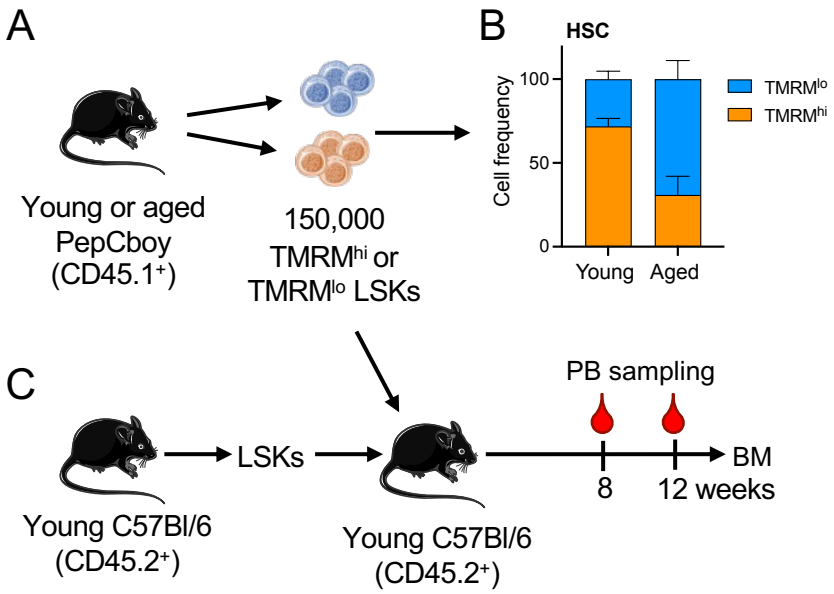

Figure 3.13. Schematic of the completive transplant of TMRM^{hi} and TMRM^{lo} LSKs from young and aged PepCboy mice.
(A) TMRM^{hi} and TMRM^{lo} LSKs were FACS purified from young and aged PepCboy (CD45.1) mice. (B) The relative distribution of TMRM^{hi} and TMRM^{lo} HSCs amongst the FACS purified LSK population used for transplantation. (C) Schematic of the competitive transplant model. Both 150,000 of the FACS purified TMRM^{hi} or TMRM^{lo} LSKs from young or aged PepCboy (CD45.1) mice and 150,000 LSKs from young C57Bl/6 (CD45.2) were injected into young C57Bl/6 (CD45.2) mice by tail vein injection.

To assess engraftment of the different TMRM cell populations from young and aged mice, blood samples were taken from the transplanted mice after 8 and 12 weeks. Flow cytometry was used to determine the percentage of CD45.1+ engrafted PB cells. The TMRM^{lo} cells from both young and aged mice were shown to be engrafted (Figure 3.14A), demonstrating an HSC repopulation potential that is preserved in the TMRM^{lo} HSCs from aged mice. There was very little engraftment of TMRM^{hi} cells from young mice and no engraftment of TMRM^{hi} cells from aged mice. After 12 weeks the mice were sacrificed and their BM extracted for analysis of engraftment as well as TMRM levels. Analysis of HSC, LSK, MPP and LS-K populations were consistent with the PB findings, with good engraftment of the TMRM^{lo} cells from both young and aged mice but little or no engraftment of the TMRM^{hi} cells (Figure 3.14B).

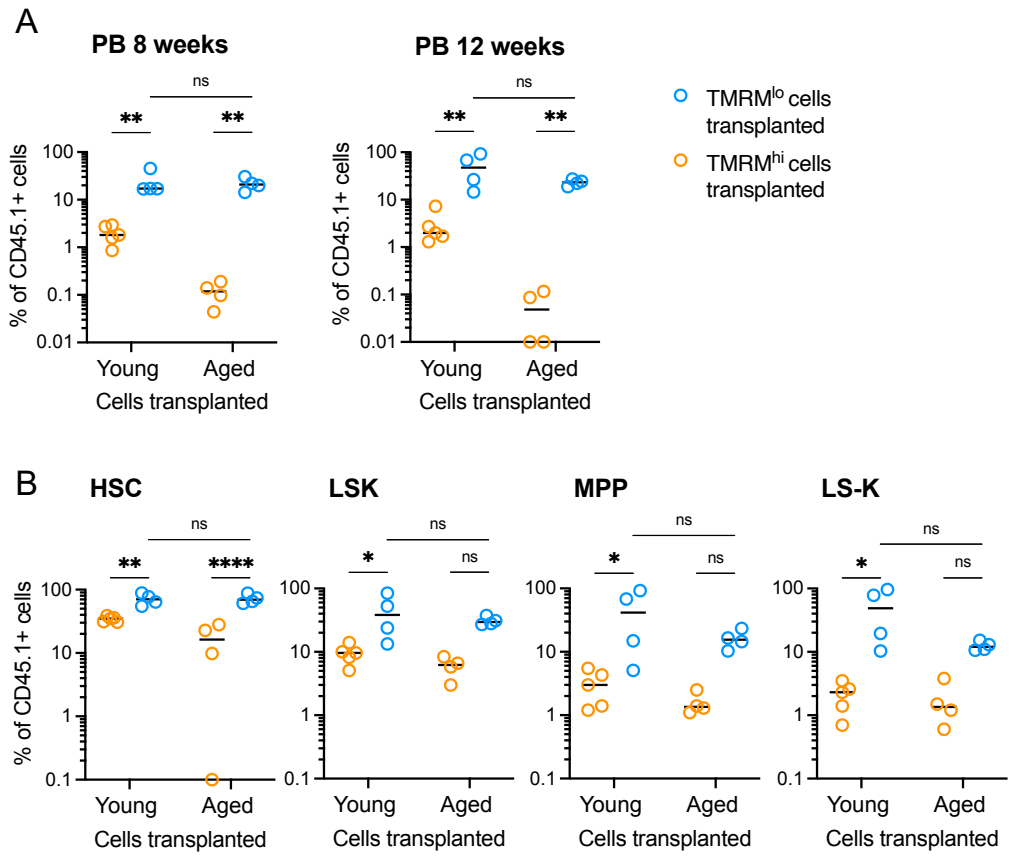

Figure 3.14. TMRM^{lo}, but not TMRM^{hi} HSCs, from young and aged mice are able to repopulate the BM of young mice following transplantation. *(A) PB samples were taken from mice 8 and 12 weeks after the tail vein injection of either TMRM^{hi} or TMRM^{lo} LSKs from young or aged mice. The percentage engraftment, measured by the percentage of CD45.1 donor PB cells detected by flow cytometry, is at 8 and 12 weeks is shown. (B) 12 weeks after transplantation the mice were sacrificed and the percentage engraftment of the CD45.1 HSC, LSK, MPP and LS-K populations was analysed by flow cytometry. *P < 0.05, **P < 0.01, ****P<0.0001, ns = not significant using Two-way Anova.*

Next, the BM and PB from mice engrafted with TMRM^{lo} LSKs was further analysed to assess the distribution of mature nucleated CD45.1+ donor blood cell populations. In the BM there was an increase in myeloid lineages in mice engrafted with TMRM^{lo} cells from aged mice compared to young but a similar distribution of the cell populations was seen in the PB samples from both groups of mice (Figure 3.15).

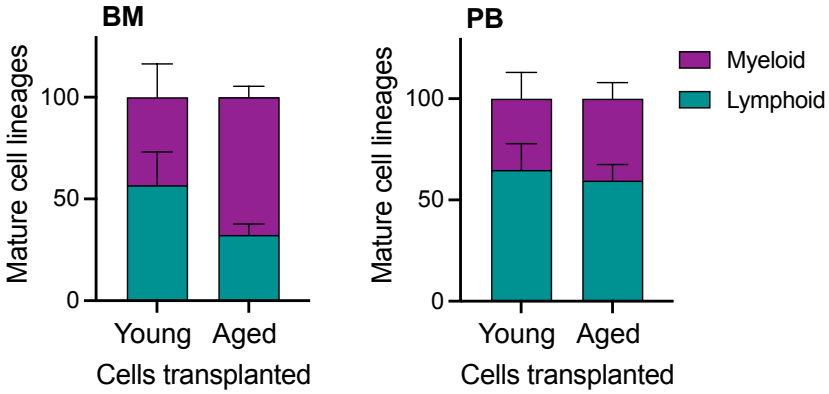

Figure 3.15.. Distribution of donor mature blood cells in the BM and PB of mice engrafted with TMRM^{lo} LSKs from young or aged mice.
Analysis of the mature blood cell populations in BM and PB samples from C57Bl/6 mice successfully engrafted with TMRM^{lo} LSKs from either young or aged mice. Relative distributions of myeloid and lymphoid cell populations are shown.

Examination of the mitochondrial membrane potential of the CD45.1+ HSCs, LSKs, MPPs and LS-Ks, using TMRM, revealed that the engrafted TMRM^{lo} cells from both young and aged mice gave rise to progeny with both TMRM^{hi} and TMRM^{lo} signatures (Figure 3.16). Furthermore, the relative frequency of engrafted TMRM^{hi} and TMRM^{lo} HSCs from young and aged mice was similar to that observed in young mice, with only a small number of TMRM^{lo} HSCs.

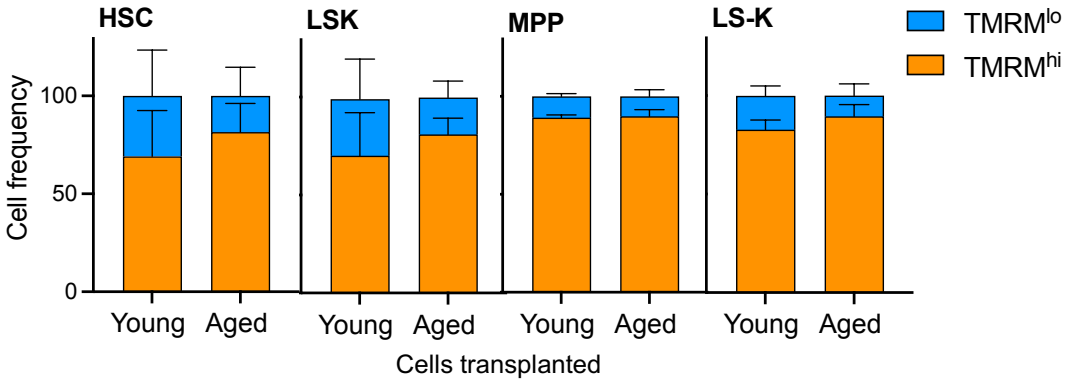

Figure 3.16.Engrafted TMRM^{lo} HSCs give rise to both TMRM^{lo} and TMRM^{hi} progeny.
Relative frequencies of TMRM^{lo} and TMRM^{hi} HSCs, LSKs, MPPs and LS-Ks in mice engrafted with TMRM^{lo} HSCs from young or aged donors are shown.

To further define the long-term repopulation potential of TMRM^{lo} HSCs from young and aged mice a subsequent secondary transplant was set up. At the termination of the first transplant, BM was isolated from C57Bl/6 (CD45.2+) mice initially engrafted with TMRM^{lo} LSKs from young or aged mice. As described previously BM was enriched for CD117 and subsequently CD45.1+ HSCs were FACS purified. For this secondary transplant HSCs rather than LSKs were used to maximise cell purity. 1000 CD45.1+ HSCs, together with 100,000 CD45.2+ support cells consisting of full BM, were injected into young C57Bl/6 mice by tail vein injection (Figure 3.17).

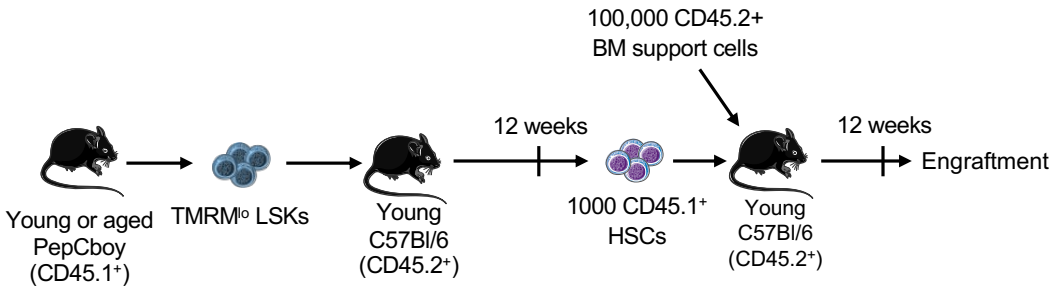

Figure 3.17.Schematic of the secondary transplant model.
CD45.1 LSKs were isolated from young and aged PepCboy mice and engrafted into young CD45.2+ C57Bl/6 mice. After 12 weeks the C57Bl/6 mice were sacrificed, their BM was isolated and CD45.1+ HSCs originating from the young and aged PepCboy mice were FACS purified. 1000 CD45.1 HSCs were subsequently transplanted into each young CD45.2+ C57Bl/6 mouse by tail vein injection together with 100,000 whole BM cells for support. After 12 weeks the experiment was terminated and BM and PB engraftment was established by flow cytometry.

After 12 weeks engraftment was assessed in both the BM and the PB. The TMRM^{lo} HSCs from young mice showed ongoing repopulation potential and engraftment was consistently demonstrated. However, the TMRM^{lo} cells that were originally taken from aged mice had significantly reduced engraftment in this secondary transplant (Figure 3.18). This demonstrates reduced repopulation and self-renewal potential of aged HSCs despite the expansion of the TMRM^{lo} cell population in aged mice.

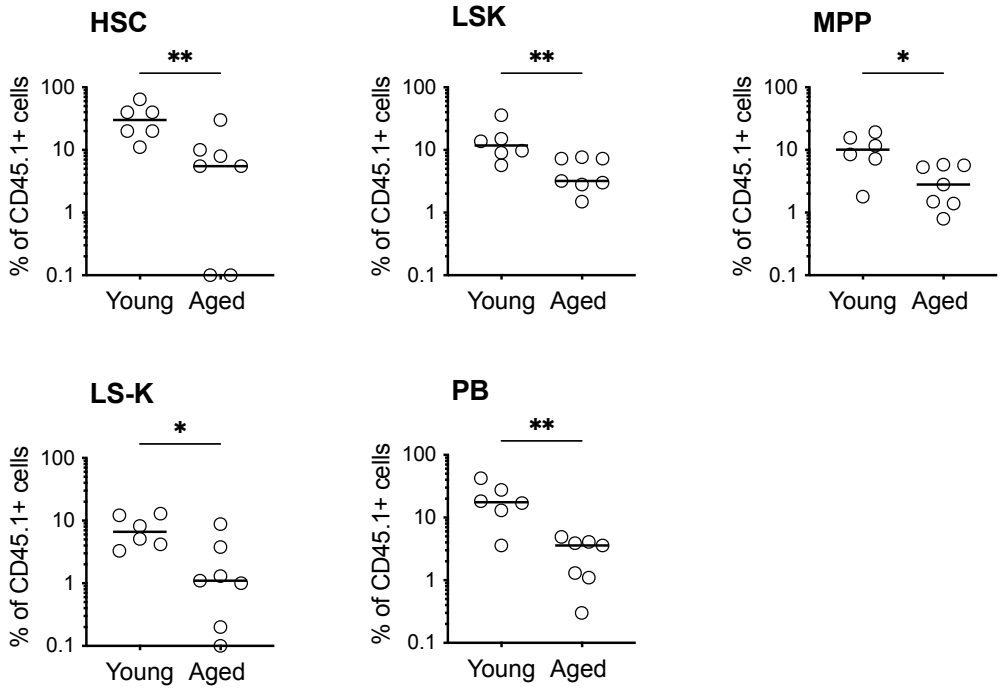

Figure 3.18. TMRM^{lo} HSCs from aged mice fail to engraft in a secondary transplant setting.

BM was isolated and terminal PB samples were taken from the C57Bl/6 mice 12 weeks following the secondary transplant. Flow cytometry was used to measure the percentage engraftment of CD45.1+ HSCs, LSKs, MPPs, LS-Ks and PB cells in the mice injected with cells originating from young or aged PepCboy mice.

Finally, the engrafted cell populations of the TMRM^{lo} HSCs from young mice following the secondary transplant were analysed. PB blood analysis revealed a persistent predominance of lymphocytes over myeloid cells as is seen in healthy young mice (Figure 3.19A). Furthermore, the TMRM^{lo} HSCs continued to give rise to similar frequencies of TMRM^{hi} and TMRM^{lo} HSCs, LSKs, MPPs and LS-Ks as seen in young mice (Figure 3.19B). Due to the reduced engraftment in mice transplanted with TMRM^{lo} HSCs from aged mice there were not sufficient CD45.1+ cells in the PB or BM to analyse the mature cell populations or TMRM levels accurately.

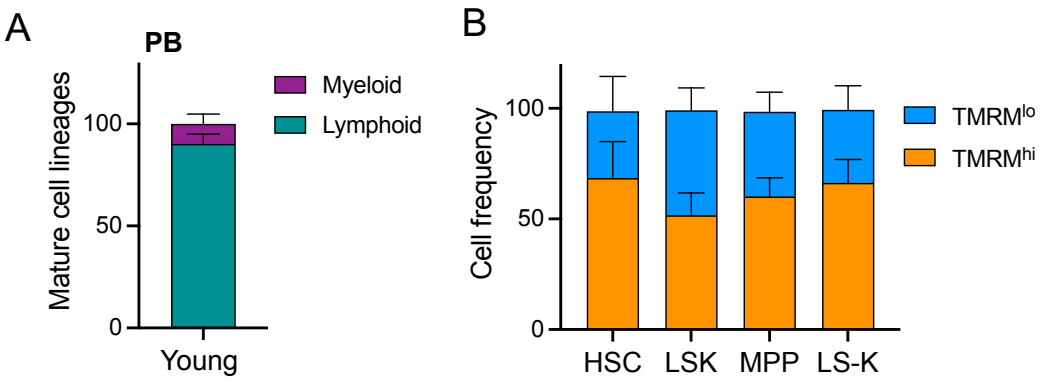

Figure 3.19. Secondary transplantation of TMRM^{lo} HSCs from young mice does not impact on their progeny.
(A) The relative distribution of donor myeloid and lymphoid cells in the PB of mice following secondary transplant of TMRM^{lo} HSCs. (B) Frequencies of TMRM^{lo} and TMRM^{hi} donor CD45.1+ HSCs, LSKs, MPPs and LS-Ks in the BM of C57Bl/6 (CD45.2+) mice following secondary transplantation of TMRM^{lo} HSCs from young mice.

The data shown here demonstrates that whilst in young mice low mitochondrial membrane potential is directly linked to the repopulation potential of HSCs, in aged mice, where the frequency of TMRM^{lo} HSCs increases, this does not correlate with preserved HSC function. Thus, not only are TMRM^{hi} HSCs functionally distinct from TMRM^{lo} cells, but it is likely that amongst the TMRM^{lo} HSCs, there are distinct sub-populations of cells with different functional profiles and self-renewal capacity. In young mice, the TMRM^{lo} HSCs appear to primarily represent the true HSCs with long-term repopulation potential. In old mice on the other hand, whilst some of these true HSCs may remain and therefore allow for some limited self-renewal capacity, the majority of TMRM^{lo} HSCs appear to lose their long-term repopulation potential. In order to further define these different cell populations, BM was isolated from two young and two aged mice and after CD117 enrichment, stained for TMRM and HSC cell surface markers. Single TMRM^{lo} and TMRM^{hi} HSCs were FACS purified for single cell sequencing using the SmartSeq2 protocol (Figure 3.20). Processing and sequencing of these samples is in progress at the time of writing.

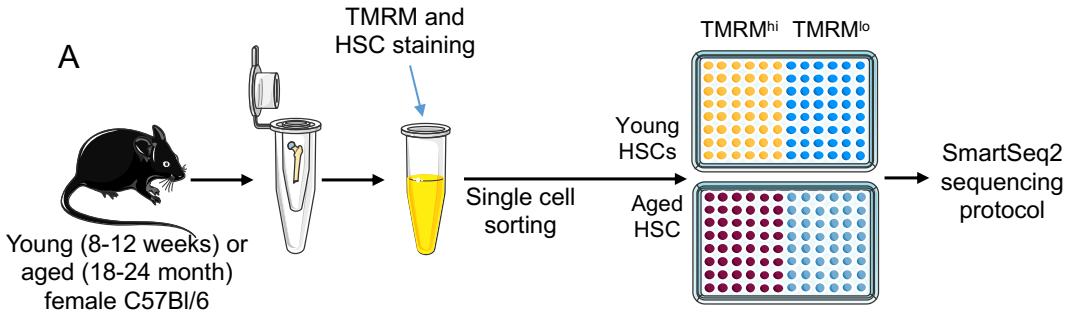

Figure 3.20. Experimental schematic.
BM was isolated from young and aged C57Bl/6 mice and first stained with TMRM and then the HSC antibody panel. Single TMRM^{hi} and TMRM^{lo} HSCs were sorted from each mouse in preparation for SmartSeq2 sequencing.

3.5. Summary

In this chapter I have investigated the mitochondrial health of HSCs in the aged BM and how this impacts on overall HSC function and self-renewal capacity. I have demonstrated that mitochondrial function in HSCs from aged mice declines and that this change can be reversed to an extend by transplanting these cells into a young BM microenvironment. This highlights the importance of the BM microenvironment in supporting HSC function. Finally, I describe how HSCs in young mice can be clearly functionally distinguished based on their mitochondrial membrane potential, with only $TMRM^{lo}$ HSCs having true repopulation potential. Whilst in aged mice a small population of these self-renewing $TMRM^{lo}$ HSCs appears to persist, their repopulation ability is limited and successful engraftment in a secondary transplant was not achieved. In order to be able to characterise these individual HSCs populations in young and aged single cell sequencing is being undertaken, however, the completion and analysis of this is beyond the scope of this thesis.

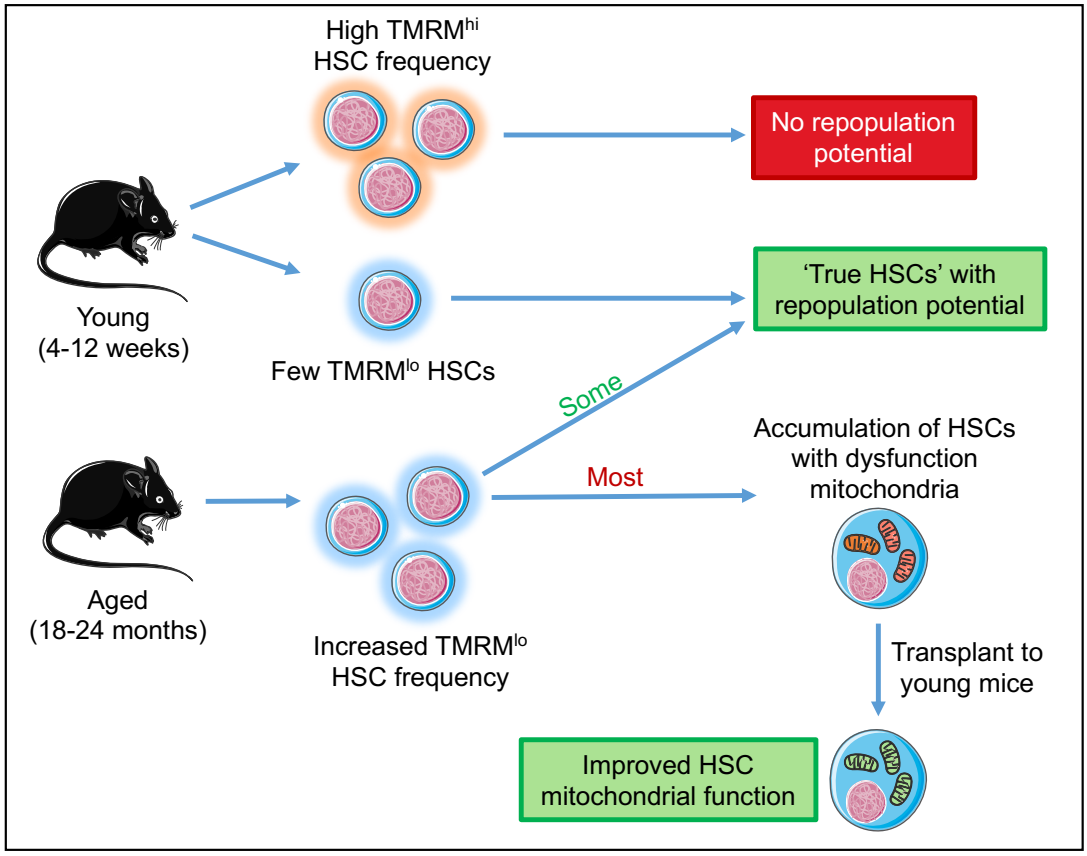

Figure 3.21. Characterising the metabolic profile of aged HSCs.
In young mice most HSCs (Lin-, CD117+, Sca1+, CD150+, CD48-) have a TMRM^{hi} phenotype. However, the transplant model in this chapter demonstrates that it is only the TMRM^{lo} HSCs that have repopulation potential and therefore reflect the true stem cell population. In aged mice the frequency of TMRM^{lo} HSCs is increased, however, their long-term repopulation potential is impaired when compared to TMRM^{lo} HSCs from young mice. This suggests that there may be a sub-population of TMRM^{lo} HSCs in aged mice with a different functional phenotype, but with low levels of TMRM due to an accumulation of dysfunctional mitochondria. Transplantation of the HSCs from aged mice into young mice results in an increase in the TMRM^{hi} HSC frequency reflecting improved HSC mitochondrial function.

4. Defining how age-related metabolic changes alter the haematopoietic response to stress

4.1. Introduction

The burden of infection increases with age, with not only increased incidence of infections, but also an increase in associated morbidity and mortality. The body's ability to respond to and clear infections is dependent on the adequate and rapid production of immune cells and is, therefore, directly linked to HSC function. Infection is thus a model that can be used to study the BM's ability to respond to stress.

In young mice a number of metabolic changes have been described that help to drive rapid HSC expansion and mature blood cell production in response to stress. This includes the acquisition of mitochondria from the BMSC by mitochondrial transfer via Connexin 43 Gap Junctions (91) and an increase in free fatty acid uptake and metabolism (240). Together these changes allow a rapid shift from glycolysis to oxidative phosphorylation (OXPHOS) and therefore a rapid increase in energy production, which is essential to fuel the increased requirement for cell cycling, production and differentiation.

Treatment with lipopolysaccharide (LPS) is frequently used as mimic for infection in *in vivo* mouse models. LPS is the main component of the outer cell membrane of gram-negative bacteria and has been shown to activate the immune response through a number of receptors including Toll-like receptor 4 (TLR-4), LPS binding protein (LBP) and CD14 (260). In this chapter I will investigate how the haematopoietic response to stress changes with age, using LPS treatment. In particular I will determine how ageing alters the metabolic changes in the HSCs and HPC populations that occur in response to LPS treatment. Finally, I will investigate if the age-related metabolic changes can be reversed by adoptively transplanting aged HSCs into a young BM.

4.2. The metabolic response to LPS in aged mice

In young mice LPS treatment has been shown to result in HSC expansion and increased cycling within 16 hours of LPS treatment at a dose of 1mg/kg **(91)**. To determine the effect of LPS treatment on aged mice, both young and aged mice were treated with a lower dose of 0.5mg/kg LPS (Figure 4.1A). Whilst young mice were able to fully recovery from this treatment, in aged mice a relatively quick deterioration in the animals' health was observed even with this low dose of LPS. Figure 4.1B shows Kaplan Meier curve of the survival of young and aged mice following LPS treatment and demonstrates that aged mice did not survive more than 36 hours after the treatment.

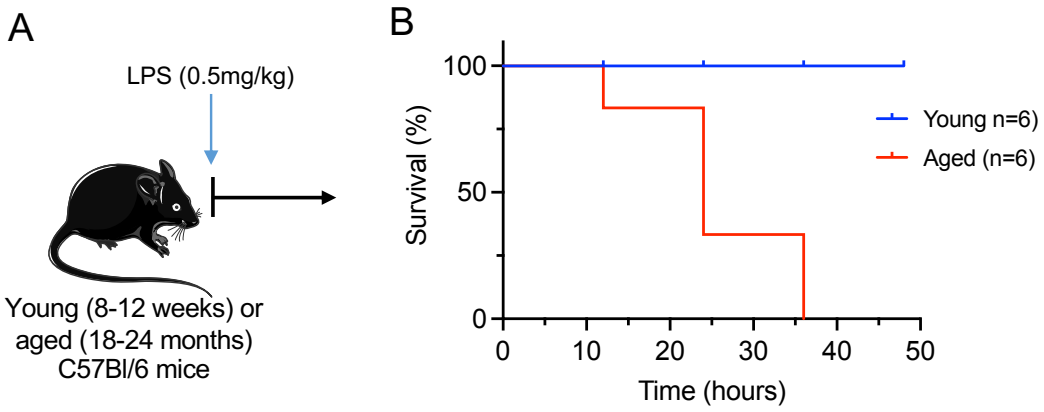

Figure 4.1. Aged mice die within 36 hours of low dose LPS treatment.
(A) Schematic of the experiment. Young or aged mice were treated with 0.5mg/kg LPS and then monitored carefully for signs of deterioration. (B) A Kaplan Meier curve for the survival of young and aged mice following LPS treatment is shown.

To investigate the BM changes in aged mice following LPS treatment, both young (8-12 weeks) and aged (18-24 months) mice were treated with 0.5mg/kg of LPS or vehicle control and sacrificed after 16 hours (Figure 4.2). Their BM was isolated and prepared for analysis by flow cytometry.

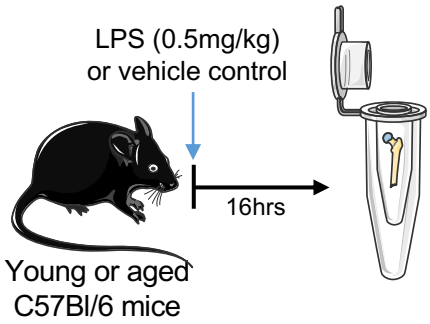

Figure 4.2. Experimental schematic.
Young and aged C57Bl/6 mice were treated with 0.5mg/kg LPS or vehicle control and 16 hours later they were sacrificed and their BM was isolated.

Consistent with previously published data, in young mice the HSC, LSK, MPP and LS-K populations expanded significantly following LPS treatment. However, in aged mice only the LSK count was increased (Figure 4.3).

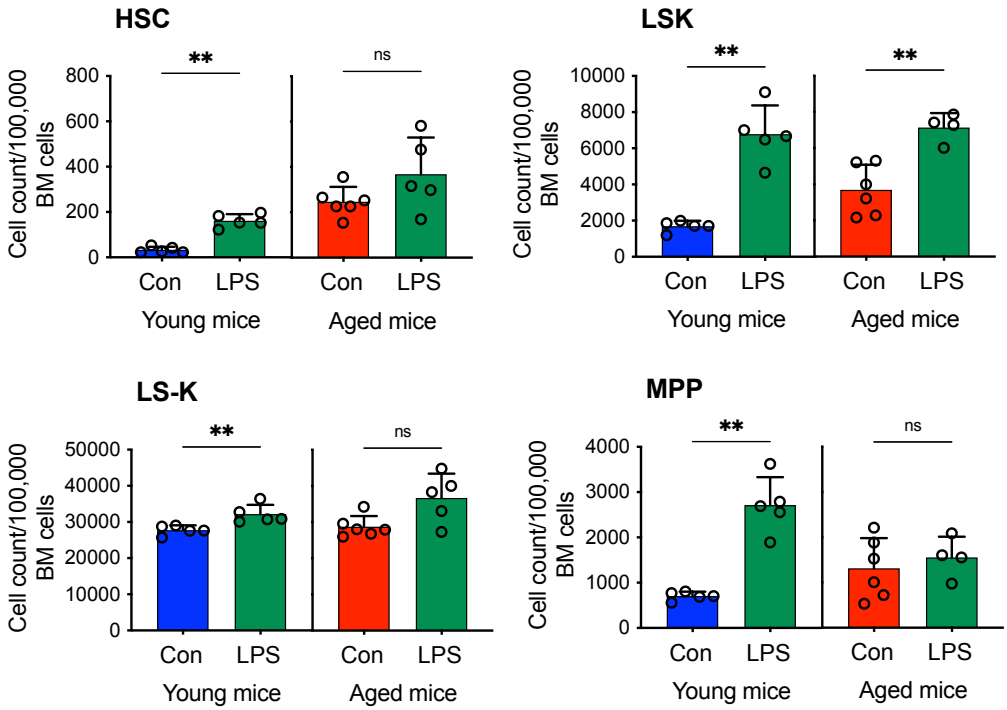

Figure 4.3. HSCs and HPCs from aged mice fail to expand after LPS treatment.
*BM was isolated from young and aged mice treated with LPS and aged matched controls. Cell counts per 100,000 BM cells of the HSCs, LSKs, MPPs and LS-Ks in control mice (con) compared to LPS treated mice are shown. *P < 0.05, **P < 0.01, ns = not significant using Mann-Whitney U test.*

To assess if this lack of expansion in the aged haematopoietic cells is due to reduced cycling, the percentage of Ki-67 positive cells was analysed by flow cytometry. The results show that Ki-67 increases in the HSCs and LSKs from young mice and also in the HSCs from aged mice (Figure 4.4). This demonstrates that in the aged mice HSC cycling is still upregulated in response to LPS treatment.

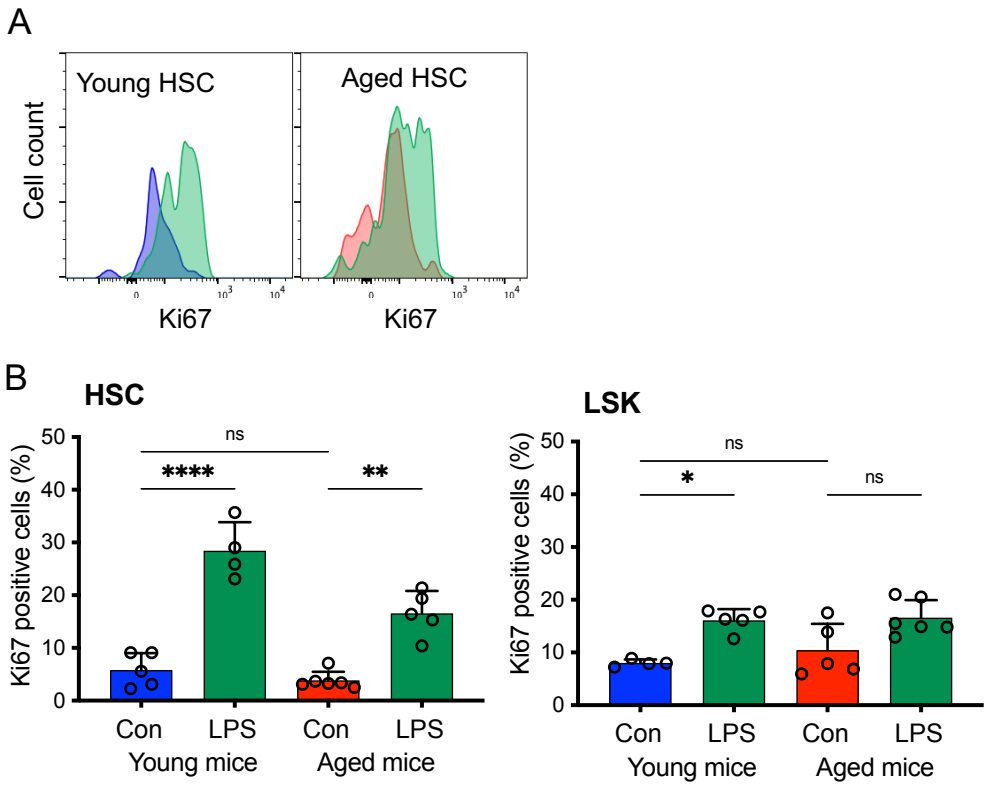

Figure 4.4. Ki67 increases in HSCs from aged mice after LPS treatment. *BM isolated from young and aged mice after LPS treatment and age matched controls was stained for Ki67. (A) Representative flow plot of Ki67 staining in HSCs from young (blue) and aged (red) controls and young and aged LPS treated mice (green). (B) Percentage of Ki67 positive cells in young and aged mice after LPS treatment compared to age matched controls. *P < 0.05, **P < 0.01, ***P < 0.001, ****P<0.0001, ns = not significant using Two-way Anova.*

Next, the metabolic profile of HSCs and HPCs from young and aged mice after LPS treatment was assessed by measuring mitochondrial membrane potential, mitochondrial content and mitochondrial ROS. In young mice, there is a clear increase in the frequency of TMRM^{hi} HSCs after LPS treatment (Figure 4.5A). Furthermore, the TMRM^{hi} LSK and MPP frequency remains stable and there is only a small decrease in the TMRM^{hi} LS-K frequency (Figure 4.5B). In aged mice, on the other hand, there is no change in the TMRM^{hi} HSC frequency and a significant drop in the TMRM^{hi} frequency of LSKs, MPPs and LS-Ks (Figure 4.5A and B). This demonstrates that whilst in young mice LPS treatment results in an increase in mitochondrial membrane potential to help meet the higher energy demands during stress, this is not observed in aged mice.

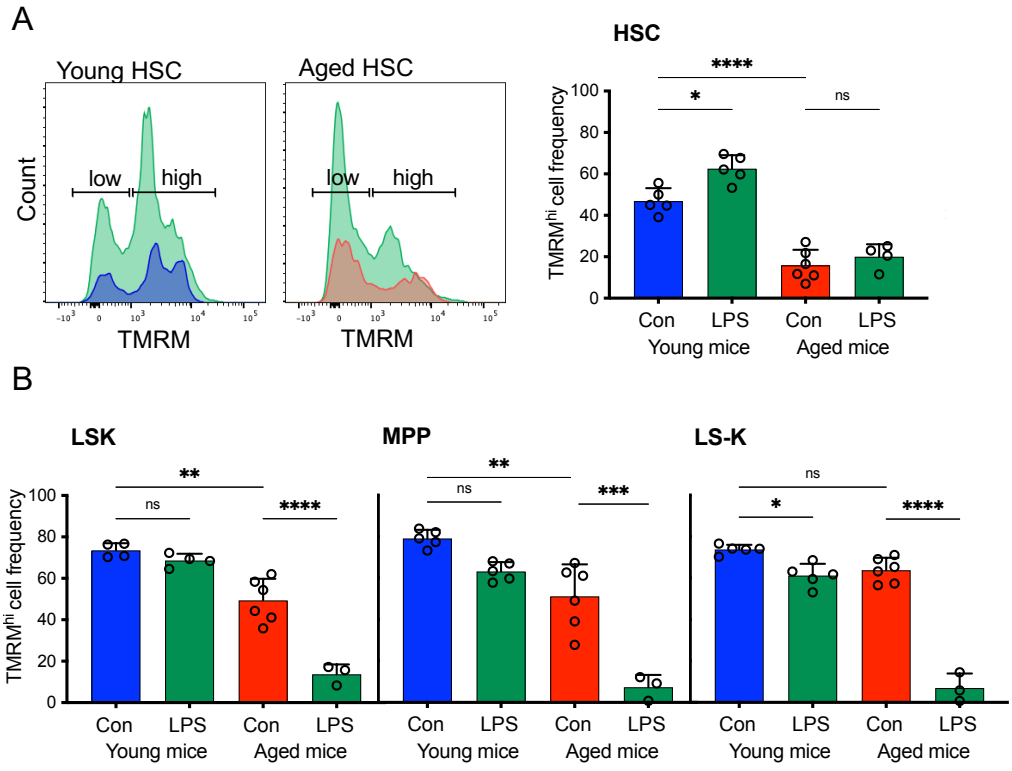

Figure 4.5. Aged HSCs and HPCs are unable to increase their mitochondrial membrane potential after LPS treatment.
*(A) Representative flow cytometry plot showing TMRM staining in HSCs from control young (blue) and aged (red) mice compared to age matched LPS treated mice (green). Frequency of TMRM^{hi} HSCs in young and aged LPS treated and control mice is shown. (B) TMRM^{hi} frequency of LSKs, MPPs and LS-Ks. *P < 0.05, **P < 0.01, ***P < 0.001, ****P<0.0001, ns = not significant using Two-way Anova.*

Next, mitochondrial content was measured using MTG. This was shown to significantly increase in the HSCs and LSKs from both young and aged mice following LPS treatment (Figure 4.6). A small increase was also observed in the MPPs from young mice but not in old mice or in the LS-K population. This may suggest that the process of mitochondrial transfer is conserved in the aged mice, even if it does not correlate with an increase in mitochondrial membrane potential and therefore mitochondrial function.

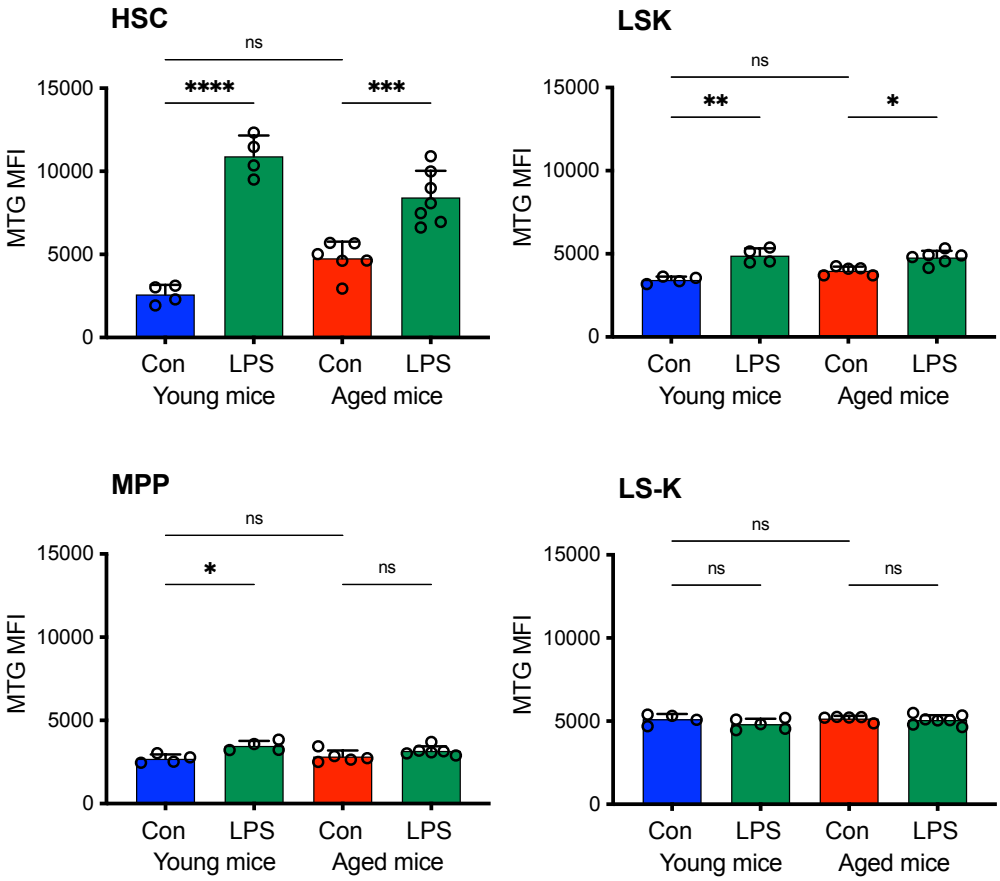

Figure 4.6. Mitochondrial content increases in HSCs and LSKs of young and aged mice following LPS treatment.
*Mean fluorescent index (MFI) of MTG staining is shown in HSCs, LSKs, MPPs and LS-Ks of young and aged mice treated with LPS compared to age matched controls. *P < 0.05, **P < 0.01, ***P < 0.001, ****P<0.0001, ns = not significant using Two-way Anova.*

Finally, MitoSox dye was used to measure mitochondrial ROS in HSC and HPCs from young and aged mice following LPS treatment. No significant changes in the MitoSox^{hi} frequency were observed in the HSC or LSK populations (Figure 4.7A). However, given the overall cell expansion following LPS treatment this simply reflects a proportionate increase in total numbers of cells with high mitochondrial ROS (Figure 4.7B). Thus, in young mice there is an increase in number of MitoSox^{hi} HSCs and LSKs and in aged mice the number of MitoSox^{hi} LSKs increases.

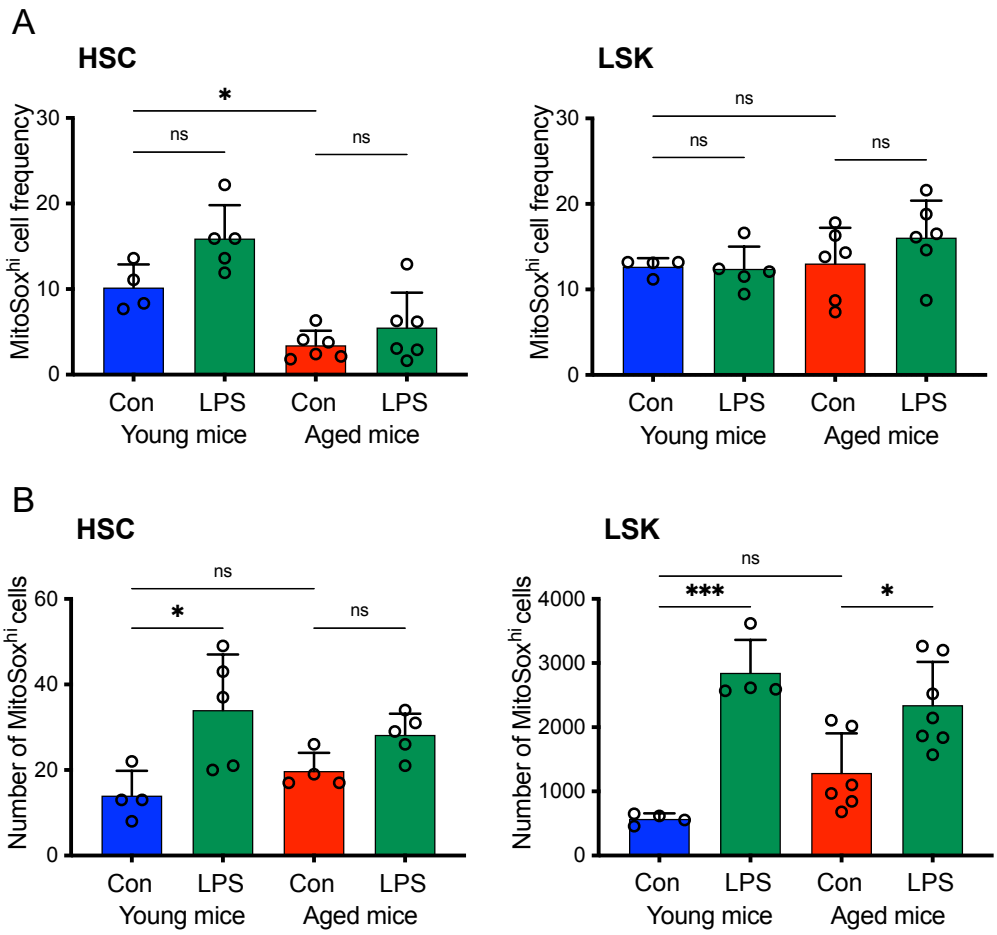

Figure 4.7. The numbers of MitoSox^{hi} HSCs and LSKs increase proportionately to overall cell expansion after LPS treatment in young and aged mice.

*(A) The frequency of MitoSox^{hi} HSCs and LSKs in young and aged controls and LPS treated mice is shown. (B) The number of MitoSox^{hi} HSCs and LSKs per 100,000 BM cells is shown. *P < 0.05, ***P < 0.001, ns = not significant using Two-way Anova.*

To directly assess the impact of the changes in mitochondrial membrane potential on levels of OXPHOS, the seahorse metabolic flux analysis was used. This allows measurement of the oxygen consumption rate (OCR) and extracellular acidification rate (ECAR) of cells, which represent levels of OXPHOS and glycolysis respectively (261, 262). For these measurements to be accurate and reliable, cells should be isolated and processed quickly and at a similar rate for all the different conditions to be analysed. Furthermore, the assay requires at least 450,000 cells for each condition. This limits the cell populations that can be used in this assay, as enough cells need to be isolated without impacting on the cell viability and delaying the processing of samples of each treatment condition. As a result, lineage depletion and CD117 enrichment was used instead of FACS purification to isolate the LK (Lin-, CD117+) cell population. This includes all the populations studied individually by flow cytometry in this chapter so far (LS-Ks, LSKs, MPPs and HSCs).

BM was isolated from young and aged mice treated with LPS or vehicle control and the samples were pooled for each of these four conditions. Next, a lineage depletion kit was used to isolate the Lin- cells, which were subsequently magnetically labelled with anti-CD117 microbeads to enrich for CD117+ cells. The isolated LK cells were counted and equal numbers of cells were used for each condition. In young mice LPS treatment resulted in an increase in OCR and therefore OXPHOS with increases in both basal and maximal respiration, whilst in aged mice there was only limited increase in maximal respiration (Figure 4.8A and B). Figure 4.8C shows the relative changes in OXPHOS and glycolysis, measured using OCR and ECAR. This demonstrates a clear increase in OCR and, therefore, a shift from glycolysis to OXPHOS in LKS from young mice after LPS treatment but very little change in both outputs in LKs isolated from aged mice treated with LPS.

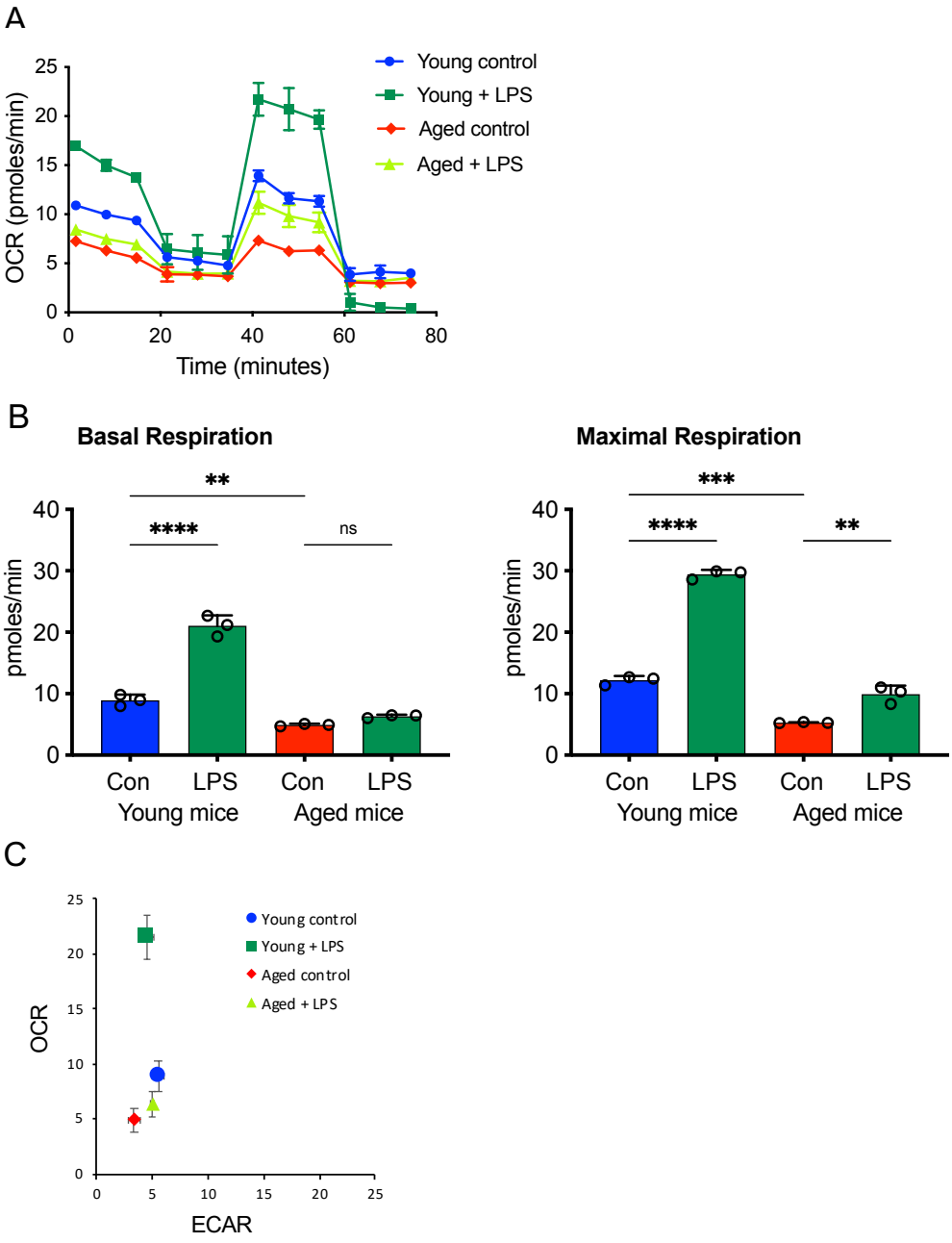

Figure 4.8. LPS treatment results in an increase in OCR in young but not aged mice.

*(A) Seahorse metabolic flux analysis of OCR in LK cells isolated from young and aged mice 16 hours after treatment with LPS or vehicle control. (B) Basal and maximal respiration for each treatment condition are shown. (C) Changes in OCR compared to ECAR in LKs from young and aged mice treated with LPS compared to controls are shown. **P < 0.01, ***P < 0.001, ****P<0.0001, ns = not significant using Two-way Anova.*

In order to further define the metabolic profile of LKs from young and aged mice after LPS treatment, substrate metabolism was measured using Mitoplates from Biolog. This allows measurement of how much of each substrate is utilised by the isolated LK cells. This assay also requires high number of cells that can processed and prepared quickly and therefore the LK population was chosen again and isolated as described above. Figure 4.9 demonstrates an overall reduction in the metabolism of both glycolytic and TCA cycle substrates in aged controls compared to young controls. Furthermore, whilst there is a significant increase in the use of TCA cycle metabolites in LKs isolated from young mice treated with LPS compared to young controls, there is little change in substrate metabolism in the aged mice after LPS treatment. Overall, this data and the results from the seahorse metabolic flux analysis reflect an increase in energy output in young mice after LPS treatment, which is not observed in aged mice.

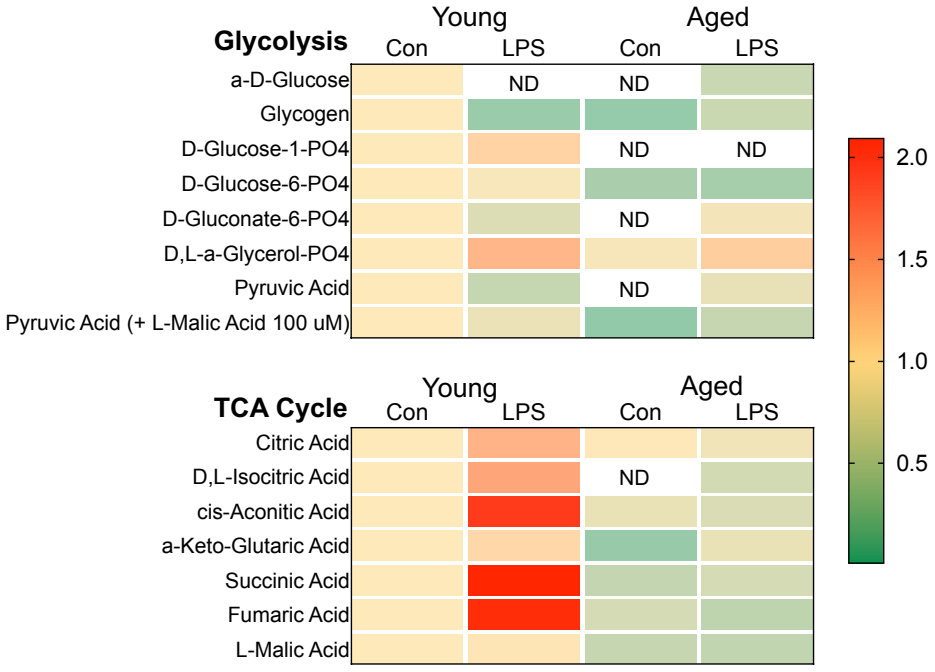

Figure 4.9. In LKs from aged mice substrate metabolism is reduced and not upregulated after LPS treatment.
LKs were isolated from young and aged mice 16 hours after treatment with LPS or vehicle control. Mitoplates from Biolog were used to measure the utilisation of glycolytic and TCA cycle substrates by the isolated LKs.

Finally, to assess how these metabolic changes in HSCs and HPCs reflect on mature blood cell blood production, terminal blood samples taken from young and aged mice treated with LPS or vehicle control. Flow cytometry was used to measure the cell counts of mature nucleated blood cells as described in Figure 3.9. In young mice, treatment with LPS results in a significant increase in the neutrophil counts and a reduction in B cell and T cell counts. In aged mice, however, no increase in neutrophil count was observed and in addition the monocyte count decreased significantly after LPS treatment (Figure 4.10). This suggests an inadequate production of neutrophils following LPS treatment in aged mice and reflects an impaired immediate immune response.

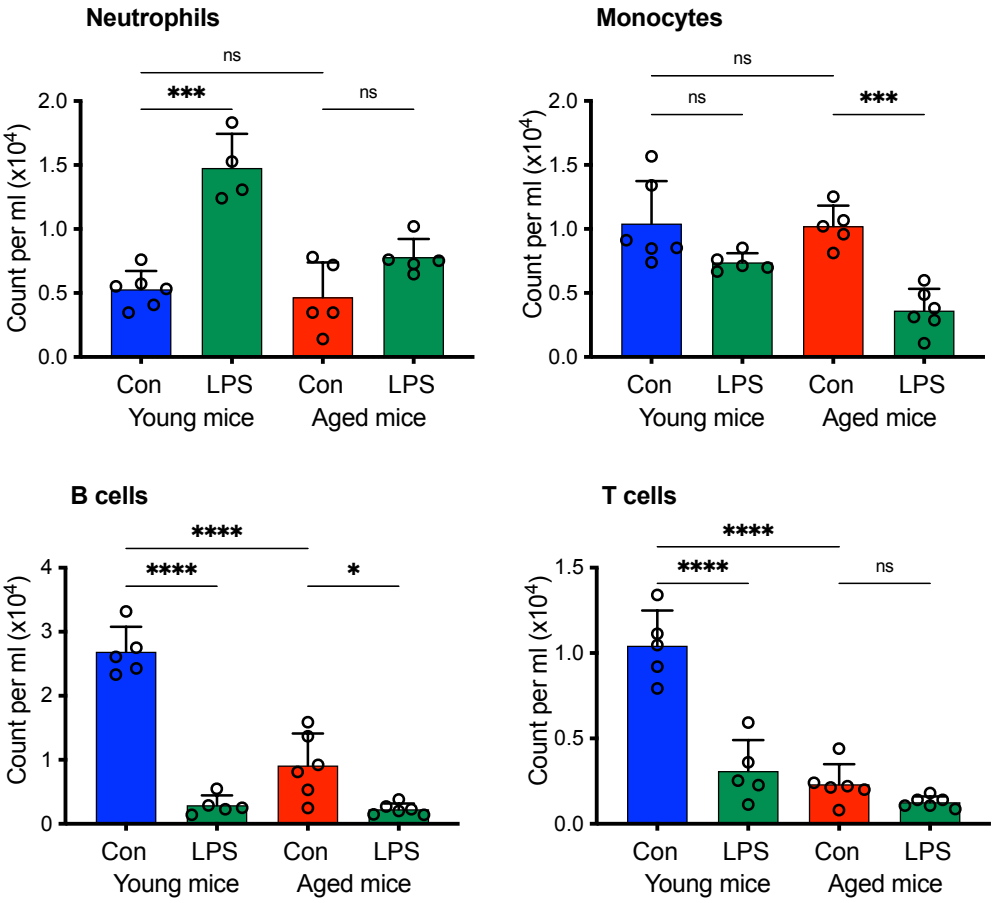

Figure 4.10. Aged mice fail to increase neutrophil production in response to LPS treatment.

*Terminal blood samples were taken from young and aged mice treated with LPS and age matched controls. Cell counts of neutrophils (CD11b+, Ly6G+), monocytes (CD11b+, Ly6G-), B cells (CD19+) and T cells (CD4+/CD8+) per ml of PB are shown. *P < 0.05, ***P < 0.001, ****P<0.0001, ns = not significant using Two-way Anova.*

4.3. Transplantation of aged haematopoietic cells improves their metabolic response to LPS

As shown in chapter 3, transplantation of aged HSCs into a young BM microenvironment resulted in an improved metabolic profile of the HSCs and HPCs. A further transplant was therefore set up to establish if this can also result in an improved metabolic response to LPS. Young C56Bl/6 (CD45.2+) mice were treated with busulfan 25mg/kg for 3 days and then injected with 100,000 FACS purified LSKs from aged PepCboy (CD45.1) mice. Blood samples were taken at 8 and 12 weeks to confirm engraftment and subsequently the engrafted mice were treated with 0.5mg/kg LPS or vehicle control (Figure 4.11). 16 hours later the mice were sacrificed and the BM was isolated.

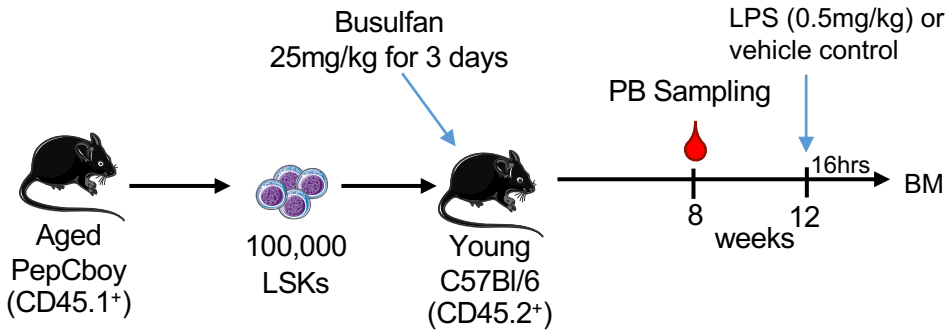

Figure 4.11. Schematic of the transplant model with LPS treatment.
LSKs were sorted from aged PepCboy (CD45.1+) mice and injected into busulfan treated C57Bl/6 by tail vein injection. After 8 weeks PB samples were taken to assess engraftment. This was repeated at 12 weeks before the mice were treated with LPS or vehicle control. After 16 hours the experiment was terminated and the BM isolated.

Engraftment was shown to be similar in the LPS treated group and the control group as demonstrated both in the peripheral blood at 8 and 12 weeks and in the BM after the mice were sacrificed (Figure 4.12).

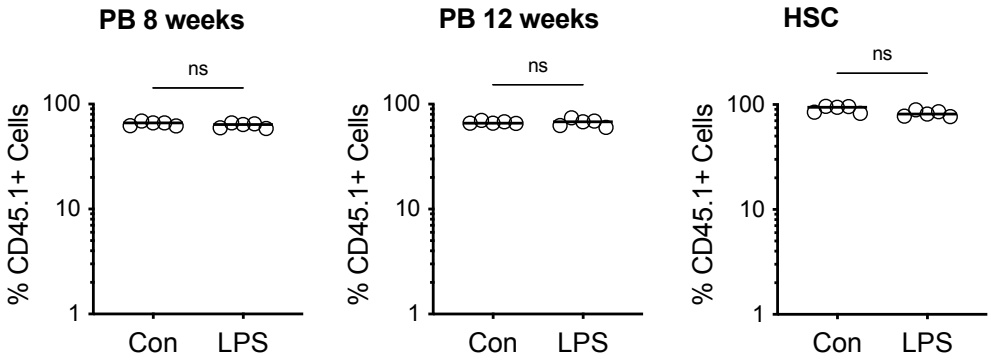

Figure 4.12. Engraftment of donor CD45.1+ cells from aged mice
Engraftment of CD45.1+ donor cells from aged PepCboy mice in the PB of young C57Bl/6 mice at 8 and 12 weeks after transplantation and of the HSC population in the BM at 12 weeks. Data is shown for control (con) mice and those treated with LPS. Ns = not significant using Mann-Whitney U test.

The isolated BM was analysed by flow cytometry for cell count and mitochondrial membrane potential. Figure 4.13 shows significant expansion in the HSC, LSK and MPP populations of the donor cells following LPS treatment and no change in the cell count of the LS-K population.

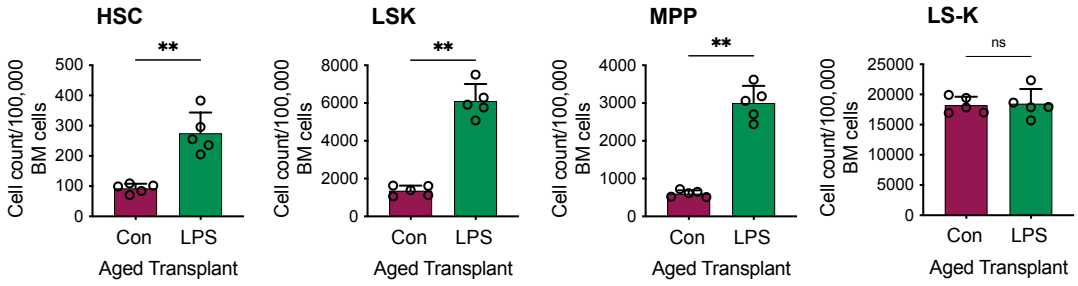

Figure 4.13. Transplantation of HSCs from aged mice into young mice results in HSC and HPC expansion after LPS treatment.
*Following transplantation of HSCs from aged PepCboy mice into young C57Bl/6 mice, the engrafted C57Bl/6 mice were treated with 0.5mg/kg LPS and sacrificed after 16 hours. Counts of engrafted CD45.1+ HSCs, LSKs, MPPs and LS-Ks per 100,000 BM cells in control mice (con) compared to LPSs treated mice are shown. *P < 0.05, **P < 0.01, ns = not significant using Mann-Whitney U test.*

Furthermore, the analysis of mitochondrial membrane potential with TMRM staining revealed an increase in TMRM^{hi} HSCs after LPS treatment in the engrafted cells and a stable TMRM^{hi} frequency of all the HPC populations (Figure 4.14). This reflects the picture seen in young mice treated with LPS and there was no drop in TMRM^{hi} cell frequency as observed in aged mice. This, therefore, suggests an improved metabolic response to LPS in the transplanted HSCs and HPCs.

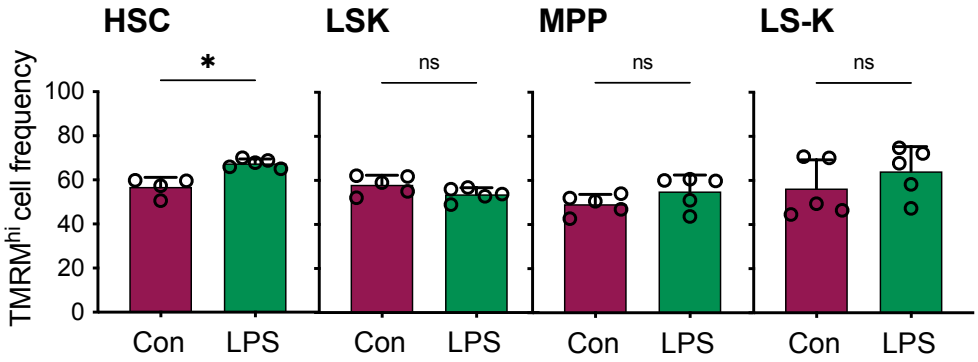

Figure 4.14. The metabolic response of aged HSCs and HPCs to LPS improves after transplantation into young mice.
*The TMRM^{hi} frequency of CD45.1+ HSCs, LSKs, MPPs and LS-Ks isolated from young C57Bl/6 (CD45.2+) mice engrafted with LSKs from aged PepCboy (CD45.1+) mice after LPS treatment compared to vehicle control is shown. *P < 0.05, ns = not significant using Mann-Whitney U test.*

Finally, the metabolic profile of the transplanted cells was analysed using the seahorse metabolic flux analysis. The LK cell population was isolated as described in chapter 3. Analysis of the LK cells showed an increase in OCR, basal respiration and maximal respiration (Figure 4.15). Together, this data suggest that the metabolic response of HSCs and HPCs from aged mice is influenced by the ageing microenvironment. Removal from this environment and placement in a new young environment can improve the haematopoietic metabolic response to LPS. This highlights the importance of the BM niche in regulating and supporting the HSC response to stress.

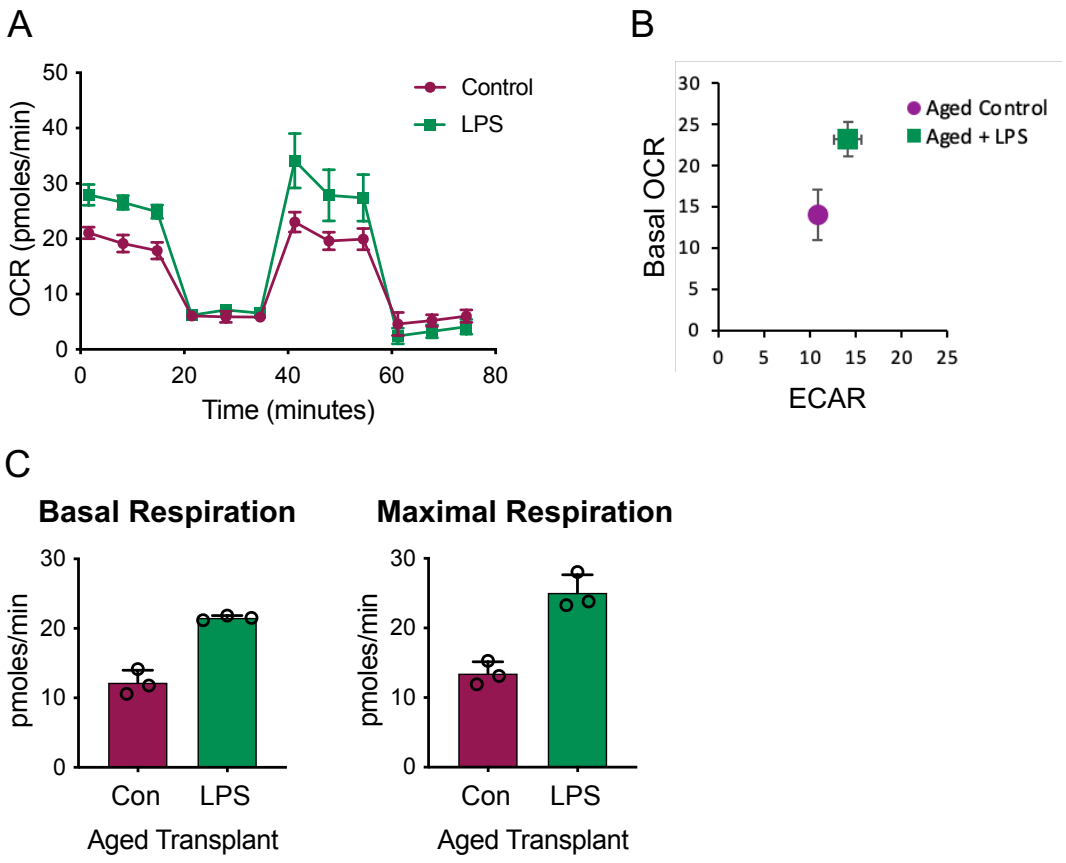

Figure 4.15. Levels of OCR increase in aged LKs in response to LPS after transplantation.
(A) Oxygen consumption rate (OCR) in LK cells isolated from mice engrafted with aged LSKs and subsequently treated with LPS or vehicle control. (B) Changes in OCR compared to extracellular acidification rate (ECAR) in LKs after LPS treatment compared to controls. (C) Basal and maximal respiration are shown.

4.4. Mitochondrial transfer is preserved in aged mice

The BM microenvironment clearly influences the metabolic response of HSCs and HPCs to stress in aged mice. Previous work has demonstrated that mitochondrial transfer from bone marrow stromal cells (BMSC) to HSCs is required to drive the rapid shift from glycolysis to OXPHOS and promote cells expansion (91). For this to remain effective in aged mice, the interaction between HSCs and BMSCs must be preserved and BMSCs must be able to supply adequate numbers of healthy mitochondria. Therefore, mitochondrial content and mitochondrial membrane potential was measured in BMSCs from young and aged mice. Whilst BMSCs can be defined in different ways, here the most commonly used cell surface markers, CD45-, Ter119-, CD31- and CD105+ were used, as shown in Figure 4.16 (121, 122, 124). Positive and negative gates were determined using FMO controls.

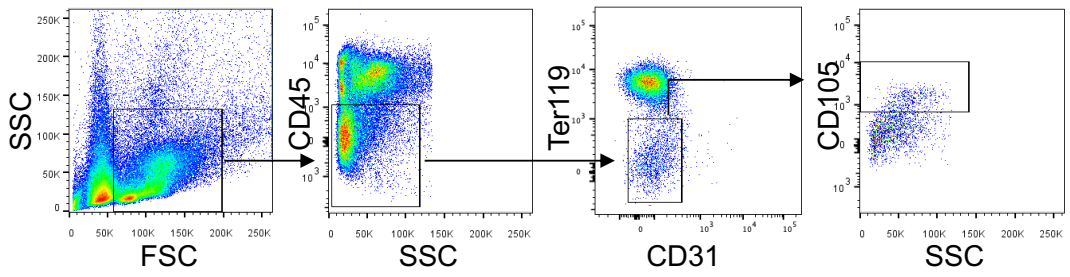

Figure 4.16. Gating strategy for bone marrow stromal cells.
Representative flow plot to show the gating strategy for BMSCs (CD45-, Ter119-, CD31- and CD105+) as determined by FMO controls.

Similarly, to other BM populations, the BMSC count per 100,000 BM cells was increased in the BM from aged mice compared to young mice (Figure 4.17A). Mitochondrial content was measured by flow cytometry using MTG and was unchanged in BMSCs isolated from aged mice compared to BMSCs from young mice (Figure 4.17B). These results were confirmed using TaqMan PCR. BMSCs from young and aged mice were FACS purified, using the same gating strategy as shown in Figure 4.16, and DNA was extracted. TaqMan PCR was used to measure the mitochondrial DNA content, which was normalised to genomic DNA content in order to account for any differences in cells numbers and analyse the relative mitochondrial copy numbers (Figure 4.17C).

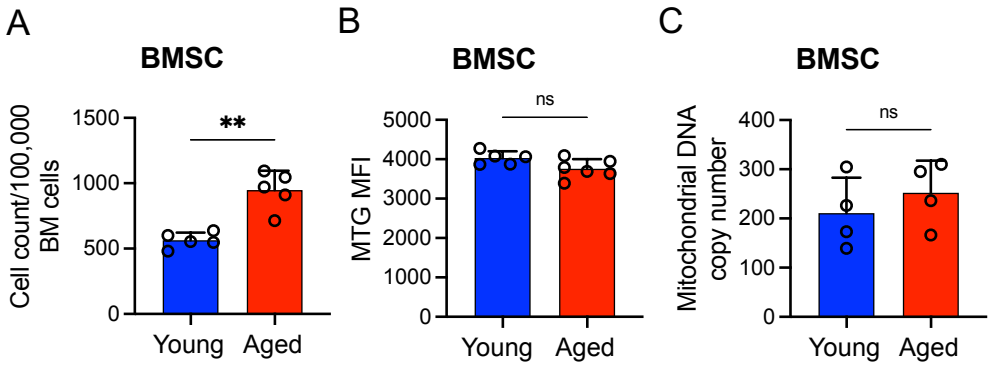

Figure 4.17. Mitochondrial content in BMSCs from aged mice is unchanged compared to young mice.

*BM was isolated from young and aged mice and stained for flow cytometry analysis. (A) Cell count of the BMSCs per 100,000 BM cells in young and aged mice. (B) The mean fluorescent index of MTG staining in BMSCs isolated from young and aged mice is shown. (C) BMSCs were isolated from young and aged mice and DNA was extracted for TaqMan PCR analysis of mitochondrial DNA relative to genomic DNA. **P < 0.01, ns = not significant using Mann-Whitney U test.*

Despite the stable numbers of mitochondria in BMSC from aged mice compared to young mice, however, the frequency of $TMRM^{hi}$ BMSCs was reduced (Figure 4.18A). To measure the OCR of BMSCs from young and aged mice, BM was isolated from young and aged mice and BMSCs were cultured *in vitro.* Subsequently, cells were counted and equal numbers were plated onto seahorse plates. Seahorse metabolic flux analysis showed a decrease in OCR, basal and maximal respiration in BMSCs isolated from aged mice compared to young mice (Figure 4.18B and C). Although this data could have been influenced by changes occurring ex vivo during the culturing process of the BMSC, together with the reduction in $TMRM^{hi}$ BMSC frequency it suggests an overall decline in the mitochondrial function of BMSCs from aged mice.

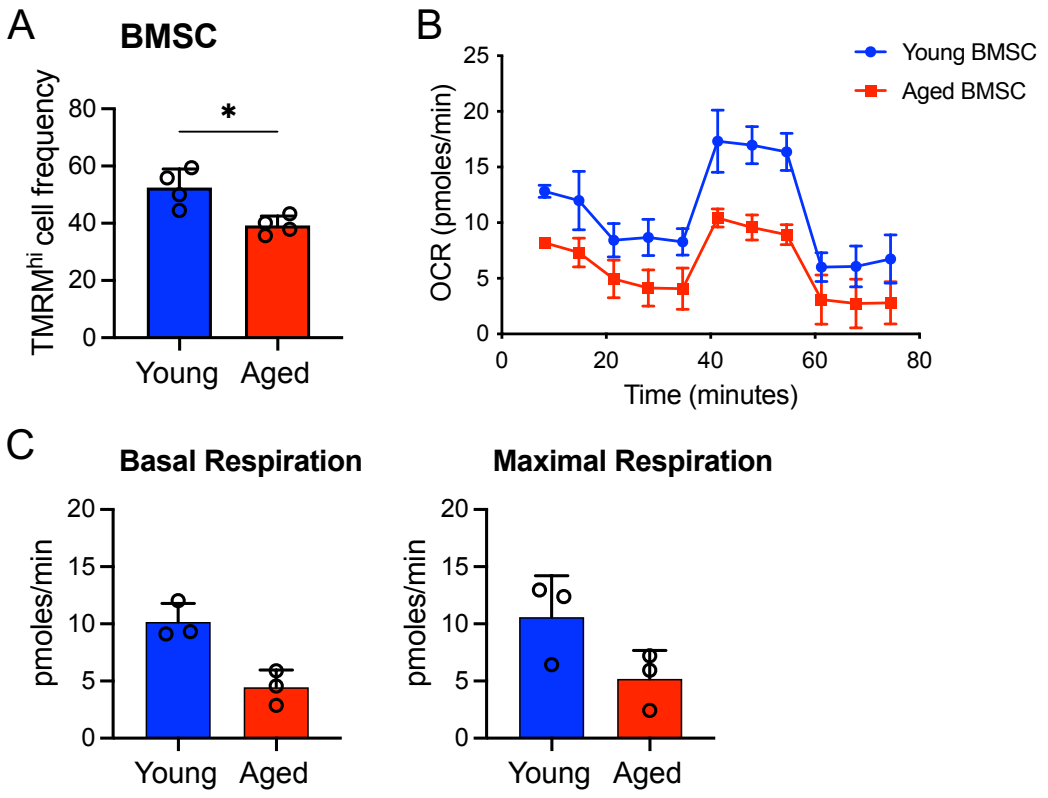

Figure 4.18. Mitochondrial function in BMSCs from aged mice declines. *(A) The $TMRM^{hi}$ BMSC frequency in young and aged mice is shown. (B) Seahorse metabolic flux measurement of oxygen consumption rate (OCR) in BMSCs isolated from young and aged mice. (C) Basal and maximal respiration of BMSCs from young and aged mice are shown.*

Data in this chapter demonstrates that mitochondrial content of HSCs and LSKs increases in both young and aged mice after LPS treatment (Figure 4.6). However, in aged mice this does not correlate with increased mitochondrial membrane potential as measured by TMRM. This, together with the decline in mitochondrial function in the BMSC population from aged mice, suggests that the mechanism of mitochondrial transfer is, in fact, preserved in aged mice, but that the mitochondria being transferred have reduced function. To confirm this, BMSCs from young and aged C57Bl/6 mice were cultured *in vitro*. These were then co-cultured with LKs from young CBA mice and mitochondrial transfer was stimulated with H_2O_2 treatment for 24 hours (Figure 4.19).

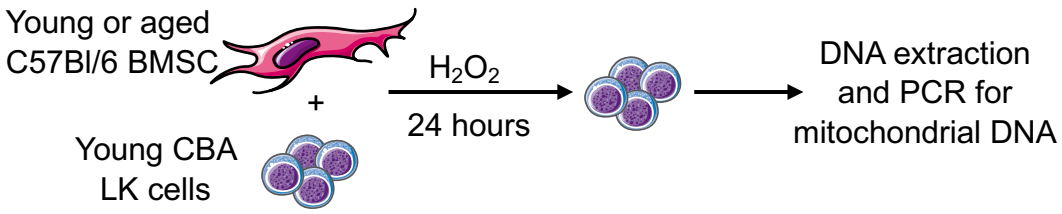

Figure 4.19. Experimental set up to study mitochondrial transfer in aged BMSC.
Young and aged C57Bl/6 stroma cells were co-cultured with young CBA LK cells and the treated with H_2O_2 to stimulate mitochondrial transfer. After 24 hours DNA was extracted from the LK cells to analyse the mitochondrial DNA content by TaqMan PCR.

The C57Bl/6 and CBA mitochondrial genome can be distinguished by two single-nucleotide polymorphisms (SNP). SNP analysis by TaqMan PCR therefore allows quantification of mitochondria originating from the C57Bl/6 BMSCs in the CBA LKs. Figure 4.20 shows that mitochondrial transfer occurs both from young and aged BMSCs to LKs, with increased levels of donor mitochondrial DNA detected after H_2O_2 treatment. This supports the hypothesis that the mechanism of mitochondrial transfer is preserved in aged mice.

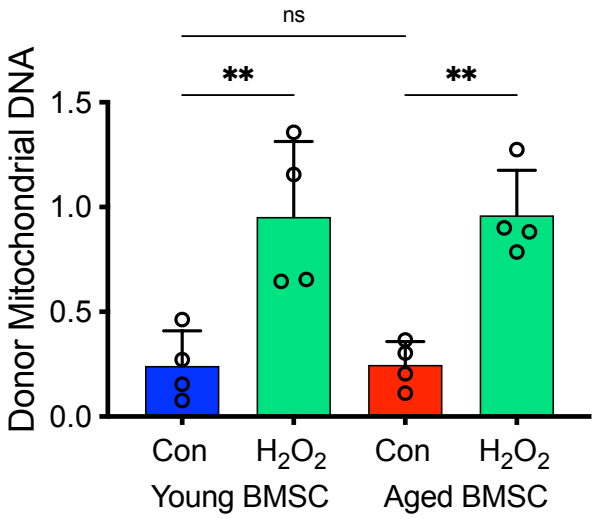

Figure 4.20. Mitochondrial transfer in conserved in aged BMSCs.
Levels of transferred donor mitochondrial DNA from BMSCs in LK cells are shown relative to total genomic DNA. LK cells were either cultured with young or aged BMSCs alone (Con) or also treated with H_2O_2 in order to stimulate mitochondrial transfer.

Finally, the metabolic changes in BMSCs in young and aged mice following LPS treatment or vehicle control were analysed by flow cytometry. No significant changes were seen in the frequency of $TMRM^{hi}$ BMSC after LPS treatment in young or aged mice (Figure 4.21A) Mitochondrial content on the other hand was shown to decrease after LPS treatment in both young and aged mice, which would be consistent with the transfer of mitochondria from BMSC to HSCs and HPCs (Figure 4.21B). Interestingly, whilst in young mice this is associated with an increase in mitochondrial ROS measured by MitoSox, in aged mice the frequency of $MitoSox^{hi}$ BMSCs decreases after LPS

treatment (Figure 4.21C). Here this is mirrored by the change in numbers of MitoSox^{hi} cells and therefore does not appear to be a result of a change in total cell numbers. One possible explanation for this is that as dysfunction mitochondria are transferred out of the BMSCs their level of mitochondrial ROS improves at least temporarily.

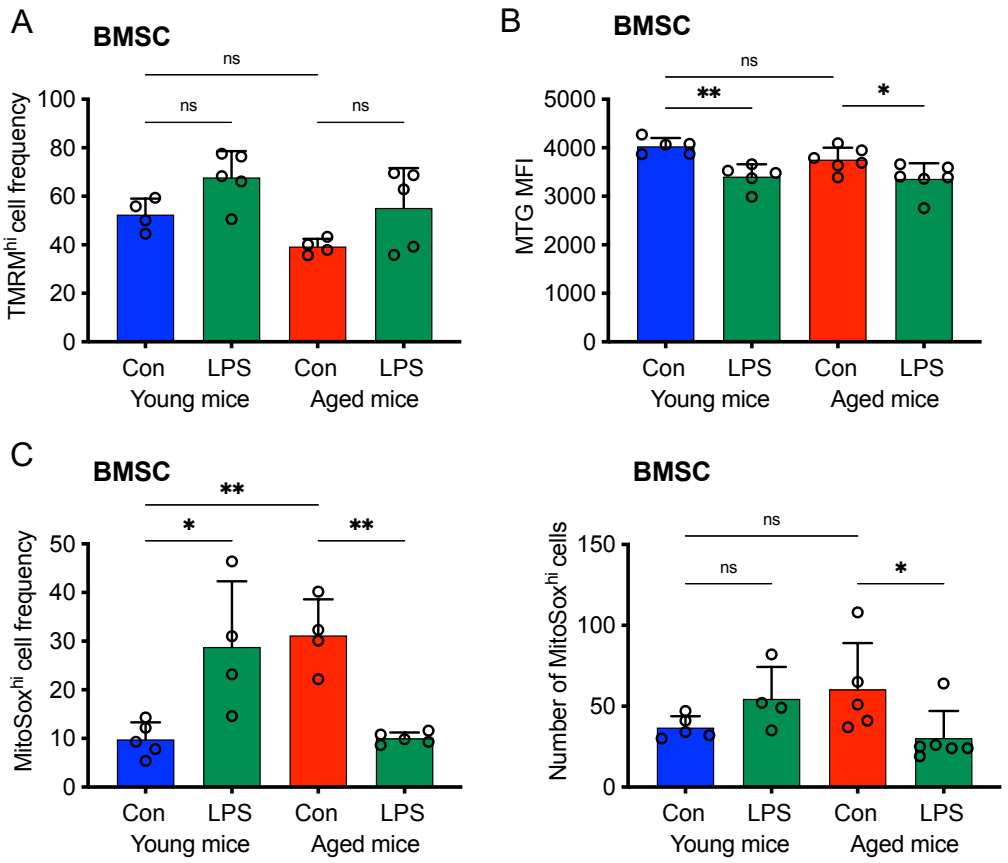

Figure 4.21. Metabolic changes of BMSCs after LPS treatment.
BMSCs were isolated from young and aged mice after LPS treatment and compared to BMSCs isolated from age matched controls by flow cytometry. (A) The frequency of TMRM^{hi} BMSCs is shown. (B) Mean fluorescent index (MFI) after MTG staining of BMSCs. (C) MitoSox^{hi} cell frequency and total number of MitoSox^{hi} BMSCs are shown.

4.5. Summary

The data shown here demonstrates the HSC and HPC metabolic response to infections is impaired in aged mice. This leads to reduced cell expansion, inadequate production of mature immune cells and overall reduced survival. Fundamentally, HSCs and HPCs in aged mice appear to be unable to increase their mitochondrial membrane potential and sufficiently upregulate their TCA cycle metabolism and subsequent levels of OXPHOS. As a result, the increased energy requirements associated with emergency granulopoiesis cannot be met and overall production of mature blood cells in response to LPS is insufficient. Importantly, this change is at least partially driven by the changes in the aged BM microenvironment and can be reversed when aged HSCs are transplanted into young mice. Furthermore, whilst the mechanism of mitochondrial transfer is preserved in aged mice, it does not appear to drive an increase in mitochondrial membrane potential as it does in young mice. Instead, it is likely that both functional and dysfunctional mitochondria are transferred and therefore the shift to OXPHOS cannot be supported. Overall, this results in an impaired ability to effectively respond to LPS treatment, which is reflected by the short overall survival of aged mice treated with LPS.

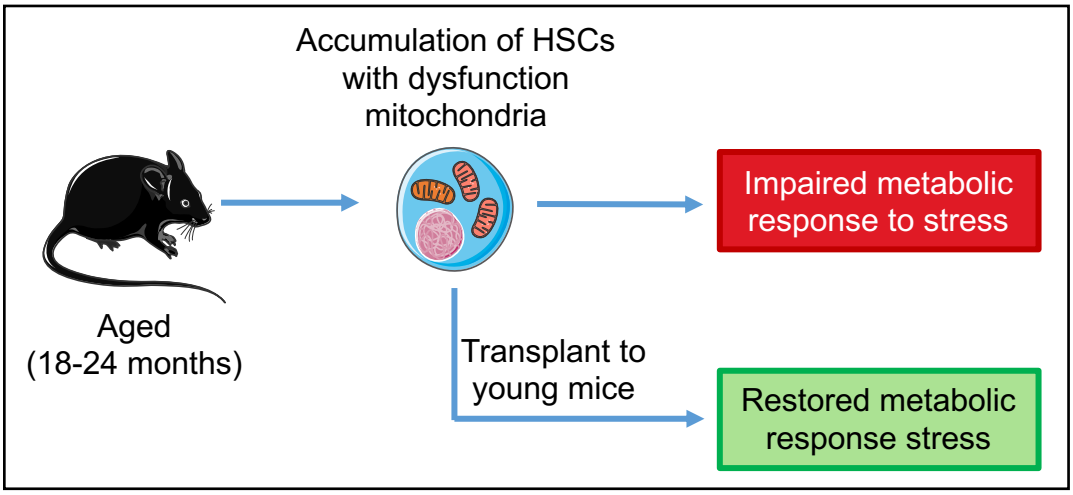

Figure 4.22. Defining how age-related metabolic changes alter the haematopoietic response to stress.
Aged mice accumulate HSCs with dysfunctional mitochondrial leading to an impaired metabolic response to stress and an inability to switch from glycolysis to OXPHOS. Transplantation of aged HSCs into young mice reverses this effect and restores the HCS and HPC metabolic response to stress.

5. Investigating the role of senescent cells in the haematopoietic response to stress

5.1. Introduction

The role of the BM microenvironment in HSC maintenance and, in particular in response to stress is becoming increasingly evident. The data discussed in chapters 3 and 4 demonstrates that the BM microenvironment contributes to age-related changes in the haematopoietic response to stress. Cellular senescence is a major driver of many age-related phenotypes and diseases and has been associated with mitochondrial dysfunction (18). The earlier chapters demonstrate that dysfunctional mitochondria accumulate in HSCs, HPCs and BMSCs in aged mice. However, cellular senescence is defined as the irreversible arrest of cell proliferation and it is therefore questionable whether HSCs, which are directly defined by their proliferative potential, can become senescent. Nevertheless, it is possible that a subgroup of HSCs or HPCs may acquire a senescent-like phenotype in the ageing BM, which could impact on their function and proliferative potential. Furthermore, the cellular components of the BM microenvironment, including BMSCs, can certainly become senescent, as has been demonstrated in a number of BM malignancies including AML and myeloma (25, 263). As the supportive cells of the BM microenvironment can directly influence, alter and control HSC function, a senescent phenotype in these cell populations could have detrimental effects on HSC and HPC function.

If, however, these cells could be eliminated and the BM microenvironment rejuvenated it may be possible to improve the haematopoietic response to stress. There are a number of ways to target senescent cells *in vivo*. One is to use specifically designed mouse models, such as the p16-3MR mouse model. In this model, the p16 promotor drives the expression of HSV-TK, which phosphorylates the pro-drug ganciclovir (GCV) causing cell death (Figure 1.4) (21). Thus, in this mouse model senescent cells can be selectively depleted by treatment with GCV by intraperitoneal injection. This allows the study of the

role of senescent cells in disease development and how depletion of senescent cells can improve the ageing phenotype.

Senescent cells can also be targeted more indirectly with pharmaceutical agents. The drug ABT-263, which targets the anti-apoptotic proteins BCL-2, BCL-XL and BCL-W, has been shown to have senolytic activity and effectively reverse premature ageing of the haematopoietic system in irradiated animals (57). Whilst the anti-apoptotic BCL-2 family of proteins are known to be upregulated in senescent cells (42), their expression is not unique to senescent cells and ABT-263 may therefore not only specifically target senescent cells. Thus, for example, it has a direct impact on platelets, causing severe thrombocytopenia, which has significantly limited its clinical use (64). Nevertheless, its senolytic activity is well established and it remains a useful tool to study how the *in vivo* elimination of senescent cells can alter tissue function.

In this chapter I aim to study the senescent changes present in the ageing BM and to determine the effect of depleting senescent cells in the BM microenvironment on HSC metabolic health. I also plan to determine if targeting the BCL-2 family of proteins with ABT-263 can improve the HSC metabolic response to stress in aged mice.

5.2. Senescence in the aged BM microenvironment

A number of senescence markers were used to determine which cell populations acquire a senescent phenotype in the aged BM. First, the p16-tdTom mouse model was used, in which the $p16^{INK4A}$ promotor is linked to the ultrabright fluorochrome tandem dimer Tomato (tdTom). This allows detection of senescent cells, defined by p16 expression, using flow cytometry. BM was isolated from both young and aged p16-tdTom mice and stained for flow cytometry analysis of HSCs, LSKs and LS-Ks (Figure 5.1A). Figure 5.1B shows representative flow plots of tdTom positive HSCs and LSKs from young and aged p16-tdTom mice. HSCs had no expression of p16 measured by tdTom in both young and aged p16-tdTom mice. In the LSK and LS-K cell population only low levels of tdTom were detected, with no significant differences between cells isolated from aged or young mice (Figure 5.1C).

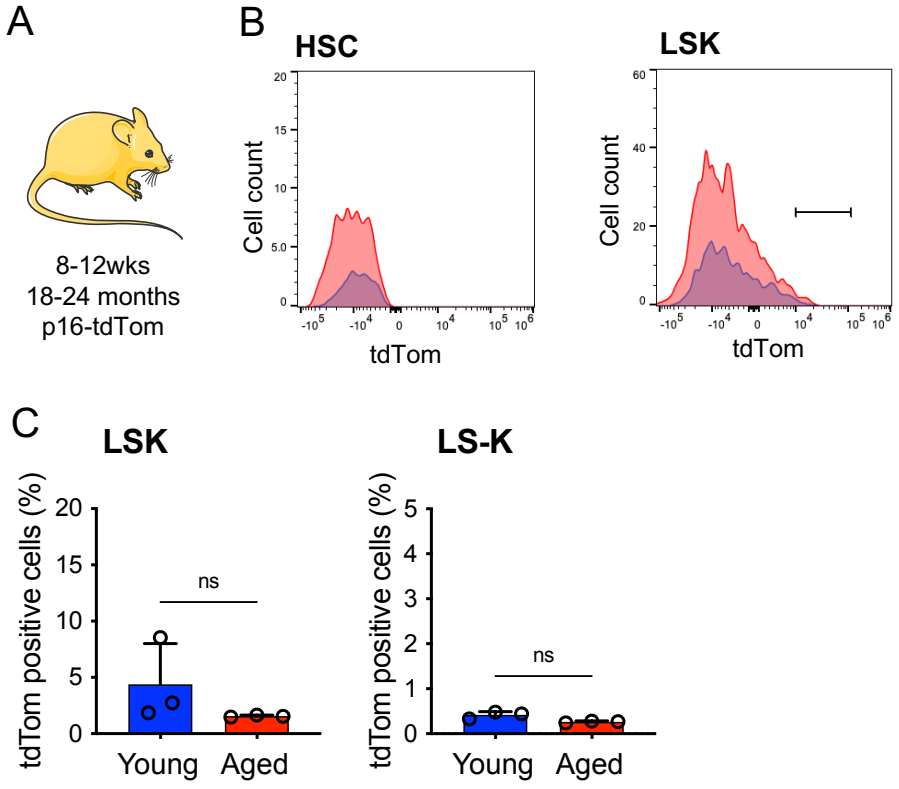

Figure 5.1. HSCs have no expression of p16-tdTom.
(A) BM was isolated from young and aged p16-tdTom mice and flow cytometry was used to measure the expression of p16-tdTom. (B) Representative flow plot of tdTom expression in HSCs and LSKs from young (blue) and aged (red) mice. (C) The percentage of tdTom positive LSKs and LS-Ks in young and aged mice is shown. ns = not significant using Mann-Whitney U test.

Next, LSKs were FACS purified and RNA was extracted and analysed for expression of the senescence associated genes p16 and p21 by qPCR. This showed no change in p16 expression in LSKs from aged mice compared to young and a decrease in p21 expression (Figure 5.2A). Finally, LK (Lin-, CD117+) cells were isolated from aged and young mice as described previously using lineage depletion followed by CD117 enrichment. LKs were used here to minimise the effects of ex-vivo processing of the BM cells. The cells were stained to measure senescence associated beta-galactosidase (SA-β-gal), which is defined as detectable β-gal activity at a pH of 6 (264). This pH dependent β-gal is a well characterised hallmark of senescent cells and is a widely used marker for senescence (265). Consistent with data from both the p16-tdTom mouse model and the qPCR analysis, no change was detected in the levels of SA-β-gal in the LKs from aged mice compared to LKs from young mice (Figure 5.2B). Together, this data demonstrates that aged HSCs and HPCs do not acquire a senescent phenotype and this is therefore not the driver of the observed age-related metabolic changes.

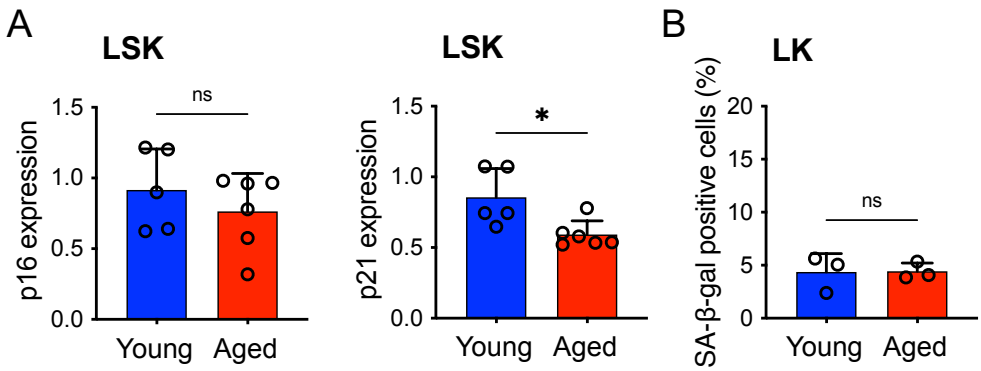

Figure 5.2. HPCs do not become senescent in aged mice.
*(A) The relative expression of p16 and p21, normalised to GAPDH, in LSKs from young and aged C57Bl/6 mice, measured by qPCR is shown. (B) Percentage of SA-β-gal positive LK cells measured by evaluation of blue colour staining. *P < 0.05, ns = not significant using Mann-Whitney U test.*

Examination of senescent markers in BMSCs, on the other hand, revealed a different picture. BMSCs (CD45-, Ter119-, CD31-, CD105+) were defined and gated for as described in Figure 4.16. Using the p16-tdTom mouse model p16-tdTom expression was found to be significantly increased in BMSCs isolated from aged mice compared to young mice. Figure 5.3A shows a representative flow plot of tdTom expression in BMSCs isolated from a young and an aged p16-tdTom mouse. A clear shift in tdTom expression was detected in the BMSC from aged mice compared to young mice (Figure 5.3B).

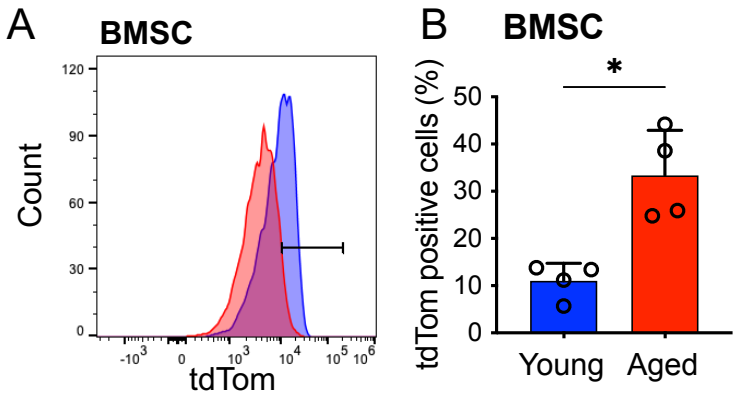

Figure 5.3. p16-tdTom expression is increased in BMSCs from aged mice.
*(A) Example of the distribution of tdTom expression in BMSCs from young (blue) and aged (red) mice. (B) Percentage of tdTom positive BSMCs measured by flow cytometry. *P < 0.05 using Mann-Whitney U test*

Finally, BMSC from young and aged mice were FACS purified and RNA was extracted for qPCR analysis for the expression of p16 and p21, as well as IL-6, a common component of the senescence associated secretory phenotype (SASP), and laminin B1, which is known to decrease in senescent cells (266). Expression of p16 and IL-6 were upregulated in BMSC from aged mice compared to BMSC from young mice and there was no change in p21 expression (Figure 15.4). In addition, laminin B1 expression was reduced in BMSC from aged mice. Thus BMSCs, but not HSCs or HPCs, acquire a senescent phenotype with age.

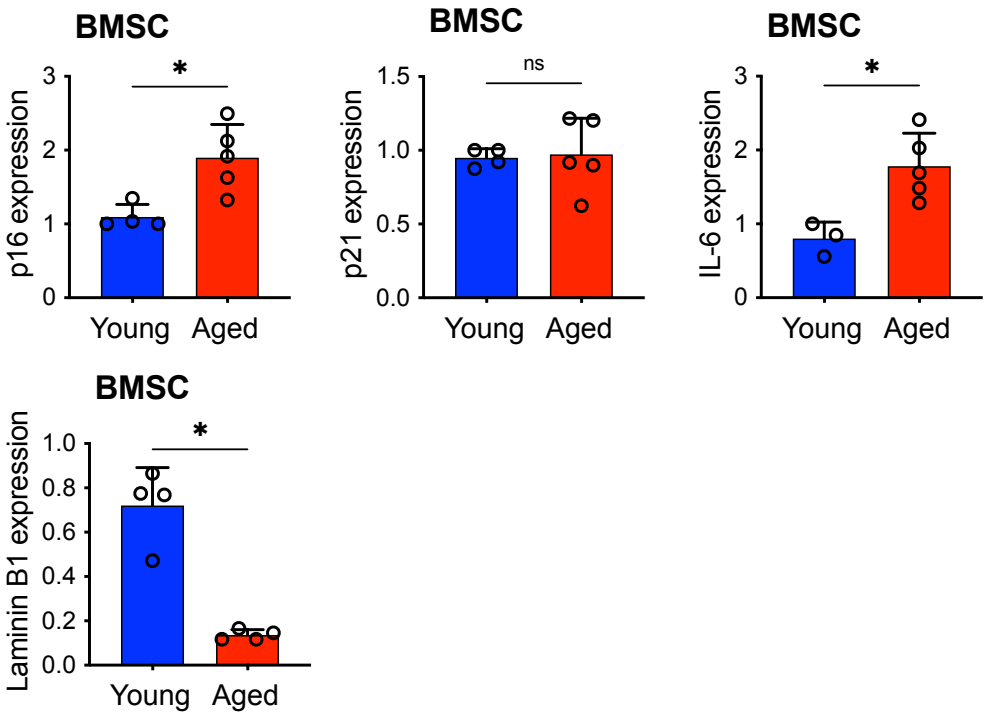

Figure 5.4. BMSCs from aged mice express a senescent phenotype.
*qPCR analysis of the expression of p16, p21, IL-6 and Laminin B1, normalised to GAPDH in BMSC sorted from young and aged C57Bl/6 mice. *P < 0.05, ns = not significant using Mann-Whitney U test.*

5.3. Selective depletion of senescent BMSCs improves the metabolic response of haematopoietic cells to LPS

In order to determine whether the elimination of the senescent BMSCs can improve the metabolic response of HSCs to stress, the p16-3MR mouse model was used. Aged p16-3MR mice were treated with GCV 25mg/kg for 5 days by intraperitoneal injection to deplete p16 expressing senescent cells. Age-matched C57Bl/6 mice were used as controls and also treated with GCV to ensure that the treatment itself did not impact on the HSC population or its response to stress. After a further 7 days, to allow full recovery from the treatment, mice were sacrificed and their BM was isolated for analysis by flow cytometry (Figure 5.5).

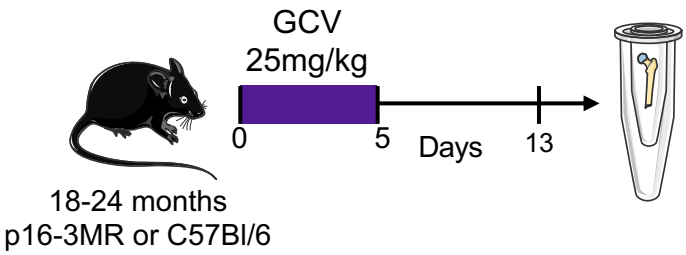

Figure 5.5. Schematic of the experimental set up.
Aged p16-3MR or C57-Bl/6 mice were treated with 25mg/kg GCV for 5 days. After a 7 day rest period the mice were sacrificed and their BM was isolated by centrifugation.

BM analysis demonstrated a reduction in BMSC counts in p16-3MR mice treated with GCV compared to C57Bl/6 control mice (Figure 5.6A). No change was observed in the mitochondrial membrane potential, measured by TMRM, of the BMSCs from GCV treated p16-3MR mice compared to C57Bl-3 controls (Figure 5.6B). However, analysis of the HSC population revealed an increase in $TMRM^{hi}$ cell frequency in the p16-3MR aged mice treated with GCV (Figure 5.6C). This suggests that targeting the senescent cells in the BM microenvironment can have a direct impact on the mitochondrial health of HSCs.

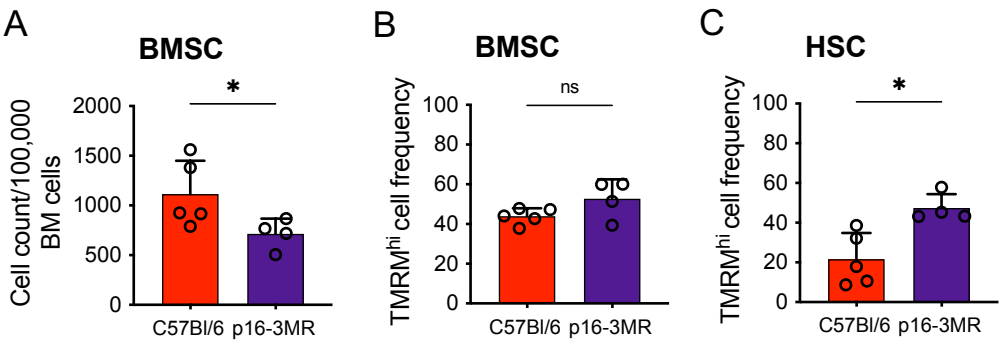

Figure 5.6. Depletion of senescent BMSCs improved HSC mitochondrial membrane potential.
*(A) Flow cytometry analysis of BMSC cell counts per 100,000 BM cells in aged C57Bl/6 and p16-3MR mice treated with GCV. (B and C) Frequency of TMRM^{hi} BMSCs and HSCs is shown. *P < 0.05, ns = not significant using Mann-Whitney U test.*

Next, to determine how this impacts the HSC and HPC response to stress, aged p16-3MR mice were first treated with GCV for 5 days, and after a 7-day recovery period, they were treated with 0.5mg/kg LPS or vehicle control (Figure 5.7). The mice were sacrificed after 16 hours and their BM isolated for flow cytometry and seahorse analysis.

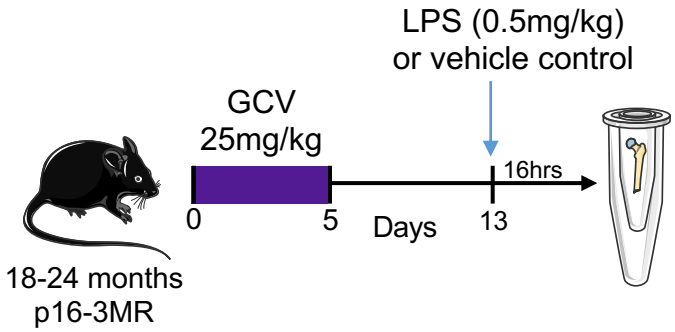

Figure 5.7. Schematic of the experimental design.
Aged p16-3MR mice were treated with 25mg/kg GCV daily for 5 days and after a further 7 days they were treated with either 0.5mg/kg LPS or vehicle control. After 16 hours the experiment was terminated and the BM was extracted for analysis.

No significant change was seen in the HSC, LSK and MPP counts following LPS treatment of aged GCV treated p16-3MR mice and there was a small increase in the LS-K count (Figure 5.8). This could suggest that depletion of senescent cells does not directly affect HSC and HPC expansion in response to stress. However, this data is limited by the small number of mice due to the limited availability of aged p16-3MR mice, the impact of adverse effects resulting from both GCV and LPS treatment and the variability in results observed in all aged mice.

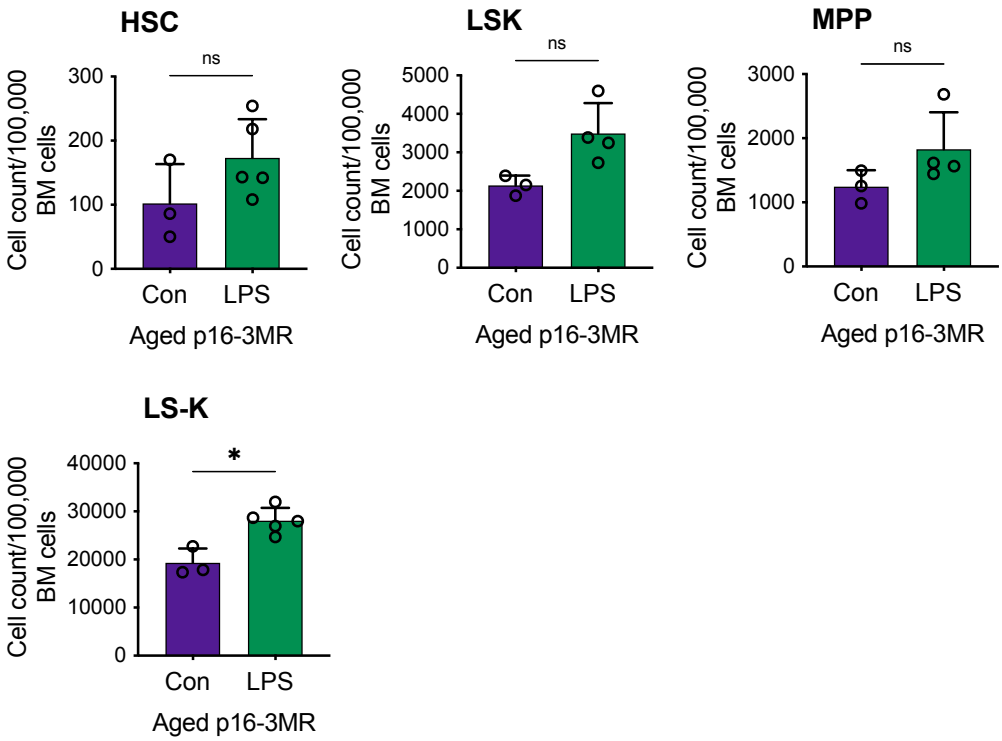

Figure 5.8. LPS treatment does not result in significant haematopoietic cell expansion in aged GCV treated p16-3MR mice.
*BM was extracted from aged p16-3MR mice first treated with GCV for 5 days and then with LPS or vehicle control (Con). Cell counts per 100,000 BM cells for HSCs, LSKs, MPPs and LS-Ks were analysed by flow cytometry. *P < 0.05, ns = not significant using Mann-Whitney U test.*

Analysis of the TMRM^{hi} cell frequency of the HSC and HPC populations revealed that this remained stable following LPS treatment after depletion of senescent cells with GCV (Figure 5.9). Thus, although there was no increase in TMRM^{hi} HSC frequency, as is seen in young mice, there was also no decrease observed in the TMRM^{hi} frequency of any of the HPC populations, as occurs in aged mice.

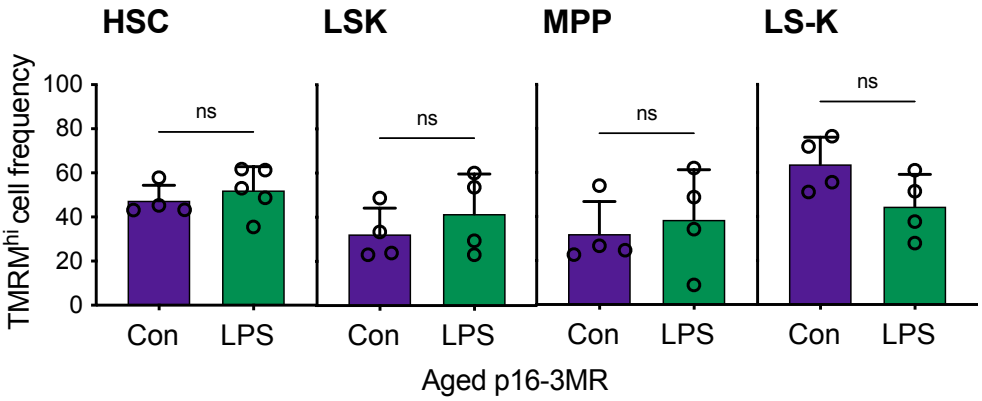

Figure 5.9. TMRM^{hi} cell frequency remains stable in HSCs and HPCs of aged GCV treated p16-3MR mice following LPS treatment.
Frequency of TMRM^{hi} HSCs, LSKs, MPPs and LS-Ks isolated from aged p16-3MR mice treated with GCV and LPS or vehicle control measured by flow cytometry. ns = not significant using Mann-Whitney U test.

Mitochondrial content increased following LPS treatment in the HSCs and LSKs from aged p16-3MR mice treated with GCV (Figure 5.10). This is consistent with the change observed in both young and aged mice treated with LPS and most likely a result of mitochondrial transfer from BMSCs. The levels of mitochondrial ROS were quite variable in p16-3MR mice treated with both GCV and then LPS compared to controls, with an overall upward trend in the MitoSox^{hi}cell frequency of HSCs and HPCs (Figure 5.10).

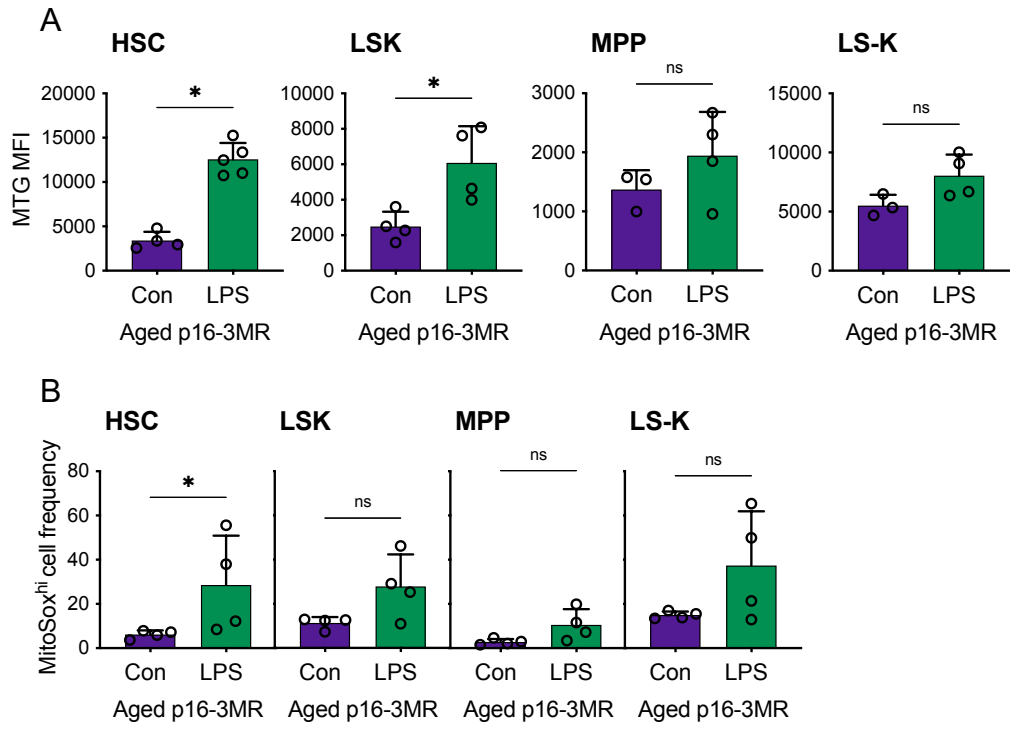

Figure 5.10. Changes in mitochondrial content and ROS after GCV and LPS treatment in p16-3MR mice.
*(A) Mean fluorescent index (MFI) of MTG stained HSCs, LSKs, MPPs and LS-Ks measured by flow cytometry in p16-3MR mice treated with GCV and LPS or vehicle control (Con). (B) Frequencies of MitoSox^{hi} HSCs, LSKs, MPPs and LS-Ks in GCV and LPS treated p16-3MR mice compared to mice treated with GCV alone. *P < 0.05, ns = not significant using Mann-Whitney U test.*

Finally, seahorse metabolic flux analysis was carried out to study the changes in HPC metabolism following depletion of senescent cells in the BM microenvironment and LPS treatments. As previously described LK cells were used for this assay and cells from aged C57Bl/6 mice were used as controls (Figure 5.11A). Figure 5.11B and C show that in aged p16-3MR mice, treated with GCV and then LPS, there is an increase in OCR and therefore, a shift towards OXPHOS which was not observed in aged C57Bl/6 mice treated with LPS. This is also reflected in a significant increase in the basal and maximal respiration rate in the aged p16-3MR mice (Figure 5.6D). Together, the data shown here suggests that depletion of senescent cells in the BM microenvironment results in an improved metabolic response of haematopoietic cells to stress.

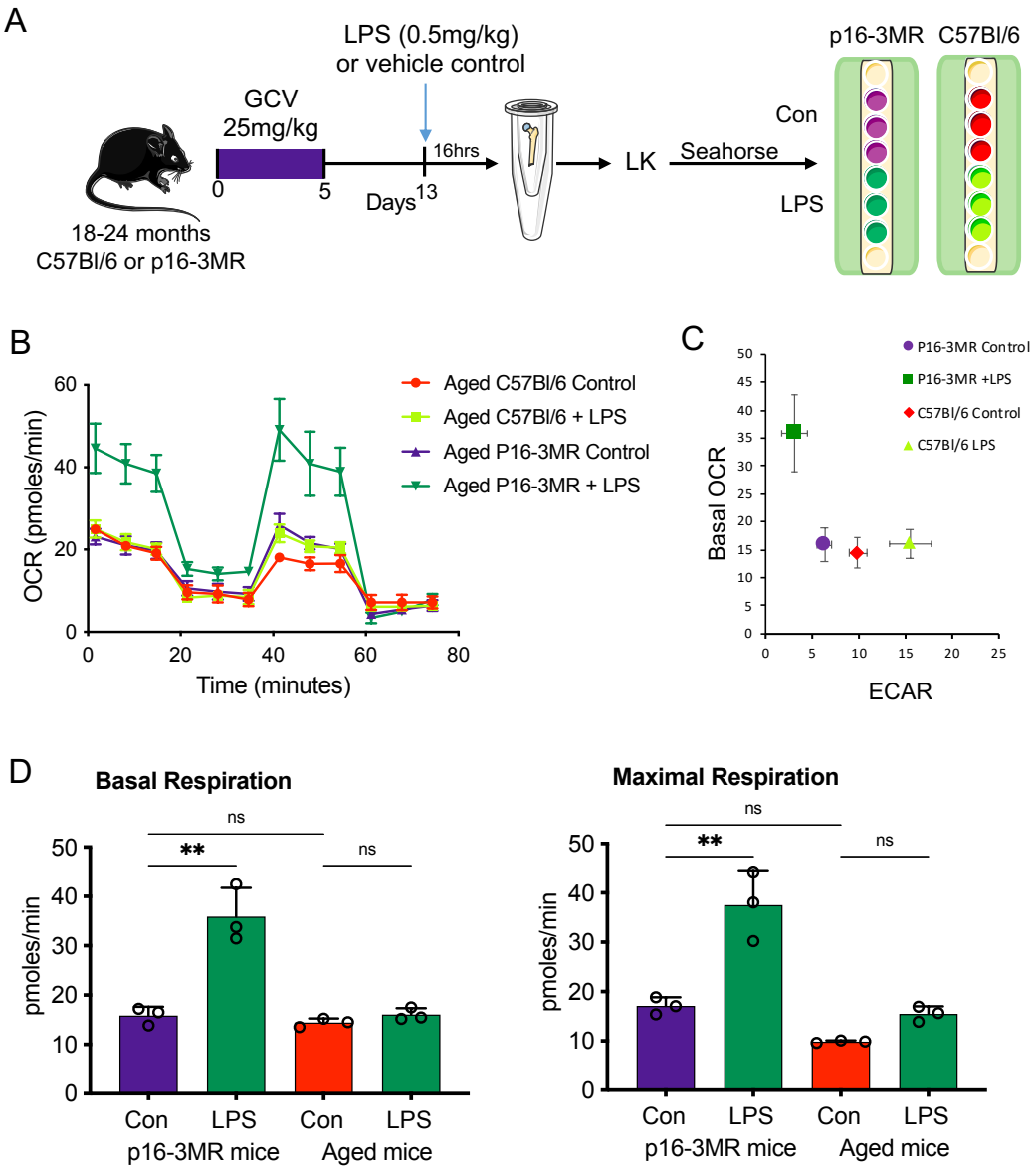

Figure 5.11. LKs from p16-3MR mice treated with GCV and then LPS show a shift towards OXPHOS.

*(A) Experimental schematic. Aged p16-3MR and C57Bl/6 mice were treated with GCV for 5 days. They were then treated with LPS or vehicle control and 16 hours later their BM was extracted and LK cells were isolated for seahorse metabolic flux analysis. (B) Levels of oxygen consumption rate (OCR) in aged p16-3MR or C57Bl/6 mice treated with LPS compared to controls. (C) Relative changes in levels of OCR and extracellular acidification rate (ECAR) in LPS treated mice compared to controls. (D) Basal and maximal respiration rates are shown for each of the four treatment groups. **P < 0.01, ns = not significant using Two-way Anova.*

5.4. Targeting pro-apoptotic BCL-2 proteins in the aged BM microenvironment allows recovery of HSC and HPC mitochondrial health

The overexpression of the anti-apoptotic BCL-2 family of proteins has been associated with a senescent phenotype. The data in this chapter demonstrates that BMSC, but not HSCs or HPCs, become senescent in aged mice. To determine how this change is reflected on the expression of the anti-apoptotic BCL-2 proteins both BMSCs and LSKs from young and aged mice were FACS purified. RNA was extracted and expression of BCL-2 and BCL-XL were analysed by qPCR. LSKs from aged mice showed a decrease in BCL-2 expression compared to LSKs from young mice and no change in the BCL-XL expression (Figure 5.12A). In BMSC on the other hand, whilst there was no difference BCL-2 expression in BMSCs from young and aged mice, the expression of BCL-XL was significantly increased in BMSCs from aged mice compared to young mice (Figure 5.12B). Thus, the senescent BMSCs, but not the HPCs, show overexpression of the anti-apoptotic protein BCL-2 and could therefore potentially be targeted using ABT-263.

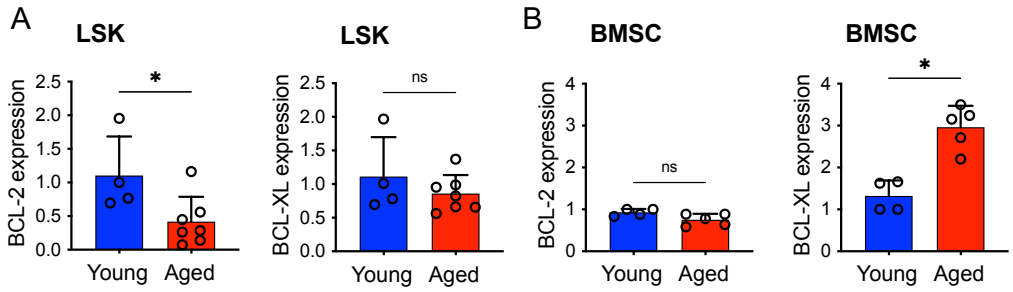

Figure 5.12. BCL-XL expression is increased in BMSCs from aged mice. *qPCR was used to measure the expression of BCL-2 and BCL-XL, normalised to GAPDH, in sorted (A) LSKs and (B) BMSCs from young and aged C57Bl/6 mice. *P < 0.05, ns = not significant using Mann-Whitney U test.*

To study the effect of in vivo inhibition of the anti-apoptotic BCL-2 proteins, aged mice were treated with ABT-263 or vehicle control daily for 7 days via oral gavage. Subsequently, after a seven-day recovery period they were treated with LPS or vehicle control and sacrificed 16 hours later (Figure 5.13)

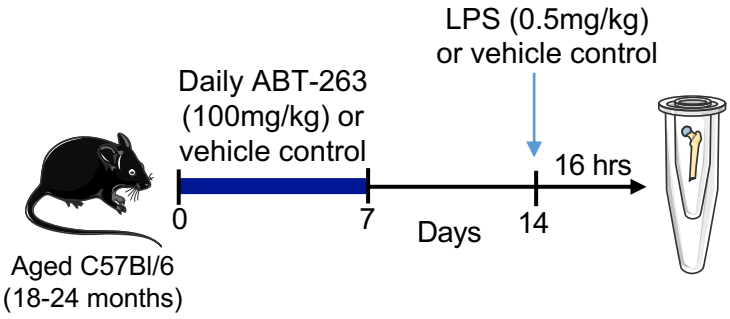

Figure 5.13. Schematic of the experiment.
18-24 months old C57Bl/6 mice were treated daily with 100mg/kg ABT-263 or vehicle control for 7 days followed by 0.5mg/kg LPS or vehicle control. 16 hours after the LPS treatment the mice were sacrificed and their BM was extracted for analysis.

Flow cytometry was used to assess the effect of ABT-263 treatment on BMSC frequency, which was shown to be reduced in aged mice treated with ABT-263 compared to age matched controls (Figure 5.14A). Furthermore, the expression of p16 was downregulated in the ABT-263 treated mice and there was no change in p21 expression (Figure 5.14B). Together this data shows that treatment with ABT-263 successfully depletes the senescent BMSCs in the aged BM microenvironment.

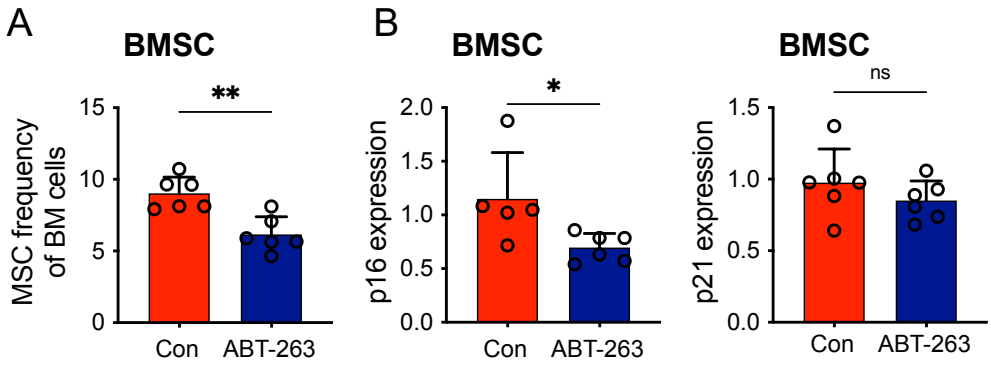

Figure 5.14. ABT-263 treatment reduced BMSC frequency and p16 expression.
*(A) Flow cytometry analysis of BMSC frequency in aged mice treated with ABT-263 compared to vehicle control (con). (B) Expression of p16 and p21, analysed by qPCR and normalised to GAPDH in BMSCs sorted from aged ABT-263 treated C57Bl/6 mice and age-matched controls. *P < 0.05, **P < 0.01, ns = not significant using Mann-Whitney U test.*

Next, the effect of targeting the senescent BMSCs with ABT-263 on the HSC and HPC populations following LPS treatment was analysed by flow cytometry. Treatment with ABT-263 followed by LPS resulted in significant expansion of the HSC, LSK and MPP populations, which is not seen in the age matched controls treated with LPS alone (Figure 5.15).

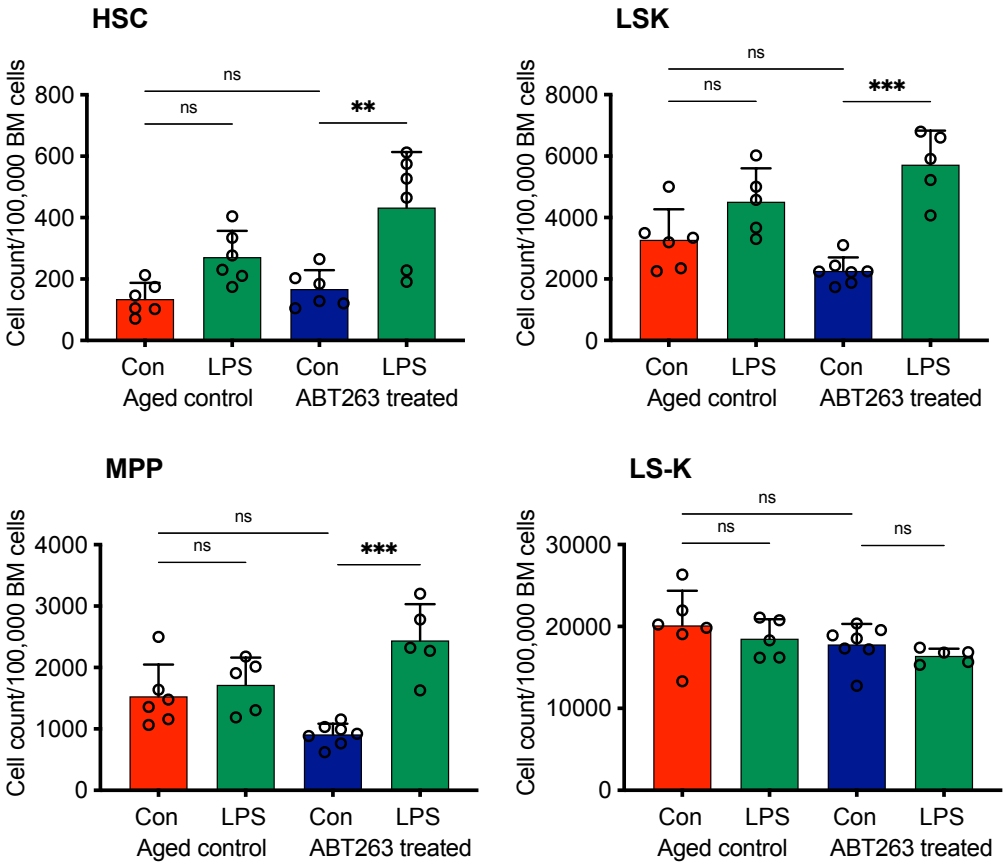

Figure 5.15. ABT-263 treatment of aged mice promotes expansion of haematopoietic cells after LPS treatment.
*Flow cytometry analysis of HSC, LSK, MPP and LS-K counts per 100,000 BM cells in aged C57Bl/6 mice treated with ABT-263 or vehicle control with or without LPS. **P < 0.01, ***P < 0.001, ns = not significant using Two-way Anova.*

In addition, analysis of the mitochondrial membrane potential showed a significant increase in TMRM^{hi} HSC frequency and stable TMRM^{hi} frequency of LSKs and MPPs in mice treated first with ABT-263 and then LPS (Figure 5.16). These changes are similar to those observed in young mice after LPS treatment. In aged controls on the other hand, LPS treatment resulted in no change in TMRM^{hi} HSC frequency and the TMRM^{hi} frequency of LSKs, MPPs and LS-Ks was reduced following LPS treatment, consistent with earlier data from aged mice.

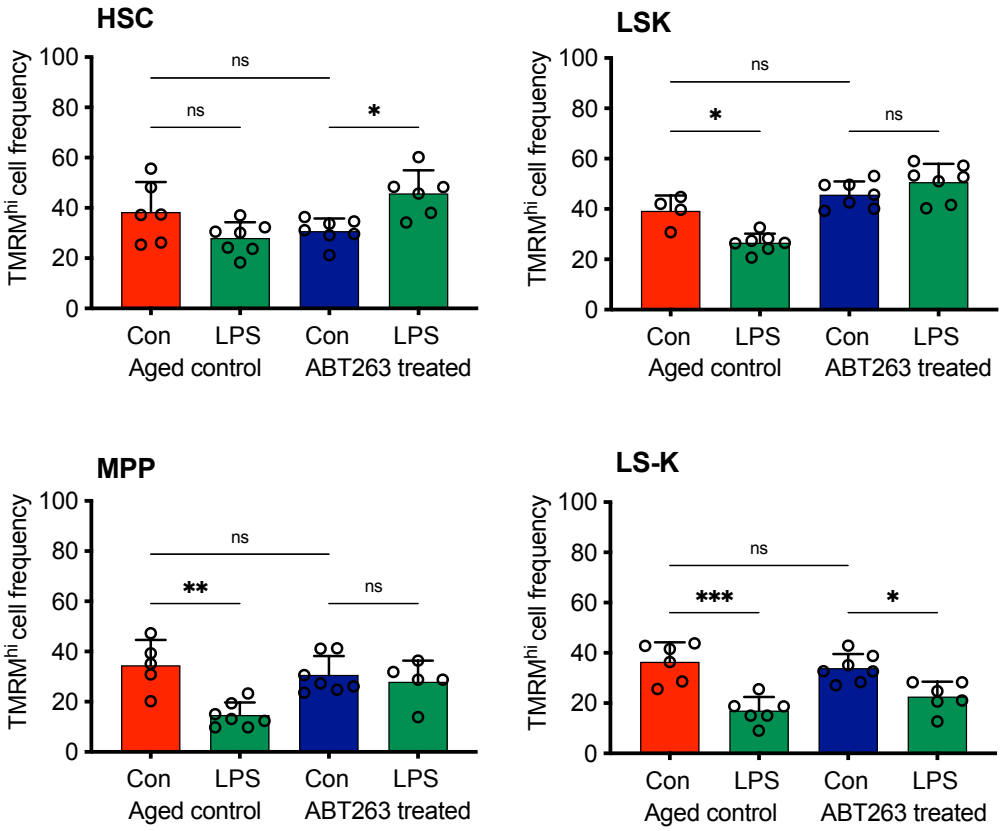

Figure 5.16. TMRM^{hi} HSC frequency increased in aged mice pre-treated with ABT-263 in response to LPS.
*Effects of LPS treatment on TMRM^{hi} frequency of HSCs, LSKs, MPPs and LS-Ks in aged mice treated with ABT-263 or vehicle control are shown. *P < 0.05, **P < 0.01, ***P < 0.001, ns = not significant using Two-way Anova.*

To fully investigate the impact of the changes in the BM microenvironment resulting from ABT-263 treatment on the haematopoietic metabolic profile metabolic output of LKs was measured by seahorse metabolic flux analysis.

This showed that ABT-263 treatment alone promoted an increase in OCR in the LK population with increases in both basal and maximal respiration compared to LKs from aged controls (Figure 5.17). This was, however, further increased after LPS treatment, demonstrating an improved response to stress in the LKs from aged mice treated with ABT-263.

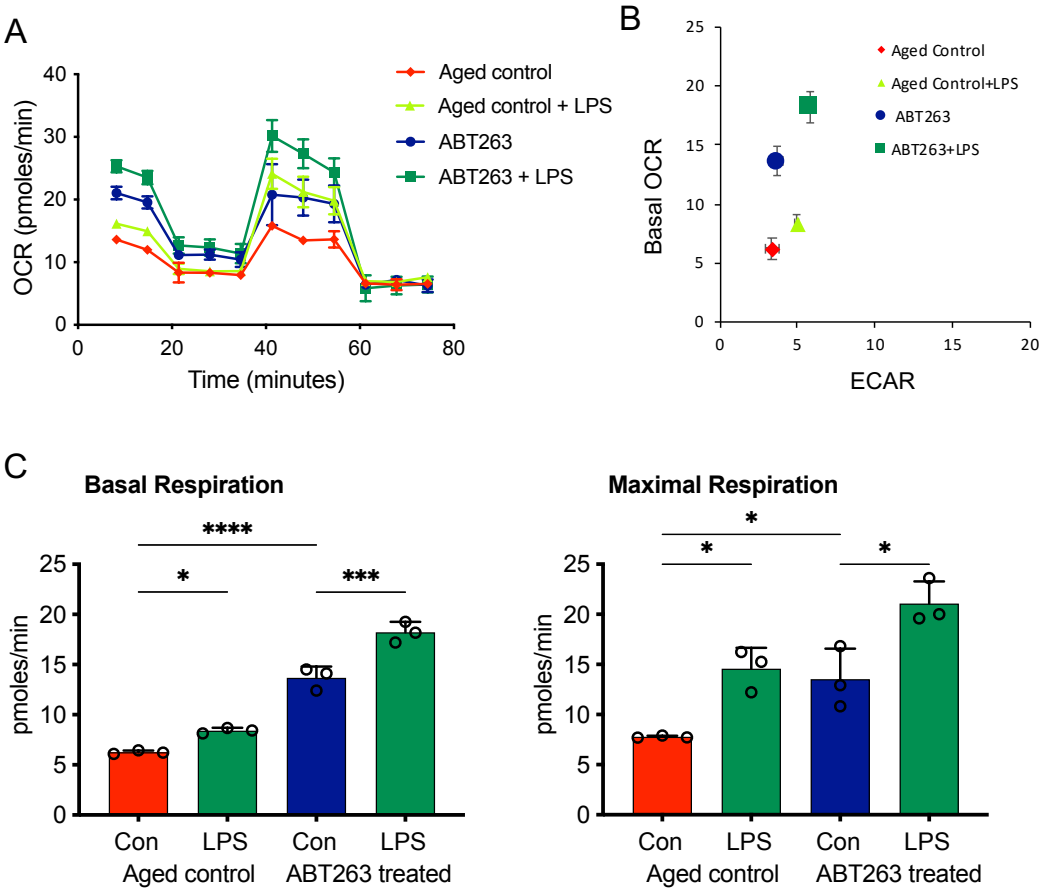

Figure 5.17. ABT-263 treatment improves the metabolic response to stress in aged mice.
*(A) Seahorse metabolic flux analysis was used to measure OCR in aged control C57BL/6 mice, aged C57Bl/6 mice treated with LPS, aged C57Bl/6 mice treated with ABT-263 alone and aged C57Bl/6 mice treated with ABT-263 and LPS. (B) The relative changes in OCR and ECAR in the four treatment groups are shown. (C) Changes in basal and maximal respiration in ABT-263 or vehicle control (con) treated mice with and without LPS treatment. *P < 0.05, ***P < 0.001, ****P<0.0001 using Two-way Anova.*

Finally, metabolic substrate analysis of the LKs was carried out using Mitoplates from Biolog. This revealed an increased use of TCA cycle metabolites in mice treated with ABT-263, which was further enhanced following LPS treatment (Figure 5.18). Together, this data demonstrates that targeting of senescent BMSCs with ABT-263 improves the metabolic response to HPCs to infection.

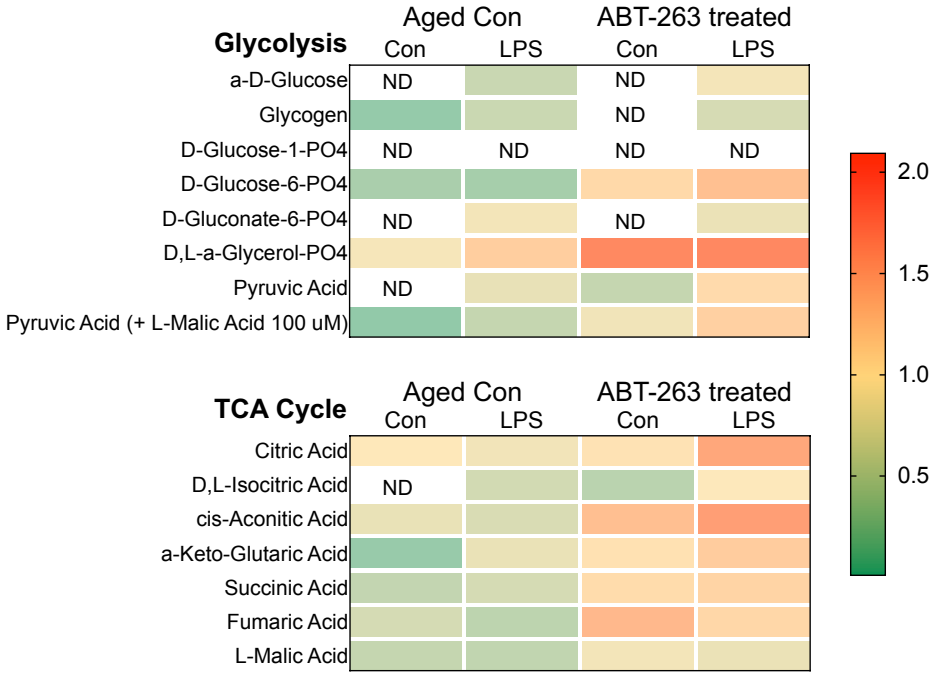

Figure 5.18. Substrate metabolism is upregulated in HPCs from aged mice treated with ABT-263 and LPS.
LKs were isolated from aged mice treated with ABT-263 or vehicle control followed by LPS or vehicle control. Biolog analysis of the utilisation of glycolytic and TCA cycle substrates by the isolated LKs is shown. ND = not detected.

5.5. Summary

The results discussed here highlight the key role of the BM microenvironment in regulating and promoting HSC and HPC function and health. BMSCs, but not HSCs or HPCs, were shown to acquire a senescent phenotype in aged mice with associated overexpression of the anti-apoptotic protein BCL-XL. Interventions that target the senescent BMSC in the microenvironment both in the p16-3MR mouse model and using the drug ABT-263 resulted in an improved metabolic responses of HSC and HPCs to LPS treatment. This was demonstrated by an increased or stable $TMRM^{hi}$ cell frequency, a shift towards OXPHOS and an increased use of TCA cycle metabolites. Overall, this suggests a healthier haematopoietic response to stress that is similar to the response observed in young mice. Furthermore, it supports the hypothesis that the age-related metabolic changes observed in chapters one and two are not solely driven by intrinsic changes of the HSC and HPC populations but that the BM microenvironment significantly contributes to these changes.

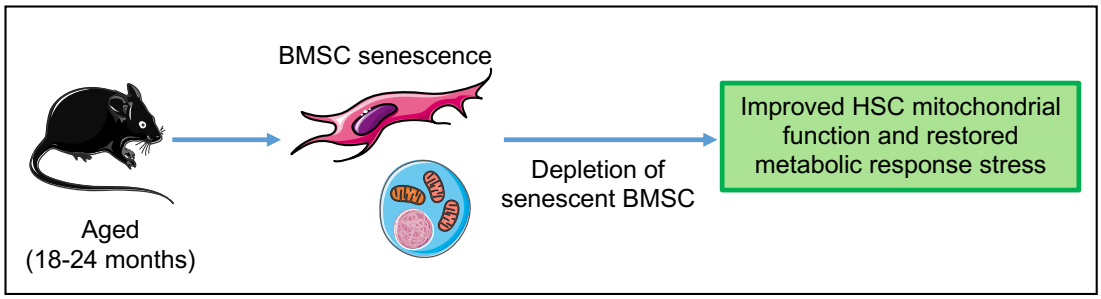

Figure 5.19. Investigating the role of senescent cells in the haematopoietic response to stress.
BMSCs from aged mice acquire a senescent phenotype that directly affects HSC and HPC function, in particular their mitochondrial health. Depletion of senescent cells in the BM microenvironment results in improved HSC mitochondrial function and restores the HSC and HPC metabolic response to stress.

6. Discussion

6.1. General Discussion

Humans are living longer than ever. The average life expectancy continues to increase. This is a result of extensive medical advances and societal changes. However, this progress has also created new challenges, diseases that were once fatal have now become chronic conditions and entirely new disease entities have been described. Moreover, diseases that occur rarely in younger populations are becoming increasingly common as the population ages. Together, these changes have transformed the landscape of medicine, patient numbers are continually increasing and their care needs are becoming ever more complex. In haematology, this is, for example, reflected in patients with myeloma. Only 20 years ago the 5- and 10-year survival rate was 27.6% and 14.3%, respectively, and this has now almost doubled to 47.0% and 32.5% (267). This, of course shows fantastic progress in the management of the disease and has had an enormous impact on patients and their families. With this success, however, also comes an ongoing need for monitoring and treatment of these patients and this, in turn, has an effect on the healthcare services. Moreover, as patients with myeloma live longer, they develop other age-related conditions and their care needs therefore become more complex and treatment plans must consider co-morbidities and drug interactions. A holistic and patient individualised approach is needed and this requires both time and resources. This is just one example of how the combination of a growing ageing population and medical advances are shaping current medical care provision.

The purpose of ageing research is not, as some may believe, to indefinitely increase life expectancy, but instead to actually reduce disease development and morbidity in this ageing population. By understanding the age-related changes that drive disease development, it may be possible to slow down this process, reduce morbidity and, as a result, improve the quality of life for older people whilst reducing the burden on the health services and society. To start this process, it essential to understand the biological changes that occur with

age. In this thesis I have focused on localised age-related changes in the BM and how these may have a systemic impact by altering the haematopoietic response to stress. I have investigated the metabolic changes of haematopoietic cells in the aged BM and how the ageing BM microenvironment influence these changes.

The data in this study demonstrates that HSCs and HPCs do acquire some intrinsic metabolic changes with age and that these may impact on their overall function, their expansion and differentiation potential, and, of course, their re-renewal capacity. However, examination of the BMSCs revealed that their senescent phenotype in aged mice, at least in part, drives some of the age-related changes observed in the haematopoietic cell populations. This was supported by the observation of improved metabolic function following transplantation or depletion of senescent cells.

Understanding the metabolic changes that occur with age and how these contribute to the impaired haematopoietic stress response may in the future shed light on how these changes also promote the development of haematological malignancies. Most haematological malignancies increase with age and in some of them cellular senescence has directly been shown to promote growth and disease progression (25, 263). Understanding of the changes that occur in the BM during physiological ageing may inform future research of how these changes can promote tumour development and chemotherapy resistance.

6.2. Key Findings

6.2.1. In young and aged mice two distinct HSC populations can be defined based on the mitochondrial membrane potential

In this study I have shown that the metabolic profile of HSCs from aged mice differs from that of young mice. The vast majority of HSCs from aged mice have a low mitochondrial membrane potential, whilst in young mice $TMRM^{lo}$ HSCs are seen infrequently. The reasons HSCs primarily rely on glycolysis is to minimise oxidative stress and mitochondrial ROS as this has been implicated in reducing long-term HSC health and self-renewal potential (268, 269). Studies have shown that lowering the mitochondrial activity of HSCs promotes self-renewal over differentiation (259). The transplant model described in this study confirms that HSCs with low mitochondrial membrane potential have superior repopulation potential compared to HSCs with high mitochondrial membrane potential measured by TMRM. Thus, $TMRM^{hi}$ HSCs were unable to repopulate the BM following transplantation. $TMRM^{lo}$ HSCs, on the other hand, engrafted in the competitive transplant setting. This was observed in HSCs from both young and aged mice. Thus, this study clearly identifies two functionally distinct HSC populations based on their metabolic profile. It suggests that the true HSC population, with self-renewal capacity, is much smaller than the total population of cells defined by the HSC cell surface markers (Lin-, CD117+, Sca1+, CD150+, CD48-).

Whilst $TMRM^{lo}$ HSCs from aged mice successfully engrafted in the first transplant, in a secondary transplant their engraftment was significantly reduced compared to $TMRM^{lo}$ HSCs from young mice. As aged mice have significantly more $TMRM^{lo}$ HSCs compared to young mice, this raises the question whether this $TMRM^{lo}$ HSC population is heterogenous and not all cells in this population have the same functional profiles. The single cell sequencing analysis that is currently underway will hopefully shed some light on this and help identify distinct subpopulations within this metabolically defined HSC population. The results may make it possible to further define the

characteristics of the true HSC population that drive engraftment in the BM and maintain the HSC renewal capacity.

6.2.2. Mitochondrial function is impaired in HSCs from aged mice

In aged mice, the decline in mitochondrial membrane potential of HSCs is associated with an increase in mitochondrial content and a reduction in the frequency of MitoSox^{hi} HSCs. The reason for the reduction in mitochondrial ROS is unclear, however it could simply reflect an overall reduction in mitochondrial activity. Together with the changes in mitochondrial membrane potential, this could indicate an accumulation of mitochondria with impaired or reduced function in the HSCs from aged mice. It is therefore possible that the mechanism that drives low mitochondrial membrane potential in HSCs from young and aged mice is different. Whilst in young mice this is a well-regulated protective mechanism to minimise oxidative stress and promote long-term health, in aged mice this actually reflects a decline in mitochondrial health and an accumulation of dysfunctional mitochondria. Mitochondrial dysfunction is one of the hallmarks of ageing and has been associated with the development of age-related diseases (14, 270, 271). It therefore follows that age-related changes in mitochondrial function could drive or contribute to pathological changes in the haematopoietic compartment. Moreover, mitochondrial dysfunction has been directly associated with cellular senescence, as both a driver for and a result of the senescent phenotype (18, 272).

6.2.3. The haematopoietic response to stress is impaired in aged mice

A key function of the BM is its ability to respond quickly and effectively to external stress, including bleeding and infection (273). In the case of infection, the BM response is essential for the initiation of an adequate immune response, timely control of the infection and, ultimately, a complete systemic recovery (91). When this is disrupted, infections can lead to local and systemic inflammatory changes, sepsis and widespread organ damage leading to delayed or impaired recovery (274, 275). The older population is known to be

more susceptible to infections and more likely to experience severe symptoms due to an overall diminished immune response (276-278). Patients often recover more slowly and their risk of long-term morbidity and mortality following infections is increased (7, 279).

Whilst there is some understanding of how the aged BM changes, with cell expansion, myeloid shift and overall reduction in the self-renewal capacity of HSCs, exactly how this alters the haematopoietic response to stress remains largely unknown. In this study I have focussed on the metabolic changes in the HSC and HPC populations, which previous work has shown to be key in regulating the HSC response to stress in the young (91). This study shows that not only is the baseline metabolic function of HSCs and HPCs impaired, but they are also unable to upregulate their metabolic output effectively in response to stress. LPS was used as a mimic for infection in this study and whilst in young mice this drives HSC and HPC expansion and a rapid shift to OXPHOS, in aged mice this shift is not observed. OXPHOS is the most efficient way to produce ATP and therefore is favoured by HSCs and HPCs when demands for proliferation and differentiation are high (91, 280). The metabolic pathway analysis showed that HPCs from aged mice are metabolically less active both at baseline and after LPS than HPCs from young mice, with reduced metabolism of glycolytic and TCA cycle substrates. The baseline changes likely reflect the accumulation of dysfunctional mitochondria, whilst the impaired response to LPS suggests a possible disruption of the support from the BM microenvironment. This study demonstrates that this is not caused by a fault in the mechanism of mitochondrial transfer, but rather that the mitochondria being transferred may not have the functional capacity to support the increased energy demand of the HSCs and HPCs in response to stress.

6.2.4. Transplantation of aged HSCs into young mice improves their mitochondrial function and the haematopoietic response to stress

HSCs and HPCs rely heavily on the BM microenvironment and its supportive cellular components, including BMSCs, adipocytes, endothelial cells osteoblasts and osteoclasts (281). The impact of ageing in the BM microenvironment on HSC and HPC health and their mitochondrial function becomes evident when cells are removed from aged microenvironment and transplanted into young mice. It is known that HSCs from aged mice have an overall reduced repopulation potential. I confirmed this and showed that HSCs from aged mice can repopulate the BM of young mice and engraft, but that this is slightly less effective compared to transplanting young HSCs. Moreover, the TMRM based transplant model demonstrates that the repopulation potential of HSCs from aged mice significantly reduces in a secondary transplant. However, once engrafted into a young BM microenvironment, HSCs from aged mice show a potential to recover from the impact of the aged BM microenvironment. Not only does their baseline mitochondrial membrane potential improve, but they can also mount a more effective response to LPS treatment, with increase in mitochondrial activity measured by TMRM and OCR. This demonstrates that the changes observed in the aged HSCs and HPCs are to some extent reversible and targeting of the microenvironment could improve the mitochondrial health of haematopoietic cell populations.

6.2.5. BMSCs, but not HSCs or HPCs, become senescent in aged mice

Cellular senescence is the irreversible arrest of cell proliferation and is usually characterised by the secretion of the SASP (19). Many factors have been shown to promote cellular senescence, including mitochondrial dysfunction, oxidative stress and DNA damage (22). The acquisition of the senescent phenotype can be beneficial or detrimental to tissue function and systemic recovery from injury. This is determined by the physiological context driving the senescent changes and has been described as an example of antagonistic pleiotropy – the concept that a biological process is beneficial in young organisms with a short lifespan but becomes harmful when the lifespan is

significantly extended (282, 283). Thus, the accumulation of senescent cells observed in ageing has been associated with impaired tissue function and the development of age-related diseases (23-28).

Although mitochondrial dysfunction has been described to directly induce senescence in some cell populations, in this study I demonstrate that this is not the case in HSCs and HPCs. In keeping with previous suggestions that stem cells by definition cannot become senescent as this would mean losing their self-renewal potential (143), I show that both HSCs and HPCs from aged mice do not express the senescent markers p21 or p16 or other characteristics of cellular senescence including SA-β-gal staining. It therefore appears that in these cell populations mitochondrial dysfunction, whilst it may impact on overall cellular function and health, does not drive senescence. However, the haematopoietic cell populations should not be studied in isolation. They have such a significant dependence on their environment that it is essential to consider any age-related changes in the BM microenvironment in conjunction with the changes observed in the HSC populations. Here, I show that the BMSCs in aged mice acquire a senescent phenotype and secrete a SASP and that this has a direct impact on HSC and HPC mitochondrial health and overall function.

6.2.6. Depletion of senescent cells in the aged BM microenvironment improves HSC and HPC function.

The transplant models demonstrate that the BM microenvironment plays an important role in HSC and HPC function and can alter their mitochondrial health. Next, I wanted to determine whether the aged microenvironment can be modulated *in vivo* in order to improve the mitochondrial health of HSCs and HPCs. The senescent BMSCs presented a good potential target for this, particularly as BMSCs are known to directly regulate HSC function and maintenance. Furthermore, a number of mouse models exist which allow direct targeting and elimination of senescent cells *in vivo*. Two models were used to determine how the depletion of senescent cells in the BM microenvironment alters the haematopoietic stress response: the p16-3MR

mouse models and the BCL-2/BCL-XL/BCL-W inhibitor ABT-263. Using both of these models I show that elimination of senescent cells allows recovery of HSC and HPC metabolic health and an improved metabolic response to stress. The frequency of $TMRM^{hi}$ HSCs increased in both models, suggesting overall improved mitochondrial function and this increased further or remained stable following LPS treatment. These findings were similar to those observed in young mice, but contrast with the results from aged mice where $TMRM^{hi}$ HSC and HPC frequency is low and reduced further after LPS treatment. In addition, ABT-263 treatment alone increased the utilisation of TCA and glycolytic metabolites reflecting increased metabolic activity in the HPC population, this was again enhanced by LPS treatment and reflects the data observed in young mice.

The data in this study shows that in both of these models senescent BMSCs are targeted and eliminated by treatment with ABT-263 and GCV in the p16-3MR mouse model. This is demonstrated by the reduction in BMSC counts and a downregulation of p16 and p21 expression. Interestingly, this was not associated with a change in TMRM levels in the BMSCs, suggesting that the senescent phenotype is not directly linked to mitochondrial function in this setting. Although it is clear that senescent BMSC contribute to the age-related metabolic changes in HSC and HPC and are effectively targeted in both *in vivo* models, it is also important to consider the role of other supportive cell populations in the BM microenvironment. Neither the GCV treatment, nor ABT-263 are specifically targeted at BMSCs and would instead deplete any senescent cell populations both in the BM and systemically. It would, therefore, be of interest to investigate the role of senescence in other cell populations within the ageing BM microenvironment and their impact on the haematopoietic metabolic function in the future. Furthermore, whilst ABT-263 has been shown to have senolytic activity, the expression of the anti-apoptotic BCL-2 family of proteins is not unique to senescent cells. As a result, ABT-263 treatment may have a wider, less specific, target cell population that would be more difficult to fully define. Finally, the systemic effects of these treatments are likely to be complex and would be challenging to decipher.

This highlights the clinical limitations of senescent cell depletion and the wider use of senolytics. *In vivo* models are a good tool to demonstrate the effect of eliminating senescent cells and it would even be possible to develop models in which only specific cell populations are depleted when they acquire a senescent phenotype. However, as is the case with ABT-263, when using pharmaceutical agents this specificity is usually lost. Most known targets associated with the senescent phenotype are not unique to senescent cells and have other essential functions which, when disrupted, result in unwanted side effects. Furthermore, one must remember that the process of senescence and the secretion of the SASP developed as protective mechanisms that are vital for effective wound healing and tissue repair. Thus, elimination of all senescent cells or blocking the SASP could have negative implications in the long term.

The key to ageing research may, therefore, not be to remove senescent cells entirely but rather to inhibit the effect they have on their surrounding tissues. Understanding how the accumulation of senescent cells contributes to pathologies could help to promote tissue health by targeting the processes impaired by this accumulation. An alternative approach would be to identify the driving mechanism for the accumulation and impaired clearance of senescent cells in ageing. It is evident, however, that senescent cells are key to many age-related pathologies and understanding these processes better can only be beneficial to our ageing population.

6.3. Limitations

Although the data in this study improves our understanding of how ageing alters the metabolic profile of HSCs and HPCs, in particular in response to stress, it nevertheless has a number of limitations. These relate both to restrictions when carrying out *in vivo* work and the ability to isolate and preserve cell populations *ex vivo*. The majority of the work for this study was carried out using *in vivo* models. *In vitro* work was limited as any culturing of cells could alter their phenotypes and particularly affect the ability to compare young and aged cell populations.

Whilst a primary focus of this study was the HSC population, for many of the in vitro assays LK populations were used instead. This was partly because some assays, particularly the seahorse metabolic flux analysis and the metabolic pathway analysis, require large numbers of cells. Thus, it would have been difficult to isolate enough HSCs even when pooling samples from multiple mice. Furthermore, the process of separating out the HSC population by FACS would have taken much longer than the methods of lineage depletion and CD117 enrichment. This would have removed the cell populations from the microenvironment for longer and could potentially have acted a direct stress stimulus and could, therefore, have influenced the metabolic pathways of the cell populations.

For the same reason, the majority of transplants were performed using LSKs and not HSCs, as these can be sorted much faster, therefore limiting the time the cells are outside the BM microenvironment. However, this could have resulted in some small differences in the total number of HSCs sorted from each mouse and subsequently transplanted. This is particularly relevant as the HSC frequency of LSKs in aged mice is slightly higher than in young mice. It is therefore possible that in the transplants using LSKs from aged mice more HSCs were injected than in those using LSKs from young mice. Despite this, the results remain pertinent as aged mice showed reduced engraftment compared to young mice and if higher numbers of HSCs had been engrafted, if anything this difference would be underestimated.

Another limitation was working with aged mice. All experiments were designed in keeping with the 3Rs (Replacement, Reduction and Refinement) and Home Office guidelines to perform humane animal research and prevent animal suffering. As a result, the total numbers of mice were kept low for all experiments. As more variability is often observed in aged mice more mice were used in each treatment group where possible. However, this was at times limited by the availability of aged mice. In particular, only a small number of aged p16-3MR mice were available. In addition, occasionally, mice were found to have tumours at the time of dissection that had not been evident before the experiment was started, or significant outlying results on analysis and were therefore excluded.

The availability of aged mouse colonies also limited the transplant set ups. In all but one transplant, cells from PepCboy mice were engrafted into C57Bl/6 mice whilst in the final transplant this was reversed. This was primarily due to the mice available at the time of the transplant. This is particularly important for the competitive transplants, as CD45.2 engraftment has been shown to be slightly favoured over CD45.1 in competitive transplants (255). However, for each transplant the different treatment groups always had the same direction of transplant and therefore remain comparable to each other.

It would have been interesting to investigate the effect of transplanting young HSCs into an aged BM microenvironment. However, this would have required busulfan treatment of aged mice for three days followed by the transplantation. Given the vulnerability of the aged mice, it was decided that this would not be feasible.

Finally, the age of the mice also influenced the treatments that could be given. Thus, only LPS was used as an infection mimic and at a reduced dose of 0.5mg/kg. As even this low dose caused significant deterioration in aged mice after 16 hours, alternatives of whole bacterial infections such as salmonella were not felt to be appropriate given the risk of animal suffering. LPS only has one target and therefore results in a relatively well controlled and limited

immune response, whilst whole bacterial infections secrete a number of virulent factors and therefore trigger a more widespread inflammatory response. Nevertheless, whilst LPS treatment may not fully reflect the systemic and localised effect of bacterial infection it remains a useful tool in studying the kinetics of the BM response to stress.

6.4. Future work

All primary aims and objectives of this study were addressed in this thesis. However, as is often the case with research, the result has been a new list of unanswered questions that could be addressed in the future. In addition, whilst this study improves our understanding of how ageing changes the haematopoietic stress response, many aspects of this remain unclear or unknown.

Firstly, the data from the single cell sequencing of $TMRM^{lo}$ and $TMRM^{hi}$ HSCs from young and aged mice remains outstanding. It will be interesting to see whether this successfully identifies functionally different subpopulations in HSCs from both young and the aged mice. Furthermore, this could help identify potential specific targets for interventions to improve overall HSC function, particularly in the aged HSCs.

In addition, this study only focusses on the BMSCs within the BM microenvironment. Other BM cell populations are known to be equally important both in HSC maintenance and in supporting the HSC response to stress. Adipocytes and the provision of free fatty acids have, for example, been shown to also be essential for an effective metabolic response to infection in HSCs (240). Moreover, macrophage function, or rather dysfunction, has been implicated as a potential mechanism for impaired clearance of senescent cells in ageing. Investigating how macrophage phenotypes and polarisation changes both in the BM and in tissue specific macrophages may help to understand how ageing alters their function and prevents effective clearance of senescent cells.

Finally, it would be interesting to determine how the observed age-related changes influence the development of BM malignancies. The incidence of most BM malignancies increases with age and they appear to thrive in the senescent BM microenvironment (25, 263). Understanding how the metabolic changes in the aged BM described in this study promote malignant growth may help to identify specific targets in the aged BM microenvironment. This

would require investigations of both animal models and primary human BM samples from patients with malignancies such as AML or myeloma to determine how ageing creates a more pro-tumoral microenvironment.

6.5. Conclusion

In this thesis I have shown how senescent BMSCs drive metabolic changes of the HSC and HPC populations in aged mice and that this has a direct impact on the haematopoietic stress response. In addition, I have identified two functionally distinct HSC populations in both young and aged mice based on their mitochondrial membrane potential. The significance of this remains to be explored further once the single cell sequencing has been completed. Here, I show that HSCs and HPCs from aged mice have impaired metabolic function at baseline and that their metabolic output cannot be adequately upregulated in response to stress. Furthermore, this is not simply due to intrinsic changes of the haematopoietic cell populations, which themselves do not acquire a senescent phenotype, but rather driven by the accumulation of senescent BMSCs in the BM microenvironment. Thus, removal of HSCs from the aged BM microenvironment and transplantation into young mice results in the recovery of the HSC metabolic health and an improved response to stress. In addition, depletion of senescent cells from the BM microenvironment using the p16-3MR mouse model or the senolytic ABT-263 has a similar effect and results in an improved metabolic response to LPS treatments. Overall, this study is yet another example of how the accumulation of senescent cells can impair normal physiological processes and drive disease development. It will never be possible to entirely reverse or stop the ageing process. Complete elimination of senescent cells may not be clinically feasible or desirable. However, perhaps it will one day be possible to target the mechanisms by which senescent cells drive pathologies and thereby improve the quality of life of our ageing population. Not to enable them to live forever but, rather so that they can enjoy a longer disease-free period towards the end of their lives.

7. References

The Figures were partly generated using Servier Medical Art, provided by Servier, licensed under a Creative Commons Attribution 3.0 unported license

1. Hellmich C, Wojtowicz E, Moore JA, Mistry JJ, Jibril A, Johnson BB, et al. p16INK4A dependent senescence in the bone marrow niche drives age-related metabolic changes of hematopoietic progenitors. Blood Adv. 2022.
2. Partridge L, Deelen J, Slagboom PE. Facing up to the global challenges of ageing. Nature. 2018;561(7721):45-56.
3. Crimmins EM. Lifespan and Healthspan: Past, Present, and Promise. Gerontologist. 2015;55(6):901-11.
4. Lee RD. Rethinking the evolutionary theory of aging: transfers, not births, shape senescence in social species. Proc Natl Acad Sci U S A. 2003;100(16):9637-42.
5. Vaupel JW, Carey JR, Christensen K, Johnson TE, Yashin AI, Holm NV, et al. Biodemographic trajectories of longevity. Science. 1998;280(5365):855-60.
6. Oeppen J, Vaupel JW. Demography. Broken limits to life expectancy. Science. 2002;296(5570):1029-31.
7. Foreman KJ, Marquez N, Dolgert A, Fukutaki K, Fullman N, McGaughey M, et al. Forecasting life expectancy, years of life lost, and all-cause and cause-specific mortality for 250 causes of death: reference and alternative scenarios for 2016-40 for 195 countries and territories. Lancet. 2018;392(10159):2052-90.
8. Kontis V, Bennett JE, Mathers CD, Li G, Foreman K, Ezzati M. Future life expectancy in 35 industrialised countries: projections with a Bayesian model ensemble. Lancet. 2017;389(10076):1323-35.
9. Burger O, Baudisch A, Vaupel JW. Human mortality improvement in evolutionary context. Proc Natl Acad Sci U S A. 2012;109(44):18210-4.
10. Fogel RW, Costa DL. A theory of technophysio evolution, with some implications for forecasting population, health care costs, and pension costs. Demography. 1997;34(1):49-66.
11. Niccoli T, Partridge L. Ageing as a risk factor for disease. Curr Biol. 2012;22(17):R741-52.
12. Palmer RD. Aging clocks & mortality timers, methylation, glycomic, telomeric and more. A window to measuring biological age. Aging Med (Milton). 2022;5(2):120-5.
13. López-Otín C, Blasco MA, Partridge L, Serrano M, Kroemer G. The hallmarks of aging. Cell. 2013;153(6):1194-217.
14. Sun N, Youle RJ, Finkel T. The Mitochondrial Basis of Aging. Mol Cell. 2016;61(5):654-66.
15. Petersen KF, Befroy D, Dufour S, Dziura J, Ariyan C, Rothman DL, et al. Mitochondrial dysfunction in the elderly: possible role in insulin resistance. Science. 2003;300(5622):1140-2.
16. Passos JF, Nelson G, Wang C, Richter T, Simillion C, Proctor CJ, et al. Feedback between p21 and reactive oxygen production is necessary for cell senescence. Mol Syst Biol. 2010;6:347.

17. Velarde MC, Flynn JM, Day NU, Melov S, Campisi J. Mitochondrial oxidative stress caused by Sod2 deficiency promotes cellular senescence and aging phenotypes in the skin. Aging (Albany NY). 2012;4(1):3-12.
18. Wiley CD, Velarde MC, Lecot P, Liu S, Sarnoski EA, Freund A, et al. Mitochondrial Dysfunction Induces Senescence with a Distinct Secretory Phenotype. Cell Metab. 2016;23(2):303-14.
19. Hayflick L. The biology of human aging. Am J Med Sci. 1973;265(6):432-45.
20. HAYFLICK L, MOORHEAD PS. The serial cultivation of human diploid cell strains. Exp Cell Res. 1961;25:585-621.
21. Demaria M, Ohtani N, Youssef SA, Rodier F, Toussaint W, Mitchell JR, et al. An essential role for senescent cells in optimal wound healing through secretion of PDGF-AA. Dev Cell. 2014;31(6):722-33.
22. Campisi J. Aging, cellular senescence, and cancer. Annu Rev Physiol. 2013;75:685-705.
23. Saez-Atienzar S, Masliah E. Cellular senescence and Alzheimer disease: the egg and the chicken scenario. Nat Rev Neurosci. 2020.
24. Chinta SJ, Woods G, Demaria M, Rane A, Zou Y, McQuade A, et al. Cellular Senescence Is Induced by the Environmental Neurotoxin Paraquat and Contributes to Neuropathology Linked to Parkinson's Disease. Cell Rep. 2018;22(4):930-40.
25. Abdul-Aziz AM, Sun Y, Hellmich C, Marlein CR, Mistry J, Forde E, et al. Acute myeloid leukemia induces protumoral p16INK4a-driven senescence in the bone marrow microenvironment. Blood. 2019;133(5):446-56.
26. Jeon OH, Kim C, Laberge RM, Demaria M, Rathod S, Vasserot AP, et al. Local clearance of senescent cells attenuates the development of post-traumatic osteoarthritis and creates a pro-regenerative environment. Nat Med. 2017;23(6):775-81.
27. Jeon OH, David N, Campisi J, Elisseeff JH. Senescent cells and osteoarthritis: a painful connection. J Clin Invest. 2018;128(4):1229-37.
28. Childs BG, Baker DJ, Wijshake T, Conover CA, Campisi J, van Deursen JM. Senescent intimal foam cells are deleterious at all stages of atherosclerosis. Science. 2016;354(6311):472-7.
29. Sharpless NE, Sherr CJ. Forging a signature of in vivo senescence. Nat Rev Cancer. 2015;15(7):397-408.
30. Kale A, Sharma A, Stolzing A, Desprez PY, Campisi J. Role of immune cells in the removal of deleterious senescent cells. Immun Ageing. 2020;17:16.
31. Muñoz-Espín D, Serrano M. Cellular senescence: from physiology to pathology. Nat Rev Mol Cell Biol. 2014;15(7):482-96.
32. Christophorou MA, Martin-Zanca D, Soucek L, Lawlor ER, Brown-Swigart L, Verschuren EW, et al. Temporal dissection of p53 function in vitro and in vivo. Nat Genet. 2005;37(7):718-26.
33. Levine AJ, Oren M. The first 30 years of p53: growing ever more complex. Nat Rev Cancer. 2009;9(10):749-58.
34. Rodier F, Coppé JP, Patil CK, Hoeijmakers WA, Muñoz DP, Raza SR, et al. Persistent DNA damage signalling triggers senescence-associated inflammatory cytokine secretion. Nat Cell Biol. 2009;11(8):973-9.
35. Coppé JP, Rodier F, Patil CK, Freund A, Desprez PY, Campisi J. Tumor suppressor and aging biomarker p16(INK4a) induces cellular senescence

without the associated inflammatory secretory phenotype. J Biol Chem. 2011;286(42):36396-403.
36. Coppé JP, Patil CK, Rodier F, Sun Y, Muñoz DP, Goldstein J, et al. Senescence-associated secretory phenotypes reveal cell-nonautonomous functions of oncogenic RAS and the p53 tumor suppressor. PLoS Biol. 2008;6(12):2853-68.
37. Coppé JP, Desprez PY, Krtolica A, Campisi J. The senescence-associated secretory phenotype: the dark side of tumor suppression. Annu Rev Pathol. 2010;5:99-118.
38. Sun Y, Campisi J, Higano C, Beer TM, Porter P, Coleman I, et al. Treatment-induced damage to the tumor microenvironment promotes prostate cancer therapy resistance through WNT16B. Nat Med. 2012;18(9):1359-68.
39. Song YS, Lee BY, Hwang ES. Dinstinct ROS and biochemical profiles in cells undergoing DNA damage-induced senescence and apoptosis. Mech Ageing Dev. 2005;126(5):580-90.
40. Parrinello S, Coppe JP, Krtolica A, Campisi J. Stromal-epithelial interactions in aging and cancer: senescent fibroblasts alter epithelial cell differentiation. J Cell Sci. 2005;118(Pt 3):485-96.
41. Childs BG, Baker DJ, Kirkland JL, Campisi J, van Deursen JM. Senescence and apoptosis: dueling or complementary cell fates? EMBO Rep. 2014;15(11):1139-53.
42. Yosef R, Pilpel N, Tokarsky-Amiel R, Biran A, Ovadya Y, Cohen S, et al. Directed elimination of senescent cells by inhibition of BCL-W and BCL-XL. Nat Commun. 2016;7:11190.
43. Popgeorgiev N, Jabbour L, Gillet G. Subcellular Localization and Dynamics of the Bcl-2 Family of Proteins. Front Cell Dev Biol. 2018;6:13.
44. Kale J, Osterlund EJ, Andrews DW. BCL-2 family proteins: changing partners in the dance towards death. Cell Death Differ. 2018;25(1):65-80.
45. Shamas-Din A, Kale J, Leber B, Andrews DW. Mechanisms of action of Bcl-2 family proteins. Cold Spring Harb Perspect Biol. 2013;5(4):a008714.
46. Warren CFA, Wong-Brown MW, Bowden NA. BCL-2 family isoforms in apoptosis and cancer. Cell Death Dis. 2019;10(3):177.
47. Tsujimoto Y, Finger LR, Yunis J, Nowell PC, Croce CM. Cloning of the chromosome breakpoint of neoplastic B cells with the t(14;18) chromosome translocation. Science. 1984;226(4678):1097-9.
48. Del Gaizo Moore V, Brown JR, Certo M, Love TM, Novina CD, Letai A. Chronic lymphocytic leukemia requires BCL2 to sequester prodeath BIM, explaining sensitivity to BCL2 antagonist ABT-737. J Clin Invest. 2007;117(1):112-21.
49. Moujalled DM, Hanna DT, Hediyeh-Zadeh S, Pomilio G, Brown L, Litalien V, et al. Cotargeting BCL-2 and MCL-1 in high-risk B-ALL. Blood Adv. 2020;4(12):2762-7.
50. DiNardo CD, Pratz K, Pullarkat V, Jonas BA, Arellano M, Becker PS, et al. Venetoclax combined with decitabine or azacitidine in treatment-naive, elderly patients with acute myeloid leukemia. Blood. 2019;133(1):7-17.
51. Adams JM, Cory S. The BCL-2 arbiters of apoptosis and their growing role as cancer targets. Cell Death Differ. 2018;25(1):27-36.
52. Souers AJ, Leverson JD, Boghaert ER, Ackler SL, Catron ND, Chen J, et al. ABT-199, a potent and selective BCL-2 inhibitor, achieves antitumor activity while sparing platelets. Nat Med. 2013;19(2):202-8.

53. Wei AH, Strickland SA, Hou JZ, Fiedler W, Lin TL, Walter RB, et al. Venetoclax Combined With Low-Dose Cytarabine for Previously Untreated Patients With Acute Myeloid Leukemia: Results From a Phase Ib/II Study. J Clin Oncol. 2019;37(15):1277-84.
54. Baker DJ, Wijshake T, Tchkonia T, LeBrasseur NK, Childs BG, van de Sluis B, et al. Clearance of p16Ink4a-positive senescent cells delays ageing-associated disorders. Nature. 2011;479(7372):232-6.
55. Bussian TJ, Aziz A, Meyer CF, Swenson BL, van Deursen JM, Baker DJ. Clearance of senescent glial cells prevents tau-dependent pathology and cognitive decline. Nature. 2018;562(7728):578-82.
56. Dolgin E. Send in the senolytics. Nat Biotechnol. 2020;38(12):1371-7.
57. Chang J, Wang Y, Shao L, Laberge RM, Demaria M, Campisi J, et al. Clearance of senescent cells by ABT263 rejuvenates aged hematopoietic stem cells in mice. Nat Med. 2016;22(1):78-83.
58. Sharma AK, Roberts RL, Benson RD, Pierce JL, Yu K, Hamrick MW, et al. The Senolytic Drug Navitoclax (ABT-263) Causes Trabecular Bone Loss and Impaired Osteoprogenitor Function in Aged Mice. Front Cell Dev Biol. 2020;8:354.
59. Pan J, Li D, Xu Y, Zhang J, Wang Y, Chen M, et al. Inhibition of Bcl-2/xl With ABT-263 Selectively Kills Senescent Type II Pneumocytes and Reverses Persistent Pulmonary Fibrosis Induced by Ionizing Radiation in Mice. Int J Radiat Oncol Biol Phys. 2017;99(2):353-61.
60. Chen J, Jin S, Abraham V, Huang X, Liu B, Mitten MJ, et al. The Bcl-2/Bcl-X(L)/Bcl-w inhibitor, navitoclax, enhances the activity of chemotherapeutic agents in vitro and in vivo. Mol Cancer Ther. 2011;10(12):2340-9.
61. Jaiswal S, Fontanillas P, Flannick J, Manning A, Grauman PV, Mar BG, et al. Age-related clonal hematopoiesis associated with adverse outcomes. N Engl J Med. 2014;371(26):2488-98.
62. Kirkland JL, Tchkonia T. Senolytic drugs: from discovery to translation. J Intern Med. 2020;288(5):518-36.
63. Hellmich C, Moore JA, Bowles KM, Rushworth SA. Bone Marrow Senescence and the Microenvironment of Hematological Malignancies. Front Oncol. 2020;10:230.
64. Tse C, Shoemaker AR, Adickes J, Anderson MG, Chen J, Jin S, et al. ABT-263: a potent and orally bioavailable Bcl-2 family inhibitor. Cancer Res. 2008;68(9):3421-8.
65. Wilson WH, O'Connor OA, Czuczman MS, LaCasce AS, Gerecitano JF, Leonard JP, et al. Navitoclax, a targeted high-affinity inhibitor of BCL-2, in lymphoid malignancies: a phase 1 dose-escalation study of safety, pharmacokinetics, pharmacodynamics, and antitumour activity. Lancet Oncol. 2010;11(12):1149-59.
66. Hickson LJ, Langhi Prata LGP, Bobart SA, Evans TK, Giorgadze N, Hashmi SK, et al. Senolytics decrease senescent cells in humans: Preliminary report from a clinical trial of Dasatinib plus Quercetin in individuals with diabetic kidney disease. EBioMedicine. 2019;47:446-56.
67. Justice JN, Nambiar AM, Tchkonia T, LeBrasseur NK, Pascual R, Hashmi SK, et al. Senolytics in idiopathic pulmonary fibrosis: Results from a first-in-human, open-label, pilot study. EBioMedicine. 2019;40:554-63.

68. Wang R, Yu Z, Sunchu B, Shoaf J, Dang I, Zhao S, et al. Rapamycin inhibits the secretory phenotype of senescent cells by a Nrf2-independent mechanism. Aging Cell. 2017;16(3):564-74.
69. Lagoumtzi SM, Chondrogianni N. Senolytics and senomorphics: Natural and synthetic therapeutics in the treatment of aging and chronic diseases. Free Radic Biol Med. 2021;171:169-90.
70. Kulkarni AS, Gubbi S, Barzilai N. Benefits of Metformin in Attenuating the Hallmarks of Aging. Cell Metab. 2020;32(1):15-30.
71. Moiseeva O, Deschênes-Simard X, St-Germain E, Igelmann S, Huot G, Cadar AE, et al. Metformin inhibits the senescence-associated secretory phenotype by interfering with IKK/NF-κB activation. Aging Cell. 2013;12(3):489-98.
72. Algire C, Moiseeva O, Deschênes-Simard X, Amrein L, Petruccelli L, Birman E, et al. Metformin reduces endogenous reactive oxygen species and associated DNA damage. Cancer Prev Res (Phila). 2012;5(4):536-43.
73. Chen D, Xia D, Pan Z, Xu D, Zhou Y, Wu Y, et al. Metformin protects against apoptosis and senescence in nucleus pulposus cells and ameliorates disc degeneration in vivo. Cell Death Dis. 2016;7(10):e2441.
74. Demaria M, O'Leary MN, Chang J, Shao L, Liu S, Alimirah F, et al. Cellular Senescence Promotes Adverse Effects of Chemotherapy and Cancer Relapse. Cancer Discov. 2017;7(2):165-76.
75. Toth LA. Identifying and Implementing Endpoints for Geriatric Mice. Comp Med. 2018;68(6):439-51.
76. Liu JY, Souroullas GP, Diekman BO, Krishnamurthy J, Hall BM, Sorrentino JA, et al. Cells exhibiting strong $p16^{INK4a}$ promotor activation in vivo display features of senescence. Proc Natl Acad Sci U S A. 2019;116(7):2603-11.
77. Burd CE, Sorrentino JA, Clark KS, Darr DB, Krishnamurthy J, Deal AM, et al. Monitoring tumorigenesis and senescence in vivo with a p16(INK4a)-luciferase model. Cell. 2013;152(1-2):340-51.
78. Yamakoshi K, Takahashi A, Hirota F, Nakayama R, Ishimaru N, Kubo Y, et al. Real-time in vivo imaging of p16Ink4a reveals cross talk with p53. J Cell Biol. 2009;186(3):393-407.
79. Wang B, Wang L, Gasek NS, Zhou Y, Kim T, Guo C, et al. An inducible. Nat Aging. 2021;1(10):962-73.
80. Marlein Christopher R RSA. Bone Marrow. eLS. 2018.
81. Gurevitch O, Slavin S, Feldman AG. Conversion of red bone marrow into yellow - Cause and mechanisms. Med Hypotheses. 2007;69(3):531-6.
82. Shafat MS, Gnaneswaran B, Bowles KM, Rushworth SA. The bone marrow microenvironment - Home of the leukemic blasts. Blood Rev. 2017;31(5):277-86.
83. Orkin SH, Zon LI. Hematopoiesis: an evolving paradigm for stem cell biology. Cell. 2008;132(4):631-44.
84. Anthony BA, Link DC. Regulation of hematopoietic stem cells by bone marrow stromal cells. Trends Immunol. 2014;35(1):32-7.
85. Silva A, Anderson AR, Gatenby R. A multiscale model of the bone marrow and hematopoiesis. Math Biosci Eng. 2011;8(2):643-58.
86. Fliedner TM, Graessle D, Paulsen C, Reimers K. Structure and function of bone marrow hemopoiesis: mechanisms of response to ionizing radiation exposure. Cancer Biother Radiopharm. 2002;17(4):405-26.

87. Dzierzak E, Speck NA. Of lineage and legacy: the development of mammalian hematopoietic stem cells. Nat Immunol. 2008;9(2):129-36.
88. Gao X, Xu C, Asada N, Frenette PS. The hematopoietic stem cell niche: from embryo to adult. Development. 2018;145(2).
89. Fan N, Lavu S, Hanson CA, Tefferi A. Extramedullary hematopoiesis in the absence of myeloproliferative neoplasm: Mayo Clinic case series of 309 patients. Blood Cancer J. 2018;8(12):119.
90. Challen GA, Boles N, Lin KK, Goodell MA. Mouse hematopoietic stem cell identification and analysis. Cytometry A. 2009;75(1):14-24.
91. Mistry JJ, Marlein CR, Moore JA, Hellmich C, Wojtowicz EE, Smith JGW, et al. ROS-mediated PI3K activation drives mitochondrial transfer from stromal cells to hematopoietic stem cells in response to infection. Proc Natl Acad Sci U S A. 2019;116(49):24610-9.
92. Cheng H, Zheng Z, Cheng T. New paradigms on hematopoietic stem cell differentiation. Protein Cell. 2020;11(1):34-44.
93. Liu L, Papa EF, Dooner MS, Machan JT, Johnson KW, Goldberg LR, et al. Homing and long-term engraftment of long- and short-term renewal hematopoietic stem cells. PLoS One. 2012;7(2):e31300.
94. Laurenti E, Göttgens B. From haematopoietic stem cells to complex differentiation landscapes. Nature. 2018;553(7689):418-26.
95. Mayani H. The regulation of hematopoietic stem cell populations. F1000Res. 2016;5.
96. Ema H, Morita Y, Suda T. Heterogeneity and hierarchy of hematopoietic stem cells. Exp Hematol. 2014;42(2):74-82.e2.
97. Cavazzana-Calvo M, Fischer A, Bushman FD, Payen E, Hacein-Bey-Abina S, Leboulch P. Is normal hematopoiesis maintained solely by long-term multipotent stem cells? Blood. 2011;117(17):4420-4.
98. Gabbianelli M, Pelosi E, Montesoro E, Valtieri M, Luchetti L, Samoggia P, et al. Multi-level effects of flt3 ligand on human hematopoiesis: expansion of putative stem cells and proliferation of granulomonocytic progenitors/monocytic precursors. Blood. 1995;86(5):1661-70.
99. Zhang CC, Lodish HF. Cytokines regulating hematopoietic stem cell function. Curr Opin Hematol. 2008;15(4):307-11.
100. Smith BR. Regulation of hematopoiesis. Yale J Biol Med. 1990;63(5):371-80.
101. D'Andrea AD. Hematopoietic growth factors and the regulation of differentiative decisions. Curr Opin Cell Biol. 1994;6(6):804-8.
102. Matsunaga T, Kato T, Miyazaki H, Ogawa M. Thrombopoietin promotes the survival of murine hematopoietic long-term reconstituting cells: comparison with the effects of FLT3/FLK-2 ligand and interleukin-6. Blood. 1998;92(2):452-61.
103. Solar GP, Kerr WG, Zeigler FC, Hess D, Donahue C, de Sauvage FJ, et al. Role of c-mpl in early hematopoiesis. Blood. 1998;92(1):4-10.
104. Sender R, Fuchs S, Milo R. Revised Estimates for the Number of Human and Bacteria Cells in the Body. PLoS Biol. 2016;14(8):e1002533.
105. Kuhn V, Diederich L, Keller TCS, Kramer CM, Lückstädt W, Panknin C, et al. Red Blood Cell Function and Dysfunction: Redox Regulation, Nitric Oxide Metabolism, Anemia. Antioxid Redox Signal. 2017;26(13):718-42.
106. Patel SR, Hartwig JH, Italiano JE. The biogenesis of platelets from megakaryocyte proplatelets. J Clin Invest. 2005;115(12):3348-54.

107. Holinstat M. Normal platelet function. Cancer Metastasis Rev. 2017;36(2):195-8.
108. Ali RA, Wuescher LM, Worth RG. Platelets: essential components of the immune system. Curr Trends Immunol. 2015;16:65-78.
109. Schmied L, Höglund P, Meinke S. Platelet-Mediated Protection of Cancer Cells From Immune Surveillance - Possible Implications for Cancer Immunotherapy. Front Immunol. 2021;12:640578.
110. Schmidt KH, Bruchelt G, Koslowski L. Granulocyte function: current knowledge and methods of assessment. J Burn Care Rehabil. 1985;6(3):261-9.
111. Rosales C. Neutrophil: A Cell with Many Roles in Inflammation or Several Cell Types? Front Physiol. 2018;9:113.
112. Yáñez A, Coetzee SG, Olsson A, Muench DE, Berman BP, Hazelett DJ, et al. Granulocyte-Monocyte Progenitors and Monocyte-Dendritic Cell Progenitors Independently Produce Functionally Distinct Monocytes. Immunity. 2017;47(5):890-902.e4.
113. LeBien TW, Tedder TF. B lymphocytes: how they develop and function. Blood. 2008;112(5):1570-80.
114. Chaplin DD. Overview of the immune response. J Allergy Clin Immunol. 2010;125(2 Suppl 2):S3-23.
115. Ginhoux F, Schultze JL, Murray PJ, Ochando J, Biswas SK. New insights into the multidimensional concept of macrophage ontogeny, activation and function. Nat Immunol. 2016;17(1):34-40.
116. Bain CC, Bravo-Blas A, Scott CL, Perdiguero EG, Geissmann F, Henri S, et al. Constant replenishment from circulating monocytes maintains the macrophage pool in the intestine of adult mice. Nat Immunol. 2014;15(10):929-37.
117. Tamoutounour S, Guilliams M, Montanana Sanchis F, Liu H, Terhorst D, Malosse C, et al. Origins and functional specialization of macrophages and of conventional and monocyte-derived dendritic cells in mouse skin. Immunity. 2013;39(5):925-38.
118. Epelman S, Lavine KJ, Beaudin AE, Sojka DK, Carrero JA, Calderon B, et al. Embryonic and adult-derived resident cardiac macrophages are maintained through distinct mechanisms at steady state and during inflammation. Immunity. 2014;40(1):91-104.
119. Ginhoux F, Jung S. Monocytes and macrophages: developmental pathways and tissue homeostasis. Nat Rev Immunol. 2014;14(6):392-404.
120. Bianco P, Cao X, Frenette PS, Mao JJ, Robey PG, Simmons PJ, et al. The meaning, the sense and the significance: translating the science of mesenchymal stem cells into medicine. Nat Med. 2013;19(1):35-42.
121. Koide Y, Morikawa S, Mabuchi Y, Muguruma Y, Hiratsu E, Hasegawa K, et al. Two distinct stem cell lineages in murine bone marrow. Stem Cells. 2007;25(5):1213-21.
122. Worthley DL, Churchill M, Compton JT, Tailor Y, Rao M, Si Y, et al. Gremlin 1 identifies a skeletal stem cell with bone, cartilage, and reticular stromal potential. Cell. 2015;160(1-2):269-84.
123. Viswanathan S, Shi Y, Galipeau J, Krampera M, Leblanc K, Martin I, et al. Mesenchymal stem versus stromal cells: International Society for Cell & Gene Therapy (ISCT®) Mesenchymal Stromal Cell committee position statement on nomenclature. Cytotherapy. 2019;21(10):1019-24.

124. Camilleri ET, Gustafson MP, Dudakovic A, Riester SM, Garces CG, Paradise CR, et al. Identification and validation of multiple cell surface markers of clinical-grade adipose-derived mesenchymal stromal cells as novel release criteria for good manufacturing practice-compliant production. Stem Cell Res Ther. 2016;7(1):107.
125. Morrison SJ, Scadden DT. The bone marrow niche for haematopoietic stem cells. Nature. 2014;505(7483):327-34.
126. Chen X, Wang Z, Duan N, Zhu G, Schwarz EM, Xie C. Osteoblast-osteoclast interactions. Connect Tissue Res. 2018;59(2):99-107.
127. Calvi LM. Osteolineage cells and regulation of the hematopoietic stem cell. Best Pract Res Clin Haematol. 2013;26(3):249-52.
128. Mansour A, Abou-Ezzi G, Sitnicka E, Jacobsen SE, Wakkach A, Blin-Wakkach C. Osteoclasts promote the formation of hematopoietic stem cell niches in the bone marrow. J Exp Med. 2012;209(3):537-49.
129. Lecka-Czernik B. Marrow fat metabolism is linked to the systemic energy metabolism. Bone. 2012;50(2):534-9.
130. Han J, Koh YJ, Moon HR, Ryoo HG, Cho CH, Kim I, et al. Adipose tissue is an extramedullary reservoir for functional hematopoietic stem and progenitor cells. Blood. 2010;115(5):957-64.
131. Zhou BO, Yu H, Yue R, Zhao Z, Rios JJ, Naveiras O, et al. Bone marrow adipocytes promote the regeneration of stem cells and haematopoiesis by secreting SCF. Nat Cell Biol. 2017;19(8):891-903.
132. BONE MARROW, THYMUS AND BLOOD: CHANGES ACROSS THE LIFESPAN. Aging health. 2009;5(3):385-93.
133. Mendelson A, Frenette PS. Hematopoietic stem cell niche maintenance during homeostasis and regeneration. Nat Med. 2014;20(8):833-46.
134. Naveiras O, Nardi V, Wenzel PL, Hauschka PV, Fahey F, Daley GQ. Bone-marrow adipocytes as negative regulators of the haematopoietic microenvironment. Nature. 2009;460(7252):259-63.
135. Ho YH, Méndez-Ferrer S. Microenvironmental contributions to hematopoietic stem cell aging. Haematologica. 2020;105(1):38-46.
136. Kunisaki Y, Bruns I, Scheiermann C, Ahmed J, Pinho S, Zhang D, et al. Arteriolar niches maintain haematopoietic stem cell quiescence. Nature. 2013;502(7473):637-43.
137. Acar M, Kocherlakota KS, Murphy MM, Peyer JG, Oguro H, Inra CN, et al. Deep imaging of bone marrow shows non-dividing stem cells are mainly perisinusoidal. Nature. 2015;526(7571):126-30.
138. Wanjare M, Kusuma S, Gerecht S. Perivascular cells in blood vessel regeneration. Biotechnol J. 2013;8(4):434-47.
139. Rafii S, Shapiro F, Pettengell R, Ferris B, Nachman RL, Moore MA, et al. Human bone marrow microvascular endothelial cells support long-term proliferation and differentiation of myeloid and megakaryocytic progenitors. Blood. 1995;86(9):3353-63.
140. Chambers SM, Shaw CA, Gatza C, Fisk CJ, Donehower LA, Goodell MA. Aging hematopoietic stem cells decline in function and exhibit epigenetic dysregulation. PLoS Biol. 2007;5(8):e201.
141. Geiger H, de Haan G, Florian MC. The ageing haematopoietic stem cell compartment. Nat Rev Immunol. 2013;13(5):376-89.

142. Dykstra B, Olthof S, Schreuder J, Ritsema M, de Haan G. Clonal analysis reveals multiple functional defects of aged murine hematopoietic stem cells. J Exp Med. 2011;208(13):2691-703.
143. de Haan G, Lazare SS. Aging of hematopoietic stem cells. Blood. 2018;131(5):479-87.
144. Bernitz JM, Kim HS, MacArthur B, Sieburg H, Moore K. Hematopoietic Stem Cells Count and Remember Self-Renewal Divisions. Cell. 2016;167(5):1296-309.e10.
145. Chung HY, Cesari M, Anton S, Marzetti E, Giovannini S, Seo AY, et al. Molecular inflammation: underpinnings of aging and age-related diseases. Ageing Res Rev. 2009;8(1):18-30.
146. Pawelec G. Immunosenescence: impact in the young as well as the old? Mech Ageing Dev. 1999;108(1):1-7.
147. Chung SS, Park CY. Aging, hematopoiesis, and the myelodysplastic syndromes. Hematology Am Soc Hematol Educ Program. 2017;2017(1):73-8.
148. Beerman I, Maloney WJ, Weissmann IL, Rossi DJ. Stem cells and the aging hematopoietic system. Curr Opin Immunol. 2010;22(4):500-6.
149. Rossi DJ, Bryder D, Zahn JM, Ahlenius H, Sonu R, Wagers AJ, et al. Cell intrinsic alterations underlie hematopoietic stem cell aging. Proc Natl Acad Sci U S A. 2005;102(26):9194-9.
150. Mevorach D, Trahtemberg U, Krispin A, Attalah M, Zazoun J, Tabib A, et al. What do we mean when we write "senescence," "apoptosis," "necrosis," or "clearance of dying cells"? Ann N Y Acad Sci. 2010;1209:1-9.
151. Irvine KM, Skoien R, Bokil NJ, Melino M, Thomas GP, Loo D, et al. Senescent human hepatocytes express a unique secretory phenotype and promote macrophage migration. World J Gastroenterol. 2014;20(47):17851-62.
152. Egashira M, Hirota Y, Shimizu-Hirota R, Saito-Fujita T, Haraguchi H, Matsumoto L, et al. F4/80+ Macrophages Contribute to Clearance of Senescent Cells in the Mouse Postpartum Uterus. Endocrinology. 2017;158(7):2344-53.
153. Prata LGPL, Ovsyannikova IG, Tchkonia T, Kirkland JL. Senescent cell clearance by the immune system: Emerging therapeutic opportunities. Semin Immunol. 2018;40:101275.
154. Hall BM, Balan V, Gleiberman AS, Strom E, Krasnov P, Virtuoso LP, et al. Aging of mice is associated with p16(Ink4a)- and β-galactosidase-positive macrophage accumulation that can be induced in young mice by senescent cells. Aging (Albany NY). 2016;8(7):1294-315.
155. Mazzoni M, Mauro G, Erreni M, Romeo P, Minna E, Vizioli MG, et al. Senescent thyrocytes and thyroid tumor cells induce M2-like macrophage polarization of human monocytes via a PGE2-dependent mechanism. J Exp Clin Cancer Res. 2019;38(1):208.
156. Lujambio A, Akkari L, Simon J, Grace D, Tschaharganeh DF, Bolden JE, et al. Non-cell-autonomous tumor suppression by p53. Cell. 2013;153(2):449-60.
157. Mills CD, Kincaid K, Alt JM, Heilman MJ, Hill AM. M-1/M-2 macrophages and the Th1/Th2 paradigm. J Immunol. 2000;164(12):6166-73.
158. Atri C, Guerfali FZ, Laouini D. Role of Human Macrophage Polarization in Inflammation during Infectious Diseases. Int J Mol Sci. 2018;19(6).

159. Behmoaras J, Gil J. Similarities and interplay between senescent cells and macrophages. J Cell Biol. 2021;220(2).
160. Elder SS, Emmerson E. Senescent cells and macrophages: key players for regeneration? Open Biol. 2020;10(12):200309.
161. Oishi Y, Manabe I. Macrophages in age-related chronic inflammatory diseases. NPJ Aging Mech Dis. 2016;2:16018.
162. Warren LA, Rossi DJ. Stem cells and aging in the hematopoietic system. Mech Ageing Dev. 2009;130(1-2):46-53.
163. Young AL, Tong RS, Birmann BM, Druley TE. Clonal hematopoiesis and risk of acute myeloid leukemia. Haematologica. 2019;104(12):2410-7.
164. Dutta AK, Fink JL, Grady JP, Morgan GJ, Mullighan CG, To LB, et al. Subclonal evolution in disease progression from MGUS/SMM to multiple myeloma is characterised by clonal stability. Leukemia. 2019;33(2):457-68.
165. Zingone A, Kuehl WM. Pathogenesis of monoclonal gammopathy of undetermined significance and progression to multiple myeloma. Semin Hematol. 2011;48(1):4-12.
166. Trowbridge JJ, Starczynowski DT. Innate immune pathways and inflammation in hematopoietic aging, clonal hematopoiesis, and MDS. J Exp Med. 2021;218(7).
167. Young AL, Challen GA, Birmann BM, Druley TE. Clonal haematopoiesis harbouring AML-associated mutations is ubiquitous in healthy adults. Nat Commun. 2016;7:12484.
168. Busque L, Mio R, Mattioli J, Brais E, Blais N, Lalonde Y, et al. Nonrandom X-inactivation patterns in normal females: lyonization ratios vary with age. Blood. 1996;88(1):59-65.
169. Heuser M, Thol F, Ganser A. Clonal Hematopoiesis of Indeterminate Potential. Dtsch Arztebl Int. 2016;113(18):317-22.
170. Bowman RL, Busque L, Levine RL. Clonal Hematopoiesis and Evolution to Hematopoietic Malignancies. Cell Stem Cell. 2018;22(2):157-70.
171. Jaiswal S, Natarajan P, Silver AJ, Gibson CJ, Bick AG, Shvartz E, et al. Clonal Hematopoiesis and Risk of Atherosclerotic Cardiovascular Disease. N Engl J Med. 2017;377(2):111-21.
172. Bouzid H, Belk J, Jan M, Qi Y, Sarnowski C, *Wirth S*, et al. Clonal Hematopoiesis is Associated with Reduced Risk of Alzheimer's Disease. Blood2021.
173. Frick M, Chan W, Arends CM, Hablesreiter R, Halik A, Heuser M, et al. Role of Donor Clonal Hematopoiesis in Allogeneic Hematopoietic Stem-Cell Transplantation. J Clin Oncol. 2019;37(5):375-85.
174. Gibson CJ, Kim HT, Zhao L, Murdock HM, Hambley B, Ogata A, et al. Donor Clonal Hematopoiesis and Recipient Outcomes After Transplantation. J Clin Oncol. 2022;40(2):189-201.
175. Jaiswal S, Ebert BL. Clonal hematopoiesis in human aging and disease. Science. 2019;366(6465).
176. Williams MJ, Zapata L, Werner B, Barnes CP, Sottoriva A, Graham TA. Measuring the distribution of fitness effects in somatic evolution by combining clonal dynamics with dN/dS ratios. Elife. 2020;9.
177. Watson CJ, Papula AL, Poon GYP, Wong WH, Young AL, Druley TE, et al. The evolutionary dynamics and fitness landscape of clonal hematopoiesis. Science. 2020;367(6485):1449-54.

178. Robertson NA, Latorre-Crespo E, Terradas-Terradas M, Lemos-Portela J, Purcell AC, Livesey BJ, et al. Longitudinal dynamics of clonal hematopoiesis identifies gene-specific fitness effects. Nat Med. 2022.
179. SanMiguel JE, E Loberg, MA Young, KA Mistry, JJ Schwartz, LS Stearns, T Challen, GA Trowbridge, JJ. Distinct Tumor Necrosis Factor Alpha Receptors Dictate Stem Cell Fitness Versus Lineage Output in Dnmt3a -Mutant Clonal Hematopoiesis. doi: https://doi.org/10.1101/2022.07.03.498502. 2022.
180. Rodriguez-Abreu D, Bordoni A, Zucca E. Epidemiology of hematological malignancies. Ann Oncol. 2007;18 Suppl 1:i3-i8.
181. Facts and information about blood cancer Blood Cancer UK2019 [Available from: https://bloodcancer.org.uk/news/blood-cancer-facts/.
182. WHO Classification of Tumours of Haematopoietic and Lymphoid Tissues. Revised 4th Edition ed. Swerdlow SH, Campo E, Harris NL, Jaffe ES, Pileri SA, Stein H, et al., editors2017.
183. Taylor J, Xiao W, Abdel-Wahab O. Diagnosis and classification of hematologic malignancies on the basis of genetics. Blood. 2017;130(4):410-23.
184. Bachireddy P, Burkhardt UE, Rajasagi M, Wu CJ. Haematological malignancies: at the forefront of immunotherapeutic innovation. Nat Rev Cancer. 2015;15(4):201-15.
185. Coiffier B, Lepage E, Briere J, Herbrecht R, Tilly H, Bouabdallah R, et al. CHOP chemotherapy plus rituximab compared with CHOP alone in elderly patients with diffuse large-B-cell lymphoma. N Engl J Med. 2002;346(4):235-42.
186. Pulte D, Gondos A, Brenner H. Ongoing improvement in outcomes for patients diagnosed as having Non-Hodgkin lymphoma from the 1990s to the early 21st century. Arch Intern Med. 2008;168(5):469-76.
187. Hochhaus A, Baccarani M, Silver RT, Schiffer C, Apperley JF, Cervantes F, et al. European LeukemiaNet 2020 recommendations for treating chronic myeloid leukemia. Leukemia. 2020;34(4):966-84.
188. Hsieh YC, Kirschner K, Copland M. Improving outcomes in chronic myeloid leukemia through harnessing the immunological landscape. Leukemia. 2021;35(5):1229-42.
189. Cohen P, Cross D, Jänne PA. Kinase drug discovery 20 years after imatinib: progress and future directions. Nat Rev Drug Discov. 2021;20(7):551-69.
190. Nowell PC. Discovery of the Philadelphia chromosome: a personal perspective. J Clin Invest. 2007;117(8):2033-5.
191. Sehn LH, Donaldson J, Chhanabhai M, Fitzgerald C, Gill K, Klasa R, et al. Introduction of combined CHOP plus rituximab therapy dramatically improved outcome of diffuse large B-cell lymphoma in British Columbia. J Clin Oncol. 2005;23(22):5027-33.
192. Extermann M. Living longer and better with haematological malignancies: a promise for older adults too? Lancet Haematol. 2021;8(11):e784-e6.
193. Juliusson G, Antunovic P, Derolf A, Lehmann S, Möllgård L, Stockelberg D, et al. Age and acute myeloid leukemia: real world data on decision to treat and outcomes from the Swedish Acute Leukemia Registry. Blood. 2009;113(18):4179-87.

194. DiNardo CD, Wei AH. How I treat acute myeloid leukemia in the era of new drugs. Blood. 2020;135(2):85-96.
195. Hartmann L, Haferlach C, Meggendorfer M, Nadarajah N, Kern W, Haferlach T, et al. Molecular characterization of acute myeloid leukemia patients who relapse more than 3 years after diagnosis: an exome sequencing study of 31 patients. Haematologica. 2020;105(4):e157-e9.
196. Verma D, Kantarjian H, Faderl S, O'Brien S, Pierce S, Vu K, et al. Late relapses in acute myeloid leukemia: analysis of characteristics and outcome. Leuk Lymphoma. 2010;51(5):778-82.
197. Döhner H, Estey E, Grimwade D, Amadori S, Appelbaum FR, Büchner T, et al. Diagnosis and management of AML in adults: 2017 ELN recommendations from an international expert panel. Blood. 2017;129(4):424-47.
198. Döhner H, Wei AH, Appelbaum FR, Craddock C, DiNardo CD, Dombret H, et al. Diagnosis and Management of AML in Adults: 2022 ELN Recommendations from an International Expert Panel. Blood. 2022.
199. Grove CS, Vassiliou GS. Acute myeloid leukaemia: a paradigm for the clonal evolution of cancer? Dis Model Mech. 2014;7(8):941-51.
200. Ley TJ, Miller C, Ding L, Raphael BJ, Mungall AJ, Robertson A, et al. Genomic and epigenomic landscapes of adult de novo acute myeloid leukemia. N Engl J Med. 2013;368(22):2059-74.
201. Kelly LM, Gilliland DG. Genetics of myeloid leukemias. Annu Rev Genomics Hum Genet. 2002;3:179-98.
202. Lagunas-Rangel FA, Chávez-Valencia V, Gómez-Guijosa M, Cortes-Penagos C. Acute Myeloid Leukemia-Genetic Alterations and Their Clinical Prognosis. Int J Hematol Oncol Stem Cell Res. 2017;11(4):328-39.
203. Grimwade D, Hills RK, Moorman AV, Walker H, Chatters S, Goldstone AH, et al. Refinement of cytogenetic classification in acute myeloid leukemia: determination of prognostic significance of rare recurring chromosomal abnormalities among 5876 younger adult patients treated in the United Kingdom Medical Research Council trials. Blood. 2010;116(3):354-65.
204. de Thé H, Chen Z. Acute promyelocytic leukaemia: novel insights into the mechanisms of cure. Nat Rev Cancer. 2010;10(11):775-83.
205. Lo-Coco F, Avvisati G, Vignetti M, Thiede C, Orlando SM, Iacobelli S, et al. Retinoic acid and arsenic trioxide for acute promyelocytic leukemia. N Engl J Med. 2013;369(2):111-21.
206. Ablain J, Rice K, Soilihi H, de Reynies A, Minucci S, de Thé H. Activation of a promyelocytic leukemia-tumor protein 53 axis underlies acute promyelocytic leukemia cure. Nat Med. 2014;20(2):167-74.
207. Löwenberg B. Sense and nonsense of high-dose cytarabine for acute myeloid leukemia. Blood. 2013;121(1):26-8.
208. Schaich M, Röllig C, Soucek S, Kramer M, Thiede C, Mohr B, et al. Cytarabine dose of 36 g/m² compared with 12 g/m² within first consolidation in acute myeloid leukemia: results of patients enrolled onto the prospective randomized AML96 study. J Clin Oncol. 2011;29(19):2696-702.
209. Singh AK, McGuirk JP. Allogeneic Stem Cell Transplantation: A Historical and Scientific Overview. Cancer Res. 2016;76(22):6445-51.
210. Shafat MS, Oellerich T, Mohr S, Robinson SD, Edwards DR, Marlein CR, et al. Leukemic blasts program bone marrow adipocytes to generate a protumoral microenvironment. Blood. 2017;129(10):1320-32.

211. Al-Matary YS, Botezatu L, Opalka B, Hönes JM, Lams RF, Thivakaran A, et al. Acute myeloid leukemia cells polarize macrophages towards a leukemia supporting state in a Growth factor independence 1 dependent manner. Haematologica. 2016;101(10):1216-27.
212. Meacham A, Wise E, Scott EW, Cogle CR. Bone Marrow Endothelial Cells Protect Acute Myeloid Leukemia From Chemotherapy By Direct Contact: The BCAM/Laminin/VLA5 Axis As a Potential Therapeutic Target. Blood. 2013;122(21):2546-.
213. Abdul-Aziz AM, Shafat MS, Mehta TK, Di Palma F, Lawes MJ, Rushworth SA, et al. MIF-Induced Stromal PKCβ/IL8 Is Essential in Human Acute Myeloid Leukemia. Cancer Res. 2017;77(2):303-11.
214. Marlein CR, Zaitseva L, Piddock RE, Robinson SD, Edwards DR, Shafat MS, et al. NADPH oxidase-2 derived superoxide drives mitochondrial transfer from bone marrow stromal cells to leukemic blasts. Blood. 2017;130(14):1649-60.
215. Kawano Y, Moschetta M, Manier S, Glavey S, Görgün GT, Roccaro AM, et al. Targeting the bone marrow microenvironment in multiple myeloma. Immunol Rev. 2015;263(1):160-72.
216. Miraki-Moud F, Anjos-Afonso F, Hodby KA, Griessinger E, Rosignoli G, Lillington D, et al. Acute myeloid leukemia does not deplete normal hematopoietic stem cells but induces cytopenias by impeding their differentiation. Proc Natl Acad Sci U S A. 2013;110(33):13576-81.
217. Yang X, Feng W, Wang R, Yang F, Wang L, Chen S, et al. Repolarizing heterogeneous leukemia-associated macrophages with more M1 characteristics eliminates their pro-leukemic effects. Oncoimmunology. 2018;7(4):e1412910.
218. Moore JA, Mistry JJ, Hellmich C, Horton RH, Wojtowicz EE, Jibril A, et al. LC3-associated phagocytosis in bone marrow macrophages suppresses acute myeloid leukemia progression through STING activation. J Clin Invest. 2022;132(5).
219. Bosse RC, Wasserstrom B, Meacham A, Wise E, Drusbosky L, Walter GA, et al. Chemosensitizing AML cells by targeting bone marrow endothelial cells. Exp Hematol. 2016;44(5):363-77.e5.
220. Grimwade D, Walker H, Harrison G, Oliver F, Chatters S, Harrison CJ, et al. The predictive value of hierarchical cytogenetic classification in older adults with acute myeloid leukemia (AML): analysis of 1065 patients entered into the United Kingdom Medical Research Council AML11 trial. Blood. 2001;98(5):1312-20.
221. Ewald JA, Desotelle JA, Wilding G, Jarrard DF. Therapy-induced senescence in cancer. J Natl Cancer Inst. 2010;102(20):1536-46.
222. Collado M, Serrano M. Senescence in tumours: evidence from mice and humans. Nat Rev Cancer. 2010;10(1):51-7.
223. Sanoff HK, Deal AM, Krishnamurthy J, Torrice C, Dillon P, Sorrentino J, et al. Effect of cytotoxic chemotherapy on markers of molecular age in patients with breast cancer. J Natl Cancer Inst. 2014;106(4):dju057.
224. Manz MG, Boettcher S. Emergency granulopoiesis. Nat Rev Immunol. 2014;14(5):302-14.
225. Nagai Y, Garrett KP, Ohta S, Bahrun U, Kouro T, Akira S, et al. Toll-like receptors on hematopoietic progenitor cells stimulate innate immune system replenishment. Immunity. 2006;24(6):801-12.

226. Zhao JL, Baltimore D. Regulation of stress-induced hematopoiesis. Curr Opin Hematol. 2015;22(4):286-92.
227. Boettcher S, Manz MG. Regulation of Inflammation- and Infection-Driven Hematopoiesis. Trends Immunol. 2017;38(5):345-57.
228. Lodish H, Flygare J, Chou S. From stem cell to erythroblast: regulation of red cell production at multiple levels by multiple hormones. IUBMB Life. 2010;62(7):492-6.
229. Tabares Calvache E, Tabares Calvache AD, Faulhaber GAM. Systematic review about etiologic association to the leukoerythroblastic reaction. Int J Lab Hematol. 2020;42(5):495-500.
230. Hui S, Ghergurovich JM, Morscher RJ, Jang C, Teng X, Lu W, et al. Glucose feeds the TCA cycle via circulating lactate. Nature. 2017;551(7678):115-8.
231. Kolditz CI, Langin D. Adipose tissue lipolysis. Curr Opin Clin Nutr Metab Care. 2010;13(4):377-81.
232. Martínez-Reyes I, Chandel NS. Mitochondrial TCA cycle metabolites control physiology and disease. Nat Commun. 2020;11(1):102.
233. Bonora M, Patergnani S, Rimessi A, De Marchi E, Suski JM, Bononi A, et al. ATP synthesis and storage. Purinergic Signal. 2012;8(3):343-57.
234. Warr MR, Passegué E. Metabolic makeover for HSCs. Cell Stem Cell. 2013;12(1):1-3.
235. Simsek T, Kocabas F, Zheng J, Deberardinis RJ, Mahmoud AI, Olson EN, et al. The distinct metabolic profile of hematopoietic stem cells reflects their location in a hypoxic niche. Cell Stem Cell. 2010;7(3):380-90.
236. Nombela-Arrieta C, Pivarnik G, Winkel B, Canty KJ, Harley B, Mahoney JE, et al. Quantitative imaging of haematopoietic stem and progenitor cell localization and hypoxic status in the bone marrow microenvironment. Nat Cell Biol. 2013;15(5):533-43.
237. Cipolleschi MG, Dello Sbarba P, Olivotto M. The role of hypoxia in the maintenance of hematopoietic stem cells. Blood. 1993;82(7):2031-7.
238. Takubo K, Nagamatsu G, Kobayashi CI, Nakamura-Ishizu A, Kobayashi H, Ikeda E, et al. Regulation of glycolysis by Pdk functions as a metabolic checkpoint for cell cycle quiescence in hematopoietic stem cells. Cell Stem Cell. 2013;12(1):49-61.
239. Ho TT, Warr MR, Adelman ER, Lansinger OM, Flach J, Verovskaya EV, et al. Autophagy maintains the metabolism and function of young and old stem cells. Nature. 2017;543(7644):205-10.
240. Mistry JJ, Hellmich C, Moore JA, Jibril A, Macaulay I, Moreno-Gonzalez M, et al. Free fatty-acid transport via CD36 drives β-oxidation-mediated hematopoietic stem cell response to infection. Nat Commun. 2021;12(1):7130.
241. Coburn CT, Hajri T, Ibrahimi A, Abumrad NA. Role of CD36 in membrane transport and utilization of long-chain fatty acids by different tissues. J Mol Neurosci. 2001;16(2-3):117-21; discussion 51-7.
242. Veglia F, Tyurin VA, Blasi M, De Leo A, Kossenkov AV, Donthireddy L, et al. Fatty acid transport protein 2 reprograms neutrophils in cancer. Nature. 2019;569(7754):73-8.
243. WARBURG O. On the origin of cancer cells. Science. 1956;123(3191):309-14.

244. Jones CL, Stevens BM, D'Alessandro A, Reisz JA, Culp-Hill R, Nemkov T, et al. Inhibition of Amino Acid Metabolism Selectively Targets Human Leukemia Stem Cells. Cancer Cell. 2018;34(5):724-40.e4.
245. Pollyea DA, Stevens BM, Jones CL, Winters A, Pei S, Minhajuddin M, et al. Venetoclax with azacitidine disrupts energy metabolism and targets leukemia stem cells in patients with acute myeloid leukemia. Nat Med. 2018;24(12):1859-66.
246. Lagadinou ED, Sach A, Callahan K, Rossi RM, Neering SJ, Minhajuddin M, et al. BCL-2 inhibition targets oxidative phosphorylation and selectively eradicates quiescent human leukemia stem cells. Cell Stem Cell. 2013;12(3):329-41.
247. Ye H, Adane B, Khan N, Sullivan T, Minhajuddin M, Gasparetto M, et al. Leukemic Stem Cells Evade Chemotherapy by Metabolic Adaptation to an Adipose Tissue Niche. Cell Stem Cell. 2016;19(1):23-37.
248. Mansell E, Sigurdsson V, Deltcheva E, Brown J, James C, Miharada K, et al. Mitochondrial Potentiation Ameliorates Age-Related Heterogeneity in Hematopoietic Stem Cell Function. Cell Stem Cell. 2021;28(2):241-56.e6.
249. Puleston D. Detection of Mitochondrial Mass, Damage, and Reactive Oxygen Species by Flow Cytometry. Cold Spring Harb Protoc. 2015;2015(9):pdb.prot086298.
250. Perry SW, Norman JP, Barbieri J, Brown EB, Gelbard HA. Mitochondrial membrane potential probes and the proton gradient: a practical usage guide. Biotechniques. 2011;50(2):98-115.
251. Kauffman ME, Kauffman MK, Traore K, Zhu H, Trush MA, Jia Z, et al. MitoSOX-Based Flow Cytometry for Detecting Mitochondrial ROS. React Oxyg Species (Apex). 2016;2(5):361-70.
252. Morganti C, Cabezas-Wallscheid N, Ito K. Metabolic Regulation of Hematopoietic Stem Cells. Hemasphere. 2022;6(7):e740.
253. Morganti C, Bonora M, Ito K. Improving the Accuracy of Flow Cytometric Assessment of Mitochondrial Membrane Potential in Hematopoietic Stem and Progenitor Cells Through the Inhibition of Efflux Pumps. J Vis Exp. 2019(149).
254. Sobecki M, Mrouj K, Camasses A, Parisis N, Nicolas E, Llères D, et al. The cell proliferation antigen Ki-67 organises heterochromatin. Elife. 2016;5:e13722.
255. Jafri S, Moore SD, Morrell NW, Ormiston ML. A sex-specific reconstitution bias in the competitive CD45.1/CD45.2 congenic bone marrow transplant model. Sci Rep. 2017;7(1):3495.
256. Zebedee SL, Barritt DS, Raschke WC. Comparison of mouse Ly5a and Ly5b leucocyte common antigen alleles. Dev Immunol. 1991;1(4):243-54.
257. Shen FW, Tung JS, Boyse EA. Further definition of the Ly-5 system. Immunogenetics. 1986;24(3):146-9.
258. Mercier FE, Sykes DB, Scadden DT. Single Targeted Exon Mutation Creates a True Congenic Mouse for Competitive Hematopoietic Stem Cell Transplantation: The C57BL/6-CD45.1(STEM) Mouse. Stem Cell Reports. 2016;6(6):985-92.
259. Vannini N, Girotra M, Naveiras O, Nikitin G, Campos V, Giger S, et al. Specification of haematopoietic stem cell fate via modulation of mitochondrial activity. Nat Commun. 2016;7:13125.

260. Park BS, Lee JO. Recognition of lipopolysaccharide pattern by TLR4 complexes. Exp Mol Med. 2013;45:e66.
261. Mookerjee SA, Goncalves RLS, Gerencser AA, Nicholls DG, Brand MD. The contributions of respiration and glycolysis to extracellular acid production. Biochim Biophys Acta. 2015;1847(2):171-81.
262. Little AC, Kovalenko I, Goo LE, Hong HS, Kerk SA, Yates JA, et al. High-content fluorescence imaging with the metabolic flux assay reveals insights into mitochondrial properties and functions. Commun Biol. 2020;3(1):271.
263. André T, Meuleman N, Stamatopoulos B, De Bruyn C, Pieters K, Bron D, et al. Evidences of early senescence in multiple myeloma bone marrow mesenchymal stromal cells. PLoS One. 2013;8(3):e59756.
264. Dimri GP, Lee X, Basile G, Acosta M, Scott G, Roskelley C, et al. A biomarker that identifies senescent human cells in culture and in aging skin in vivo. Proc Natl Acad Sci U S A. 1995;92(20):9363-7.
265. Lee BY, Han JA, Im JS, Morrone A, Johung K, Goodwin EC, et al. Senescence-associated beta-galactosidase is lysosomal beta-galactosidase. Aging Cell. 2006;5(2):187-95.
266. Freund A, Laberge RM, Demaria M, Campisi J. Lamin B1 loss is a senescence-associated biomarker. Mol Biol Cell. 2012;23(11):2066-75.
267. Cancer Research UK: Myeloma Survival Statistics 2022 [Available from:https://www.cancerresearchuk.org/health-professional/cancer-statistics/statistics-by-cancer-type/myeloma/survival#heading-Two.
268. Ito K, Hirao A, Arai F, Takubo K, Matsuoka S, Miyamoto K, et al. Reactive oxygen species act through p38 MAPK to limit the lifespan of hematopoietic stem cells. Nat Med. 2006;12(4):446-51.
269. Vannini N, Campos V, Girotra M, Trachsel V, Rojas-Sutterlin S, Tratwal J, et al. The NAD-Booster Nicotinamide Riboside Potently Stimulates Hematopoiesis through Increased Mitochondrial Clearance. Cell Stem Cell. 2019;24(3):405-18.e7.
270. Amorim JA, Coppotelli G, Rolo AP, Palmeira CM, Ross JM, Sinclair DA. Mitochondrial and metabolic dysfunction in ageing and age-related diseases. Nat Rev Endocrinol. 2022;18(4):243-58.
271. Haas RH. Mitochondrial Dysfunction in Aging and Diseases of Aging. Biology (Basel). 2019;8(2).
272. Miwa S, Kashyap S, Chini E, von Zglinicki T. Mitochondrial dysfunction in cell senescence and aging. J Clin Invest. 2022;132(13).
273. Glatman Zaretsky A, Engiles JB, Hunter CA. Infection-induced changes in hematopoiesis. J Immunol. 2014;192(1):27-33.
274. Caraballo C, Jaimes F. Organ Dysfunction in Sepsis: An Ominous Trajectory From Infection To Death. Yale J Biol Med. 2019;92(4):629-40.
275. Singer M, Deutschman CS, Seymour CW, Shankar-Hari M, Annane D, Bauer M, et al. The Third International Consensus Definitions for Sepsis and Septic Shock (Sepsis-3). JAMA. 2016;315(8):801-10.
276. Gavazzi G, Krause KH. Ageing and infection. Lancet Infect Dis. 2002;2(11):659-66.
277. El Chakhtoura NG, Bonomo RA, Jump RLP. Influence of Aging and Environment on Presentation of Infection in Older Adults. Infect Dis Clin North Am. 2017;31(4):593-608.

278. Esme M, Topeli A, Yavuz BB, Akova M. Infections in the Elderly Critically-Ill Patients. Front Med (Lausanne). 2019;6:118.
279. El Solh A, Pineda L, Bouquin P, Mankowski C. Determinants of short and long term functional recovery after hospitalization for community-acquired pneumonia in the elderly: role of inflammatory markers. BMC Geriatr. 2006;6:12.
280. Papa L, Djedaini M, Hoffman R. Mitochondrial Role in Stemness and Differentiation of Hematopoietic Stem Cells. Stem Cells Int. 2019;2019:4067162.
281. Scadden DT. Nice neighborhood: emerging concepts of the stem cell niche. Cell. 2014;157(1):41-50.
282. Williams GC. Pleiotropy, natural selection, and the evolution of senescence. Evolution.1957. p. 398-411.
283. Wiley CD, Campisi J. The metabolic roots of senescence: mechanisms and opportunities for intervention. Nat Metab. 2021;3(10):1290-301.